Pollutant transport in rivers: estimating dispersion coefficients from tracer experiments

Alexander James Heron

Thesis submitted for the degree of

Master of Philosophy

School of Energy, Geoscience, Infrastructure and Society

Heriot-Watt University

July 2015

Abstract

To better understand the dispersion characteristics of small streams which are sparsely represented in published work, eleven successful tracer experiments were carried out on the same reach of a small stream (Murray Burn) in Scotland over various flow and seasonal conditions. Four different analysis methods (Reduction of Peak, Method of Moments, Routing Procedure, Analytical Solution) were used to determine dispersion coefficients and flow velocities from observed temporal concentration profiles. A new weighted average approach for the Analytical Solution method produced improved velocity and dispersion results, i.e. ones that were more consistent with the results from the other methods. One aim was to investigate the influence of long tails (on the concentration profiles) on the results by truncating the profiles at the 1% peak concentration level, repeating the data analysis and comparing the truncated results with the original analysis. It is concluded that truncation of concentration profiles is beneficial for the methods used in the thesis. The dispersion coefficients obtained for the Murray Burn (0.15 – 1.0 m^2/s) augment our knowledge of dispersion in small streams by complementing the few previously published data for stream flow rates less than 1000 l/s.

ACADEMIC REGISTRY
Research Thesis Submission

Name*:*	Alexander James Heron		
School/PGI:	EGIS		
Version: *(i.e. First, Resubmission, Final)*	Final	Degree Sought (Award and Subject area)	MPhil (CIVIL)

Declaration

In accordance with the appropriate regulations I hereby submit my thesis and I declare that:

1) the thesis embodies the results of my own work and has been composed by myself
2) where appropriate, I have made acknowledgement of the work of others and have made reference to work carried out in collaboration with other persons
3) the thesis is the correct version of the thesis for submission and is the same version as any electronic versions submitted*.
4) my thesis for the award referred to, deposited in the Heriot-Watt University Library, should be made available for loan or photocopying and be available via the Institutional Repository, subject to such conditions as the Librarian may require
5) I understand that as a student of the University I am required to abide by the Regulations of the University and to conform to its discipline.

* *Please note that it is the responsibility of the candidate to ensure that the correct version of the thesis is submitted.*

Signature of Candidate*:*		Date:	25/7/2015

Submission

Submitted By *(name in capitals):*	ALEXANDER JAMES HERON
Signature of Individual Submitting:	
Date Submitted:	25/7/2015

For Completion in the Student Service Centre (SSC)

Received in the SSC by *(name in capitals):*			
Method of Submission *(Handed in to SSC; posted through internal/external mail):*			
E-thesis Submitted (mandatory for final theses)			
Signature:		Date:	

Table of Contents

Chapter 1 - Introduction

1.1 Background

1.2 Aim and objectives of the work

1.3 Structure of thesis

Chapter 2 – Literature Review

2.1 Introduction

2.2 Transport processes in rivers

2.3 Mathematical models of transport

2.4 Mixing zones in rivers

2.4.1 Advective zone

2.4.2 Equilibrium zone

2.4.3 Gaussian zone

2.5 Deviations from the Fickian model

2.6 Methods for estimating dispersion coefficients

2.6.1 Flow structure

2.6.2 Flux integration

2.6.3 Reduction of peak

2.6.4 Method of moments

2.6.5 Routing procedures

2.6.6 Analytical solution

2.6.7 Empirical equations

2.7 Dispersion coefficient values

2.8 Small streams

2.9 Summary

Chapter 3 - Methodology

3.1 Introduction

3.2 Reduction of peak

3.2.1 Description

3.2.2 Comments

3.3 Method of moments

3.3.1 Description

3.3.2 Comments

3.4 Routing procedure

3.4.1 Description

3.4.2 Comments

3.5 Analytical solution

3.5.1 Description

3.5.2 Comments

3.6 Stream flow rate

3.7 Truncation of data

3.8 Data interpolation

3.9 Summary

Chapter 4 - Experimental work and data processing

4.1 Introduction

4.2 Preparation of Rhodamine WT standards

4.3 Tracer Experiments

4.3.1 Introduction

4.3.2 Tracer release

4.3.3 Collection of water samples

4.4 Operation of the Turner Designs Fluorometer

4.4.1 Introduction

4.4.2 Use and Initial set-up

4.4.3 Calibration and analysis of samples

4.4.4 Estimation of calibration factor

4.5 Identification of background signal

4.6 Removal of background signal and amplification of calibration factor

4.7 Missing data

4.8 Data scaling

4.9 Data interpolation

4.10 Summary

Chapter 5 - Results and discussion

5.1 Introduction

5.2 Stream flow rate

5.3 Some preliminary issues

5.4 Velocity

5.4.1 Reduction of peak

5.4.2 Method of Moments

5.4.3 Routing Procedure

5.4.4 Analytical Solution

5.4.5 Discussion

5.5 Dispersion coefficient

5.5.1 Reduction of peak

5.5.2 Method of moments

5.5.3 Routing procedure

5.5.4 Analytical solution

5.5.5 Discussion

5.5.6 Errors

5.5.7 Summary

Chapter 6 - Conclusions

6.0 Conclusions

6.1 Suggestions for further work

Notation

The following symbols are used in this paper:

A cross-sectional area of flow (m^2)

c depth average solute concentration (μg/l)

C cross-sectional average solute concentration (μg/l)

c' deviation of the local solute concentration from the cross-sectional average solute concentration (μg/l)

C_p peak concentration (μg/l)

D diffusion coefficient (m^2/s)

g gravitational acceleration (m/s^2)

H cross-sectional average depth (m)

h local depth (m)

I dimensionless triple integral

J diffusive solute flux ($kg/(m^2 \cdot s^1)$)

K longitudinal dispersion coefficient (m^2/s)

k depth average dispersion coefficient (m^2/s)

L length scale over which velocity deviation occurs (m)

M mass of solute released (mg)

m moment of temporal solute concentration profile (various)

Q stream flow rate (l/s)

S slope of channel (-)

t time (min)

t_p time of peak concentration occurrence (min)

V cross-sectional average velocity (m/s)

v depth average velocity (m/s)

v' deviation of the local longitudinal flow velocity from the cross-sectional average velocity (m/s)

V_* shear velocity (m/s)

W width (m)

x longitudinal co-ordinate (m)

y transverse co-ordinate (m)

z vertical co-ordinate (m)

ε turbulent diffusion coefficient (m^2/s)

ε_t transverse mixing coefficient (m^2/s)

μ centroid of temporal solute concentration profile (min)

σ^2 variance of temporal solute concentration profile (min^2)

$\emptyset$ solute concentration ($\mu g/l$)

List of Tables and Figures

Table 4.1 Summary of stock solutions used

Table 4.2 Examples of dilutions

Table 4.3 Summary data of the experiments

Table 4.4 Example of readings for calibration standards and conversion to MS range

Table 5.1 Stream flow rates for each site for all experiments

Figure 2.1 Variation of dispersion coefficient with flow rate

Figure 3.1 Example of the temporal concentration profiles

Figure 3.2 Reduction of Peak Method

Figure 3.3 Example of the Routing Procedure output

Figure 3.4 Example of the Analytical Solution output

Figure 3.5 Example of a standard temporal concentration profile

Figure 3.6 Example of a truncated temporal concentration profile

Figure 4.1 Map of study site

Figure 4.2 Turner Designs model 10 Fluorometer

Figure 4.3 Example of fluorometer calibration graph

Figure 5.1 Examples of sources of land drainage upstream of Site 4

Figure 5.2 Variation of velocity with stream flow rate: Reduction of Peak Analysis

Figure 5.3 Variation of velocity with stream flow rate: Method of Moments Analysis

Figure 5.4 Variation of velocity with stream flow rate: Routing Procedure Analysis

Figure 5.5 Comparison of 3 different velocity estimates: Analytical Solution Analysis using standard data

Figure 5.6 Variation of velocity with stream flow rate: Analytical Solution Analysis

Figure 5.7 Comparison of velocities from four analysis methods using standard data

Figure 5.8 Comparison of velocities from four analysis methods using truncated data

Figure 5.9 Comparison of alternative Analytical Solution velocities

Figure 5.10 Comparison of velocity with stream flow rate: four analysis methods using standard data

Figure 5.11 Comparison of velocity with stream flow rate: four analysis methods using truncated data

Figure 5.12 Variation of dispersion coefficient with stream flow rate: Reduction of Peak Analysis

Figure 5.13 Variation of dispersion coefficient with stream flow rate: Method of Moments Analysis

Figure 5.14 Variation of dispersion coefficient with stream flow rate: Routing Procedure Analysis

Figure 5.15 Comparison of 3 different dispersion coefficient estimates: Analytical Solution Analysis using standard data

Figure 5.16 Variation of dispersion coefficient with stream flow rate: Analytical Solution Analysis

Figure 5.17 Comparison of dispersion coefficients from four analysis methods using standard data

Figure 5.18 Comparison of dispersion coefficients from four analysis methods using truncated data

Figure 5.19 Comparison of alternative Analytical Solution dispersion coefficients with other analysis methods using truncated data

Figure 5.20 Comparison of dispersion coefficient with stream flow rate: four analysis methods using truncated data; individual results

Figure 5.21 Comparison of dispersion coefficient with stream flow rate: four analysis methods using truncated data; power law trends

Figure 5.22 Variation of dispersion coefficient with stream flow rate: average of three analysis methods using truncated data

Figure 5.23 Variation of dispersion coefficient with stream flow rate: new and existing data

Figure 5.24 Variation of non dimensional dispersion coefficient using river depth as the length scale

Figure 5.25 Variation of non dimensional dispersion coefficient using river width as the length scale

Appendices

Appendix A Table for Figure 2.1

Appendix B Temporal concentration profiles

Appendix C Routing procedure profiles

Appendix D Analytical solution profiles

Appendix E Velocity and dispersion coefficient tables, all methods

Appendix F Dispersion coefficient example calculations

Appendix G Process of serial dilution used to obtain the Rhodamine WT standards

References

Chapter 1 Introduction

1.1 Background

Clean water is important for all forms of life, it is also an indication of how society values and protects the natural resources of a country. Pollution of our natural water resources whether deliberate or accidental must be prevented to the best of our abilities. It is precious to think you could drink the water from any stream in your environment. Any pollution entering even a small stream on a hillside could have an effect: the impact could be local or could be further downstream; it could be temporary or be long-lived. For example, stream pollution from a road traffic incident would normally have a local effect for a short period of time whereas stream pollution from an abandoned industrial site may carry on for many years eventually affecting a large downstream area. In either case, the pollutant transport characteristics of the stream system play a major role in the outcome. Hence phenomena such as stream flow rate, velocity of flow and solute dispersion are of interest to the water industry.

Of these, this thesis is primarily concerned with solute dispersion with an emphasis on small streams. It seems that relatively few previous studies on river dispersion have considered small streams. This is surprising because the necessary fieldwork is easier and cheaper to do compared with working on medium size and large rivers. However, probably the perception has been that water quality and pollution issues in the latter are more important. For example, the ecological and economic consequences of an industrial spill or of widespread diffuse agricultural runoff in rivers such as the Forth, Thames and Rhine would be considerably more significant than similar events in low order streams and local drainage channels. Also urban watercourses (typically medium order streams) and major rivers passing through large towns and cities are probably at higher risk of serious pollution than are headwater and upland streams. Nevertheless, pollution in small streams and in upland catchments is inevitably passed downstream so that an understanding of the transport characteristics of small streams has an important role in predicting water quality issues at the catchment scale.

Despite many tens of studies, the reliable prediction of dispersion coefficients in rivers is a difficult task. Although the ultimate goal would be to have a way of

estimating dispersion coefficients that will apply to all rivers, this remains elusive and is probably unrealistic because of the great variability between rivers of important factors such as bed slope, structure and roughness; sinuosity and channel shape; flow rate and vegetation, both of which vary during the year. Hence the most reliable approach is to undertake tracer experiments. This involves injecting a soluble tracer at an upstream location and measuring tracer concentrations at one or more locations further downstream. From these data several methods can be used to estimate dispersion coefficients for the flow conditions existing during the experiment.

This is the technique used in this thesis, and experiments were undertaken in the Murray Burn which is a small stream that crosses Heriot-Watt University's Riccarton Campus in Edinburgh. A total of eleven successful experiments were completed under steady flow conditions. The experiments covered a stream flow range of 17 l/s to 436 l/s. Previous travel time experiments conducted on this stream had sampling sites ranging from one to four, for the dispersion tracer dye experiments the reach between sites 3 and 4 were chosen for the more consistent hydraulic parameters. Each experiment yielded an upstream (Site 3) temporal concentration profile and a downstream (Site 4) temporal concentration profile from which estimates of stream flow velocity and dispersion coefficient were obtained using four different methods.

1.2 Aim and objectives of the work

Aim

The aim of the work is to improve our knowledge of the solute dispersion characteristics of small streams. This is achieved by fulfilling the following objectives.

Objectives

- Carry out tracer experiments to determine dispersion coefficients (and flow velocities) for the Murray Burn over a wide range of stream flow rates
- Use four methods of estimating dispersion coefficients (Peak Reduction, Method of Moments, Routing Procedure, Analytical Solution) with the tracer data and compare the results

- Determine the influence of long tails (on the concentration profiles) on the results by repeating the data analysis using truncated profiles and comparing the results with the original analysis
- Compare the dispersion coefficients with previous unpublished results from a nearby reach of the Murray Burn and with published data from other streams
- To augment the very small number of published dispersion coefficients for small streams (defined as streams with stream flow rate less than 1000 l/s)

1.3 Structure of thesis

The next chapter reviews the literature on dispersion in rivers and comments on the lack of data for small streams. Chapter 3 describes the methods used to analyse the tracer data, and Chapter 4 describes the tracer experiments and initial data processing. Chapter 5 presents and discusses flow velocities and dispersion coefficients obtained using the four analysis methods with standard and truncated data. Conclusions are presented in Chapter 6. Following a list of several appendices that present supportive information, a list of cited work is given.

Chapter 2 Literature Review

2.1 Introduction

Dispersion in rivers has been studied since the 1960s, and has included observations of the processes, development of theories and derivation of mathematical models. As a result numerous tools have evolved that enable the impact of pollution incidents on rivers to be estimated. This chapter reviews this work and reflects on the relative lack of information on dispersion in small streams.

2.2 Transport processes in rivers

If one looks down at a river from a distance, it appears as one simple flow; however, closer inspection reveals it consists of complex, random and variable features. To understand river mixing we must take into account many factors: the nature of the stream bed, the width and depth of the river, the velocity of the water, the slope of the river bed, the sinuosity of the channel, river bank and bed vegetation etc.

There are two main physical processes that transport solute in a moving fluid: advection and diffusion. Advection describes how the stream or river carries solute by the velocity of the flow. It can be likened to the action of currents upon "bags" of fluid: an analogy may be to think of it of as a paper bag being blown around by the wind, it will be blown in a general direction but may sample a wide area on its journey. Diffusion is the spreading of solute caused by random motions in a fluid. In a stationary fluid, the random motion occurs at the molecular scale and is known as Brownian motion (Fischer et al, 1979; Rutherford, 1994). This effect can be seen if a drop of dye is very carefully placed in a glass of water. Very gradually, the dye will spread out in all directions until there are no concentration gradients left and the dye becomes fully mixed with the water, In very slowly moving fluids in which the Reynolds number remains less than about 2000 (known as laminar flow), Brownian motion always takes place. At larger Reynolds number, turbulence in the flow promotes much more vigorous diffusion known as turbulent diffusion (Fischer et al, 1979; Rutherford, 1994). In natural water courses Reynolds numbers are large enough so that turbulent diffusion is the dominant mechanism and Brownian motion can be neglected (Chanson, 2004; Rutherford, 1994).

Dispersion is the result of the interaction of advection and diffusion. Longitudinal dispersion, the focus of the work in this thesis, is created by the interaction of cross-sectional gradients of longitudinal advection (differential longitudinal advection) and cross-sectional mixing (Chanson, 2004; Fischer et al, 1979; Rutherford, 1994) which comprises cross-sectional turbulent diffusion and cross-sectional advection (known as secondary currents). Cross-sectional gradients in longitudinal advection are caused by velocity shear, which exists due to the frictional drag of the physical boundaries at the stream bed and banks. Water in contact with the stream bed and sides travels slower; water beyond these boundaries travels much faster creating a velocity shearing effect. Thus solute in the centre of a river is carried downstream more quickly than solute near the bank or bed, creating longitudinal spreading. Turbulent diffusion mixes solute longitudinally, transversely and vertically. Whereas its longitudinal component contributes little to longitudinal solute transport, its transverse and vertical components continually re-distribute solute within the cross-section. As a result the power of velocity shear to create longitudinal spreading is reduced. Secondary currents are circulations in the plane of the cross-section that occur due to the interaction of the flow with the channel boundaries (Chanson, 2004). They are usually much smaller than the longitudinal velocity, and only in meandering channels do they contribute significantly to the cross-sectional mixing of solute (Rutherford, 1994; Boxall et al 2003; Baek et al 2006).

An additional source of mixing are eddies caused by geomorphological structures. These comprise features such as obstacles (e.g. large roughness elements, waterfalls and weirs), pool-riffle sequences (i.e. alternating sections of deep and shallow water) and dead zones (i.e. pockets of circulating water that are, to a greater or lesser extent, separate from the main flow). Eddies created by these structures exist over a wide range of scales, and although they are known to affect longitudinal dispersion, it is often difficult to predict the consequences with any degree of certainty (Zhang and Boufadel, 2010).

When a solute is put into a stream, advection and diffusion of the solute begins. Initially, the mixing of the solute is dominated by the local three dimensional transport processes and the momentum of the solute release. Usually, some vertical mixing occurs first subjecting the solute to vertical velocity shear and hence longitudinal spreading. At the same time, local turbulent diffusion and secondary currents carry the solute transversely taking the solute towards the banks and subjecting it to further

velocity shear. Quite quickly an initially small and concentrated patch of solute evolves into a much diluted and larger cloud of solute. Complete mixing over the depth is usually achieved within a longitudinal distance of 50 stream depths, complete transverse mixing takes much longer to achieve, usually within a longitudinal distance of 100 to 300 stream widths (Rutherford, 1994). Longitudinal mixing continues for ever.

2.3 Mathematical models of transport

In 1855 Fick derived equations to describe diffusion (Fischer et al, 1979). His first law describes how spatial concentration fluctuations are smoothed out with solute moving from regions of high concentration to regions of low concentration. It explains the movement of molecules in terms of Brownian motion where molecules are continually bouncing off each other with such high frequency that there can be no "memory" of a previous velocity/path, and the motion of a molecule is best described as a random walk. Generalising this motion to the one-dimensional behaviour of a patch of solute, he derived his first law of diffusion (Fischer et al, 1979):

$$J_x = -D\frac{\partial \emptyset}{\partial x} \tag{2.1}$$

where J_x is the diffusive flux (a measure of the mass of solute being transported), D is the diffusion coefficient, $\emptyset$ is the solute concentration and x is the coordinate direction.

Fick's second law describes how diffusion causes concentration to change with time. It combines the concept of mass conservation with his first law. In one dimension, this gives (Fischer et al, 1979):

$$\frac{\partial \emptyset}{\partial t} = D\frac{\partial^2 \emptyset}{\partial x^2} \tag{2.2}$$

Fick's work can be applied directly to stationary fluids or those moving under laminar flow. For turbulent flows it can be shown that under certain conditions the same basic Fickian principles and equations can also be used (Fischer et al, 1979). Essentially, the main conditions are that the mixing is caused by random motions in the fluid and that the mixing has been taking place for a long enough time such that the evolving cloud is no longer being influenced by its initial contact with the flow (Fischer et al, 1979).

A three dimensional transport equation for a turbulent flow (known as the Advection-Diffusion Equation) can be derived for a turbulent flow in a similar way to equation 2.2 and allowing for the presence of advection. Thus (Chatwin & Allen, 1985; Rutherford, 1994):

$$\frac{\partial \emptyset}{\partial t} + u_x \frac{\partial \emptyset}{\partial x} + u_y \frac{\partial \emptyset}{\partial y} + u_z \frac{\partial \emptyset}{\partial z} = \frac{\partial}{\partial x}\left(\varepsilon_x \frac{\partial \emptyset}{\partial x}\right) + \frac{\partial}{\partial y}\left(\varepsilon_y \frac{\partial \emptyset}{\partial y}\right) + \frac{\partial}{\partial z}\left(\varepsilon_z \frac{\partial \emptyset}{\partial z}\right) \quad (2.3)$$

where *x*, *y*, and *z* are longitudinal, transverse and vertical co-ordinates; $\emptyset$ is solute concentration, u_x, u_y, u_z are velocities and ε_x, ε_y, ε_z are turbulent diffusion coefficients. In this equation the 2nd, 3rd and 4th terms represent transport by advection and the terms on the right-hand side represent transport by turbulent diffusion. In contrast to transport by Brownian motion, where the mixing coefficient is a fluid property, for turbulent diffusion the mixing coefficients are properties of the flow, and hence they are likely to take different values in the three space directions and vary with location. The concentrations, velocities and diffusion coefficients in this equation are turbulent mean values, i.e. they are representative of conditions existing at a given time rather than being values that exist at a particular instant of time.

This three dimensional equation can be simplified to a two dimensional equation as the majority of rivers are wider than they are deep, so vertical mixing occurs rapidly. Hence averaging over the depth leaves the following equation (Rutherford, 1994):

$$\frac{\partial c}{\partial t} + v_x \frac{\partial c}{\partial x} + v_y \frac{\partial c}{\partial y} = \frac{1}{h}\frac{\partial}{\partial x}\left(h k_x \frac{\partial c}{\partial x}\right) + \frac{1}{h}\frac{\partial}{\partial y}\left(h k_y \frac{\partial c}{\partial y}\right) \quad (2.4)$$

where *c* is depth averaged solute concentration, v_x, v_y are depth averaged velocities, *h* is local depth and k_x, k_y are longitudinal and transverse dispersion coefficients. The two terms on the right-hand side of the equation describe transport caused by the interaction of the vertical shear with the vertical mixing, i.e. local longitudinal and transverse dispersion.

Once it is considered that sufficient transverse mixing has also occurred the transverse mixing can also be averaged out leaving us with the following one dimensional equation (Rutherford, 1994):

$$\frac{\partial C}{\partial t} + V\frac{\partial C}{\partial x} = \frac{1}{A}\frac{\partial}{\partial x}\left(AK\frac{\partial C}{\partial x}\right) \quad (2.5)$$

Where *C* is cross-sectional average solute concentration, *V* is cross-sectional average velocity, *A* is cross-sectional area of flow and *K* is longitudinal dispersion coefficient. The term on the right-hand side describes transport caused by the interaction of the cross-sectional shear with the cross-sectional mixing, i.e. longitudinal dispersion. For a uniform channel, in which *A*, *V* and *K* are constants, equation 2.5 simplifies to (Fischer et al, 1979; Rutherford, 1994):

$$\frac{\partial C}{\partial t} + V\frac{\partial C}{\partial x} = K\frac{\partial^2 C}{\partial x^2} \quad (2.6)$$

which is known as the Advection-Dispersion Equation (ADE).

The Advection-*Diffusion* Equation (equation 2.3) applies at all locations in a river and is the fundamental basis on which many simplified mathematical descriptions rely. In contrast the ADE only applies to cross-sectional average concentrations, and several important conditions must be met for it to be used. It can be noticed that dispersion only arises as an artefact of spatial averaging of the Advection-*Diffusion* Equation, so that "dispersion is not a fundamental physical process" (Rutherford, 1994). Furthermore, the form of the dispersion term is identical to the forms of the Fickian diffusion terms in equation 2.3. Hence the ADE is frequently referred to as a Fickian model (Rutherford, 1994). However, the physics of dispersion are not the same as the physics of diffusion.

The origins of the ADE lie in the work of the British scientist Sir Geoffrey Taylor. In papers on the evolution of diffusing solute clouds (Taylor, 1921), dispersion in laminar pipe flow (Taylor, 1953) and dispersion in turbulent pipe flow (Taylor, 1954) he specified the conditions under which the ADE applies. These are:

The solute has been evolving for a sufficiently long time
The turbulence is statistically stationary in time
The velocity field is steady
The flow cross-section is a constant
The solute is passive

Hence the ADE is valid for describing solute transport in steady flow in a uniform channel once sufficient time has elapsed since the solute entered the flow (Chatwin and

Allen, 1985). The latter concept and its consequences are described in the following section.

2.4 Mixing zones in rivers

There are considered to be three zones when describing the dispersion of solutes in a river or stream: these are the advective zone, the equilibrium zone and the Gaussian zone. These zones relate to different stages of the transport of a solute released to a river and may be defined in terms of the balance of the processes that create dispersion, namely velocity shear and cross-sectional mixing. For the application of Taylor's work to rivers, Fischer (1967) argued that transverse velocity gradients and transverse mixing are much more important than vertical velocity gradients and vertical mixing because most streams are much wider than they are deep. Therefore the definition of mixing zones in rivers usually relates to the degree to which transverse mixing is complete.

2.4.1 Advective zone

In this zone solute transport is initially heavily influenced by the local conditions existing at the point of solute release and by any momentum imparted to the solute during its release. However, these influences reduce as the solute mixes and eventually disappear. On entering the flow a patch of solute is stretched longitudinally by velocity shear, creating a highly skewed (asymmetrical) longitudinal concentration profile (Fischer, 1966). Over time, due to transverse mixing, solute experiences more and more of the local transport processes that exist across the width of the channel and the more times that solute moves across the width the more the influence of the initial entry conditions fade away. As a result the skewness decays, but does not necessarily disappear. Whereas in the early stages velocity shear dominates transverse mixing, as time passes this domination reduces and at some time they reach a balance. This marks the end of the advective zone and the start of the equilibrium zone. Various ways of estimating the length of the advective zone have been proposed (see, e.g. Fischer et al, 1979; Rutherford, 1994; Chanson, 2004), but none are particularly reliable because they require estimates of appropriate length scales and rates of transverse mixing, both of which are difficult to quantify. According to experimental laboratory studies carried out by Shucksmith et al (2007) the advective zone in a

channel becomes longer with increasing discharge. The ADE does not apply in the advective zone.

2.4.2 Equilibrium zone

This begins when differential longitudinal advection and cross sectional mixing are in balance. By now solute will have encountered the entire transverse distribution of the flow and mixing field. Taylor (1953, 1954) showed that the balance between the processes was required for the longitudinal dispersion to be described using a Fickian type of expression (i.e. equation 2.5 or 2.6). As a consequence of the Fickian nature of the evolution of a solute cloud, in the equilibrium zone the variance of a spatial concentration profile grows linearly with time and distance (Fischer et al, 1979; Rutherford, 1994). The skewness of the profile continues to decay (Fischer et al, 1979; Rutherford, 1994).

Shucksmith et al (2007) state that in this region the ADE can be applied because it is looking only at one dimension and the tracer is assumed to be fully mixed over the width and depth of the stream. However, Sayre (1968a) showed that for an instantaneous tracer release there will always be transverse concentration gradients because velocity shear continually creates them. Under the equilibrium of the processes, as soon as concentration gradients appear, cross-sectional mixing breaks them down. It is usually assumed that the ADE is applicable in the equilibrium zone.

2.4.3 Gaussian zone

If the balance between the processes is maintained, further evolution of the cloud constitutes continued linear growth of the variance, and the final removal of any skewness, of the spatial concentration profile. As a consequence of the Fickian nature of the system spatial profiles take the shape of a Gaussian distribution (Fischer et al, 1979; Rutherford, 1994). The ADE can be used in the Gaussian zone. Rutherford (1994) states that the Fickian model predicts that the Gaussian zone should begin at about 5 to 10 times the length of the advective zone. It is worth noting that under the Fickian model temporal concentration profiles are not Gaussian in shape, but retain some skewness. This happens because as a dispersing solute cloud passes a fixed location it continues to evolve (Fischer et al, 1979; Rutherford, 1994).

2.5 Deviations from the Fickian model

Several authors have questioned the validity of the Fickian model, often because observations of concentration profiles are not Gaussian. Although there is sometimes confusion due to observations being of temporal profiles rather than spatial profiles, the skewness of observed temporal profiles is sometimes greater than would be expected. A further complication is the difficulty of knowing in which of the mixing zones described above the observations were collected. Chatwin & Allen (1985) also raise some practical limitations of the underlying Fickian theory.

Day and Wood (1976) state they are "unaware of any Gaussian concentration distribution ever being recorded from flow in an open channel" and Day (1977), commenting on a series of 49 tracer experiments in small rough natural mountain streams, notes that temporal tracer profiles remained skewed over the sampled region of the streams. Similarly, Nordin and Troutman (1980) report on persistent skewness in observations. These and other workers (e.g. Valentine and Wood, 1979; Beer and Young, 1983; Schmid, 2002) have suggested that the presence of dead zones is a likely source of the differences between observations and the Fickian model.

Dead zones are areas in the stream where solutes may enter and then be slowly released back into the main areas of the flow. Likely areas for dead zones are usually close to stream banks where there may be slower moving pools or areas with eddies causing loops and current reversals. Another factor is the permeability of the river bed and the water exchange mechanisms that make up the hyporheic zone (i.e. the saturated zone bordering a stream channel). In recent years all these mechanisms have tended to be lumped together and are often termed "transient storage".

As a result several alternative models to the ADE have been proposed. Most prominent are the Transient Storage Model, which is an extended version of the ADE to include the effect of transient storage (e.g. Bencala and Walters, 1983; Runkel, 1998; Rutherford, 1994; Schmid et al, 2010) and the Aggregated Dead Zone Model, which has a completely different basis in which a river is modelled as a series of incompletely mixed cells (e.g. Beer and Young, 1983; Wallis et al, 1989; Rutherford, 1994).

2.6 Methods for estimating dispersion coefficients

Several methods for estimating dispersion coefficients have been proposed. Some require detailed measurements of relevant processes; some require the use of tracer experiments; some use estimates of reach average hydraulic parameters. Seven approaches are introduced below, four of which are used in this work and are described in more detail in Chapter 3.

2.6.1 Flow structure

This method follows directly from Fischer's (1967) application to rivers of Taylor's (1954) work on pipes. It is based on the interaction of transverse velocity shear and transverse mixing, from which it can be shown that (Fischer, 1967; Fischer et al, 1979; Rutherford, 1994; Wallis & Manson, 2004):

$$K = -\frac{1}{A}\int_0^W hv' \int_0^y \frac{1}{h\varepsilon_t}\int_0^y hv' \; dy\, dy\, dy \tag{2.7}$$

where K is the dispersion coefficient, A is the cross-sectional area, W is the width of the river, h is the local depth, v' is the deviation of the local longitudinal flow velocity from the cross-sectional average velocity, ε_t is the transverse mixing coefficient and y is the transverse co-ordinate. It can only be used if measurements or estimates of the transverse distribution of the required variables are available. Until recently, this was rare, but the advent of ADCP technology has improved things (see, e.g. Carr & Rehmann, 2007; Shen et al, 2010).

2.6.2 Flux integration

This method comes from the Fickian nature of the ADE, in which the dispersive flux is proportional to the concentration gradient (see, equation 2.1). Hence (Wallis, 2011):

$$K = \frac{-\frac{1}{A}\int_0^A c'v'\, dA}{\partial C/\partial x} \tag{2.8}$$

where c' is the deviation of the local solute concentration from the cross-sectional average solute concentration, C, x is the longitudinal co-ordinate and the other symbols are as defined in section 2.5.1. It can only be used if measurements or estimates of the transverse distribution of the required variables are available. This is rare, so the method is of little practical use.

2.6.3 Reduction of peak

This method is based on observations taken at the ends of a longitudinal reach during a tracer experiment. It relates the dispersion coefficient to the reduction in peak concentration between the two sites, the timing of the peak concentrations, the flow rate of the stream and the cross-sectional area of the flow. The method is based on Taylor's (1954) theoretical analysis of solute transport and uses an analytical solution of the ADE. Further details are given in section 3.2.

2.6.4 Method of moments

This method is based on observations taken at the ends of a longitudinal reach during a tracer experiment. It was developed by Fischer (1966), building on the work of Taylor (1954), and relates the dispersion coefficient to the changes in the centroid and variance of the temporal concentration profiles between the two sites. This relationship is a consequence of the Fickian nature of dispersion. Further details are given in section 3.3.

2.6.5 Routing procedures

A routing procedure was first proposed by Fischer (1968) and a few more have been proposed more recently (Barnett, 1983; Singh & Beck, 2003). The idea is to compare a temporal concentration profile observed during a tracer experiment with a corresponding temporal concentration profile created by a series of calculations that simulate solute transport as described by the ADE. The dispersion coefficient is evaluated by finding the value which gives the best fit between the two profiles. Further details are given in section 3.4.

2.6.6 Analytical solution

This is the same as a routing procedure except that the simulated concentration profile comes from an analytical solution of the ADE. Further details are given in section 3.5.

2.6.7 Empirical equations

Once values of dispersion coefficients in rivers had been estimated, workers attempted to correlate them with commonly available hydraulic variables such as flow rate, channel dimensions etc. The form of many of the resulting equations was heavily

influenced by Fischer's (1975) suggestion that equation 2.7 could be written more simply as (Wallis & Manson, 2004):

$$K = \frac{I\overline{v'^2}L^2}{\varepsilon_t} \tag{2.9}$$

where I is a dimensionless triple integral describing the interaction of the local flow structure and the local transverse mixing, $\overline{v'^2}$ is the mean square value of the velocity deviation, L is the length scale over which the velocity deviation occurs and ε_t is the transverse mixing coefficient, as before. Fischer argued that the numerical value of I would not vary much between rivers, that a reasonable estimate of L was 0.7W and that data from simple laboratory and natural channels suggested that a reasonable estimate of $\overline{v'^2}$ would be $0.2V^2$. Finally, based on knowledge of transverse mixing in channels, he suggested that the transverse mixing coefficient could be expressed as:

$$\varepsilon_t = 0.6HV_* \tag{2.10}$$

where H is the mean depth of flow and V_* is the shear velocity. Hence, he obtained:

$$K = \frac{0.011V^2W^2}{HV_*} \tag{2.11}$$

Many more empirical (and semi-empirical) equations, which to a greater or lesser extent, reflect Fischer's original equation have been proposed, see e.g. Manson & Wallis (2004); Chin (2013). Earlier ones exploited correlations between dispersion coefficients and relevant variables or dimensionless groups (e.g. Liu, 1977; Seo and Cheong, 1998; Kashefipour and Falconer, 2002), whilst others had a more theoretical background and/or incorporated improved physics (e.g. Deng et al, 2001; Seo and Baek, 2002; Deng et al, 2002). In more recent years neural networks have become a popular tool for exploring relationships between dispersion coefficients and relevant parameters (e.g. Kashefipour et al, 2002; Rowinski et al, 2005; Piotrowski et al, 2011).

2.7 Dispersion coefficient values

Many workers have evaluated dispersion coefficients using a variety of methods over the last 50 years. Figure 2.1 shows such data from several sources, and indicates that dispersion coefficients between 0.1 and 1000 m^2/s have been observed over a flow

range of 0.1 to 10,000 m^3/s. The data is also shown in the table in Appendix A alongside hydraulic variables such as width and depth.

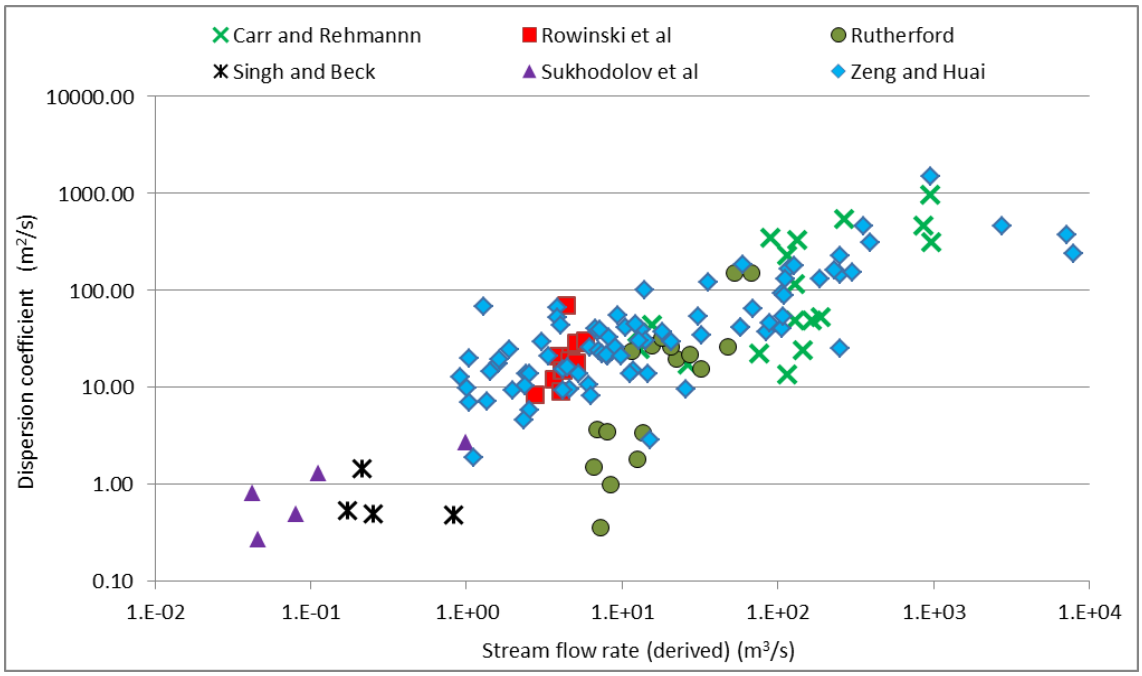

Figure 2.1 Variation of dispersion coefficient with flow rate: the legend indicates the data sources as shown in Appendix A.

Using flow rate as an indicator of a river's size, the figure illustrates an important trend namely that dispersion coefficients tend to increase with the size of the river. It is also noticeable that relatively few dispersion coefficients have been observed in small rivers (e.g. at flows less than $1m^3/s$).

Several workers (e.g. Rutherford, 1994) have tried to present dispersion coefficient data in non-dimensional forms, which has the advantage of allowing a more meaningful comparison of data obtained in different rivers and at different stream flow rates. This idea is discussed briefly in Chapter 5.

2.8 Small streams

The lack of dispersion data for small streams suggests that relatively few studies have been conducted into them. An interesting question is: what defines a small stream? Stream classification has had a long history, beginning with Davis (1899) who first divided rivers into three stages: youthful, mature and old age. Size order process was later defined by Strahler (1952) where streams are classified by size with 1 being the lowest and 12 being the highest: the Amazon River is a 12. A zero to first order stream

can begin as just a few centimetres wide as the initial run off from hill or mountain sides. When two first order streams join together they become a second order stream. First through third order streams are called headwater streams, these make up 80% of the world's waterways. Rosgen (1994) also devised a river classification system which is comprehensive as it covers a wider range of geomorphological parameters. The UK has no official stream size classification system in place but it is generally agreed that stream width is the best method of defining streams and rivers.

Although the major water pollution consequences are probably associated with the larger rivers, there are arguments supporting an interest in small streams. Firstly, small streams are at the top of the pyramid system that feeds into medium and large rivers that may feed into lochs, estuaries and seas. Clearly, any water quality issues in small streams are passed downstream. Secondly, it seems likely that small streams constitute a high proportion of the total stream and river length in many catchments (IBIS, 2012), so that when fully accounted for, they make up a far larger proportion of our natural water resources than we consider at the moment. Thirdly, small streams are not immune from being polluted. For example, in urban areas streams and burns sometimes pass through, or are very close to, housing and industrial estates and as such could be subject to a greater risk of intentional or accidental pollution incidents. Similarly in rural areas streams are subject to agricultural pollution both from pesticides and fertilisers applied to fields and from run-off from farms and storage facilities. Also streams draining forested catchments are always more acid than the streams draining non-forested catchments and have higher concentration of aluminium and manganese (Harriman and Morrison, 1982). Depending on catchment geology, stream pH may also be lowered by acid rain: rocks which are resistant to chemical weathering (e.g. granite) do not help to buffer the acidity while, for example, limestone and chalk do. (Edmunds and Kinniburgh, 1986). Fourthly, small watercourses are not generally monitored by environment agencies such as the Scottish Environment Protection Agency (SEPA) so that any pollution may go unreported and may not be recorded in any database.

Furthermore, in a report of a workshop looking into the importance of small streams in regard to salmon and trout spawning and nursery areas most of the key outcomes called for more focus on small streams (IBIS, 2012). It was also agreed that very small streams (<1.5m wide) were particularly vulnerable and that they constituted a high proportion of the total stream and river length in many catchments and in most cases

little data was available on them. The report states “the great majority of small streams fall outside the monitoring processes of the Water Framework Directive, although, since levels of diffuse pollution were proportional to length of river bank, ignoring small streams posed serious risks of downstream water bodies failing to meet WFD standards” and “the high ratio of bank length to water volume makes small streams more vulnerable to harmful effects from land use”.

2.9 Summary

This chapter has reviewed current knowledge on longitudinal dispersion in rivers. Following sections on physical processes and mathematical models, methods for estimating dispersion coefficients were introduced. A review of dispersion coefficient values showed a tendency for an increase with increasing river size, but relatively few values are available for small streams. The work in this thesis is designed to help close this particular gap of knowledge.

Chapter 3 Methodology

3.1 Introduction

This chapter describes the data analysis methods used in the research. The data was obtained from tracer experiments and, after initial pre-processing (see Chapter 4), two temporal concentration profiles were produced for each tracer experiment: one for an upstream site and one for a downstream site. Typically, each profile consisted of about 100 equally spaced concentration values. An example of the processed data is shown in Figure 3.1. Below are descriptions of the four methods used for estimating dispersion coefficients from the data. For each method at least one of the following supplementary pieces of information was required: reach length between upstream and downstream sites, mass of tracer released, stream flow rate and stream velocity. The first two were known from measurements, but the second two needed to be calculated (in one way or another) from the concentration profiles. The calculation of the stream velocity is covered separately within each dispersion coefficient method described below: the calculation of stream flow rate was common to all methods and is described in section 3.6. Finally, the way in which the effect of profile truncation was studied is described, and comments are given on data interpolation, which was necessary for a few of the concentration profiles.

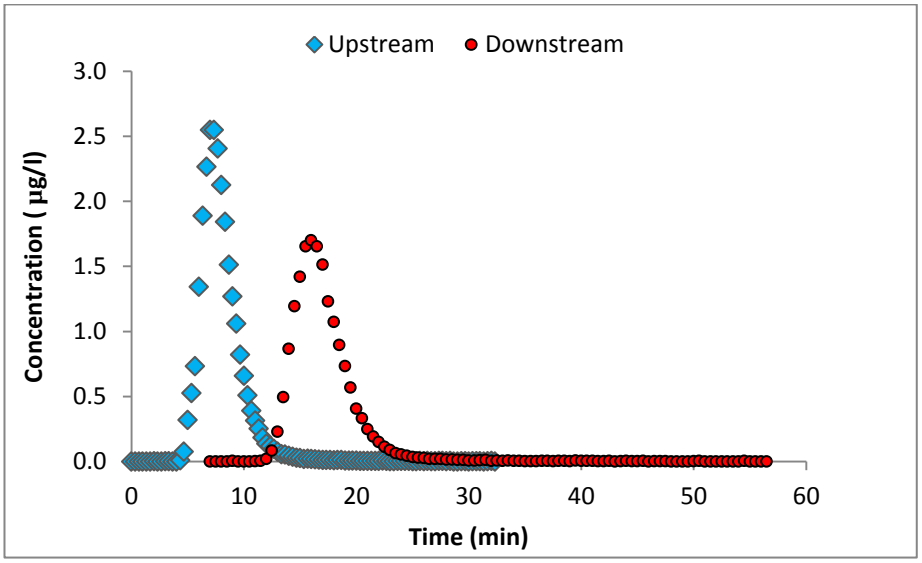

Figure 3.1: Example of the temporal concentration profiles.

3.2 Reduction of peak

3.2.1 Description

This method relates the dispersion coefficient of the reach to the reduction in peak concentration between the two sites, the timing of the peak concentrations, the flow rate of the stream and the cross-sectional area of the flow. The method is based on Taylor's (1954) theoretical analysis of solute transport. The method uses the following analytical solution of the ADE, which is valid for an instantaneous release of solute to a steady flow in a uniform channel.

$$C(x,t) = \frac{M}{(A\sqrt{4\pi Kt})} \exp\left[-\frac{(x-Vt)^2}{4Kt}\right] \tag{3.1}$$

Here: C is the solute concentration at location x at time t; M is the mass of solute released; A is the cross-sectional area of the flow; K is the dispersion coefficient; and V is the cross-sectional averaged stream velocity. According to this equation the peak concentration occurs when the exponential term has its maximum value, which is 1. Hence the peak concentrations at two locations x_1 and x_2 are given by:

$$C_p(x_1) = \frac{M}{A\sqrt{4\pi K t_p(x_1)}} \tag{3.2}$$

$$C_p(x_2) = \frac{M}{A\sqrt{4\pi K t_p(x_2)}} \tag{3.3}$$

where C_p is the peak concentration and t_p is the time of its occurrence. The reduction of peak method uses the observed peak concentration values plotted against the reciprocal of the square root of the observed peak time values, see Figure 3.2. It follows from equations 3.2 and 3.3 that the slope of the line, S, is given by:

$$S = \frac{M}{A\sqrt{4\pi K}} \tag{3.4}$$

Hence, the dispersion coefficient is given by:

$$K = \frac{1}{4\pi}\left(\frac{M}{SA}\right)^2 \tag{3.5}$$

M was known for each experiment, and *A* was estimated by dividing the stream flow rate with the stream velocity, with the latter being estimated using the method of moments (see section 3.3).

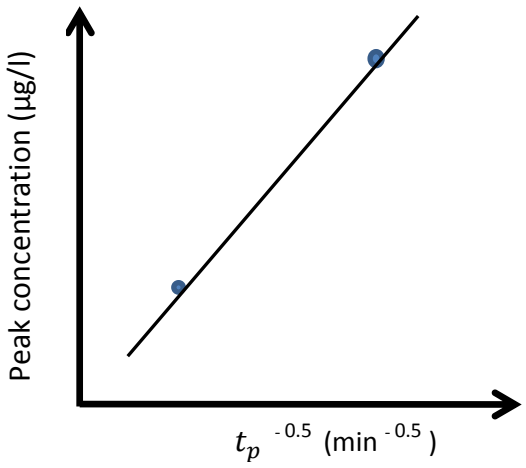

Figure 3.2: Reduction of Peak Method

3.2.2 Comments

Since the method is based on a solution of the ADE, it is only valid if the evolution of the tracer is in the equilibrium zone (see section 2.4.2).

There are two main sources of error: errors in the peak concentration values and errors in the calculation. Errors in the peak concentration values come from errors in the concentration values that make up the concentration profile and the possibility that the true peak concentration occurs between samples. Errors in the calculation come mainly from the estimation of the slope of the line from the plot and in the use of the cross-sectional area of flow, which is derived from the velocity of flow obtained using the method of moments.

3.3 Method of moments

3.3.1 Description

In this method developed by Fischer (1966) the centroid and variance of the temporal concentration profiles for both upstream and downstream sites are evaluated. The dispersion coefficient is evaluated from the changes of the variance and centroid between the two sites. The variance and centroid of a temporal concentration profile are evaluated from the moments of the profile (m_0, m_1, m_2), as defined in the following equations.

$$m_0 = \int_{-\infty}^{\infty} t^0 C(t) dt \tag{3.6}$$

$$m_1 = \int_{-\infty}^{\infty} t^1 C(t) dt \tag{3.7}$$

$$m_2 = \int_{-\infty}^{\infty} t^2 C(t) dt \tag{3.8}$$

In practice, because the profiles being analysed consist of a series of discrete values, the integrals are approximated by summations undertaken between the start and end of the profiles. Thus:

$$m_0 = \Delta t \sum_{i=1}^{N} t_i^0 C_i \tag{3.9}$$

$$m_1 = \Delta t \sum_{i=1}^{N} t_i^1 C_i \tag{3.10}$$

$$m_2 = \Delta t \sum_{i=1}^{N} t_i^2 C_i \tag{3.11}$$

where Δt is the sampling interval (or time step) in the data, C_i is the concentration of the ith sample, t_i is the time at which the ith sample was collected and N is the total number of samples in the profile. The centroid (μ) and variance (σ^2) of a profile are calculated from its moments using (Rutherford, 1994):

$$\mu = \frac{m_1}{m_0} \tag{3.12}$$

$$\sigma^2 = \frac{m_2}{m_0} - \mu^2 \tag{3.13}$$

Finally, the dispersion coefficient is evaluated using (Rutherford, 1994):

$$K = \frac{V^3}{2}\frac{(\sigma_2^2 - \sigma_1^2)}{(x_2 - x_1)} \tag{3.14}$$

where subscripts 1 and 2 refer to the upstream and downstream sites. Here, the cross-sectional averaged stream velocity, *V*, is calculated from the centroids of the profiles using:

$$V = \frac{x_2 - x_1}{\mu_2 - \mu_1} \tag{3.15}$$

3.3.2 Comments

The method is only valid if the evolution of the tracer is in the equilibrium zone (see section 2.4.2). There are two main sources of error: errors in the concentration values that make up the concentration profile and errors in the calculation. The latter include errors in the numerical evaluation of the moments (described below) and errors coming from only having two concentration profiles, one at each end of the experimental reach.

The experience of previous workers (e.g. Fischer, 1968; Yotsukura et al, 1970; Rutherford, 1994) suggests that the method suffers from problems caused by two features often observed on the tails of temporal concentration profiles. Firstly, the tails are frequently noisy and the noise can unduly influence the calculation of the variance, in particular. There are at least three sources of this noise. Firstly, small fluctuations in data values in the tails of concentration profiles are produced due to tracer being temporarily held up in slower moving parts of the stream, e.g. dead zones. Secondly, the background signal is noisy and when concentrations approach background levels, it is difficult to separate the background from the tracer concentration. Thirdly, any output readings produced by signal analysis equipment may itself be noisy at the highest sensitivities needed to detect the lowest concentration values.

The second feature to cause problems is the presence of elevated tails on the concentration profiles. These can be a true reflection of the transport characteristics of the stream, being created when there is significant contributions to dispersion from transient storage (see section 2.5). Alternatively, they may arise due to an increase in

the background signal during a tracer experiment, perhaps caused by a change in stream flow rate or a change in stream chemistry. Unfortunately, it is rarely possible to identify which of these may be the cause.

One of the consequences of these problems with the tail of a concentration profile is that it can make it difficult to identify the end of the profile. Yet, if the profile is allowed to extend beyond its true end the variance may be over-estimated because the end of the tail occurs a long time after the bulk of the profile. This happens because, in effect, this time difference is squared when the variance is calculated (see equations 3.8, 3.11 & 3.13). The consequences for the velocity and stream flow rate, which are calculated from lower moments (time difference raised to powers of 1 and 0, respectively) are less significant.

Fischer (1968) acknowledges the existence of low velocity pockets where tracer will be delayed adding to the long tails. These delayed particles do not follow the ADE therefore Fischer discounted the effect of the long tails stating that "the effect of the long tails should not be included in calculation of the moment from which a dispersion coefficient is to be derived", Fischer goes on to describe the method used, "variances were computed using a procedure resembling that of Elder. A point on the tail was chosen, entirely by eye, at which the integration was to be terminated; at this point the concentration value was generally about 5 percent of the peak".

Similarly Yotsukura et al (1970) state that "The main difficulty in evaluating dispersion by the method of moments is the large contribution to the variance from the tails of the concentration distributions. Even a small amount of tracer that is temporarily trapped in slow moving flow near the banks and is subsequently released to the main channel, where it shows up as a tail on the concentration distribution, can greatly inflate the value of dispersion".

3.4 Routing procedure

3.4.1 Description

This method, developed by Fischer (1968), compares an observed temporal concentration profile with a temporal concentration profile created by a series of calculations that simulate solute transport as described by the ADE. In this the observed temporal concentration profile at the upstream site is used as a boundary

condition and the routing procedure predicts the temporal concentration profile at the downstream site. The procedure is based on the idea that a solute cloud can be divided into a series of longitudinally consecutive parts, each of which evolves independently as it is carried downstream by the flow (Rutherford, 1994). The position and extent of the cloud at a later time can be calculated by re-combining the evolved parts using the principle of superposition, i.e. by summation. Using observed temporal concentration profiles, the procedure consists of the following six stages:

convert the upstream temporal profile to an initial spatial profile
divide the initial spatial profile into an equivalent series of solute releases
route each equivalent solute release downstream using equation 3.1
sum all the routed solute releases to create the final spatial profile
convert the final spatial profile to a predicted downstream temporal profile
compare the predicted and observed downstream profiles

The two conversions in stages 1 and 5 are made by applying the "frozen cloud" assumption (Fischer et al, 1979; Rutherford, 1994). In this, during the time it takes for a solute cloud to pass a fixed point, it is assumed that no dispersion takes place, i.e. the corresponding spatial concentration profile does not change shape. In practice, this means that a spatial profile and its equivalent temporal profile are defined by the same concentration values, but the order of the values is reversed. Using sampled data, all the required calculations can be combined into the following algorithm (Fischer, 1968; Fischer et al, 1979; Rutherford, 1994):

$$C(x_2,t) = \sum_{i=1}^{N} \frac{C(x_1,i)V\Delta\tau}{\sqrt{4\pi K(\mu_2-\mu_1)}} exp\left[-\frac{V^2(\mu_2-\mu_1-t+i\Delta\tau)^2}{4K(\mu_2-\mu_1)}\right] \quad (3.16)$$

where $C(x_2,t)$ is the predicted downstream concentration at time t, $C(x_1,i)$ is the concentration of the ith sample at the upstream site, $\Delta\tau$ is the sampling interval of the upstream profile and all other symbols are as previously defined. Unfortunately, μ_2 is not known until the downstream profile has been calculated. However, the term $\mu_2 - \mu_1$ can be evaluated by re-arranging equation 3.15 to give:

$$\mu_2 - \mu_1 = \frac{x_2 - x_1}{V} \quad (3.17)$$

which, on substitution into equation 3.16, introduces some additional dependency on V.

Clearly, the difference between the predicted and observed profiles at the downstream site depends on the values of *K* and *V* used in the calculations. By adjusting the values of these parameters the difference can be changed, and optimum parameter values are found when the difference is minimised. Since the data analysis was undertaken using MS Excel, an add-in called Solver was used to achieve the optimisation. This worked by automatically adjusting the values of dispersion and velocity such that the total squared error between observed and simulated concentration profiles was minimised. Figure 3.3 shows an example of an optimised profile together with the corresponding observed profiles.

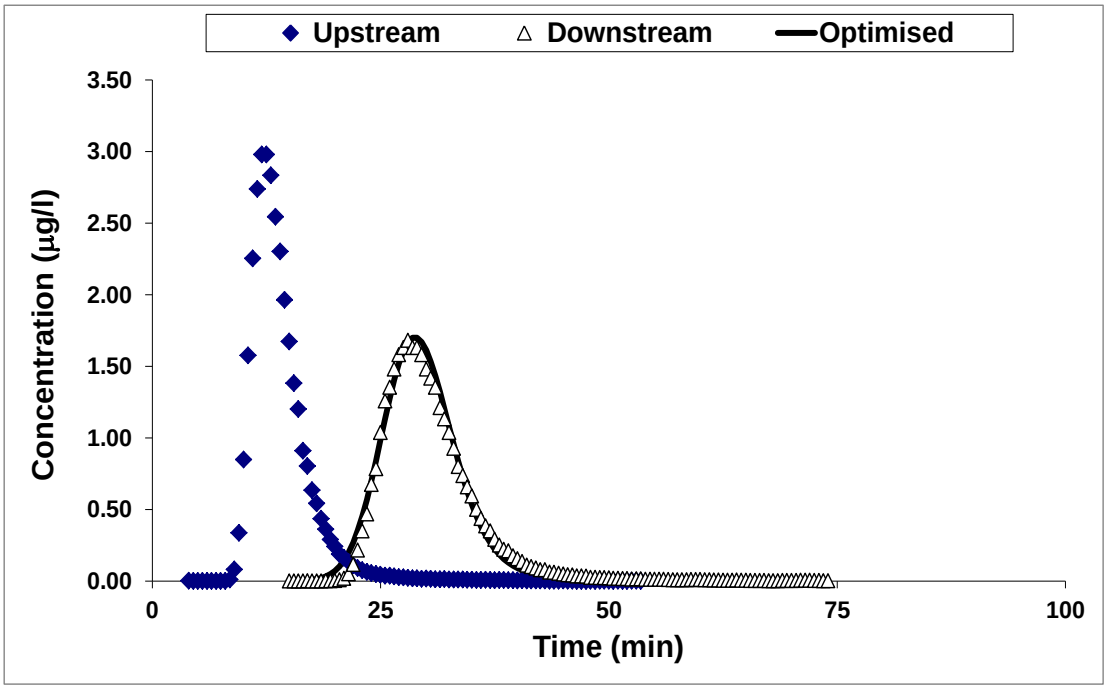

Figure 3.3: Example of the Routing Procedure output.

3.4.2 Comments

Since the method is based on a solution of the ADE, it is only valid if the evolution of the tracer is in the equilibrium zone (see section 2.4.2). There are three potential sources of error: errors in the concentration values that make up the concentration profile, errors induced by the frozen cloud assumption and errors in the calculation. The latter are mainly concerned with minimising the squared error between the observed and simulated profiles.

A convenient feature of the method is that the time step in the observed upstream and downstream profiles need not be the same. However, the time step in both profiles

needs to be constant, so that if observations are not taken at a fixed sampling interval, the data needs to be interpolated to a constant time step.

3.5 Analytical solution

3.5.1 Description

This method compares an observed temporal concentration profile with a temporal concentration profile predicted by an analytical solution of the ADE, see e.g. Ani et al (2009). The analytical solution is the same one used in the Reduction of Peak and Routing Procedure methods, i.e. equation 3.1. The cross-sectional area of flow was calculated by dividing the stream flow rate with the stream velocity which introduced an additional dependency on V. Similarly to the Routing Procedure, the difference between the two profiles depends on the values of stream velocity and dispersion coefficient used in the calculations. So, optimised values of velocity and dispersion were obtained in the same way as described in section 3.4. Figure 3.4 shows an example of an optimised analytical solution profile together with the corresponding observed profile at the downstream site.

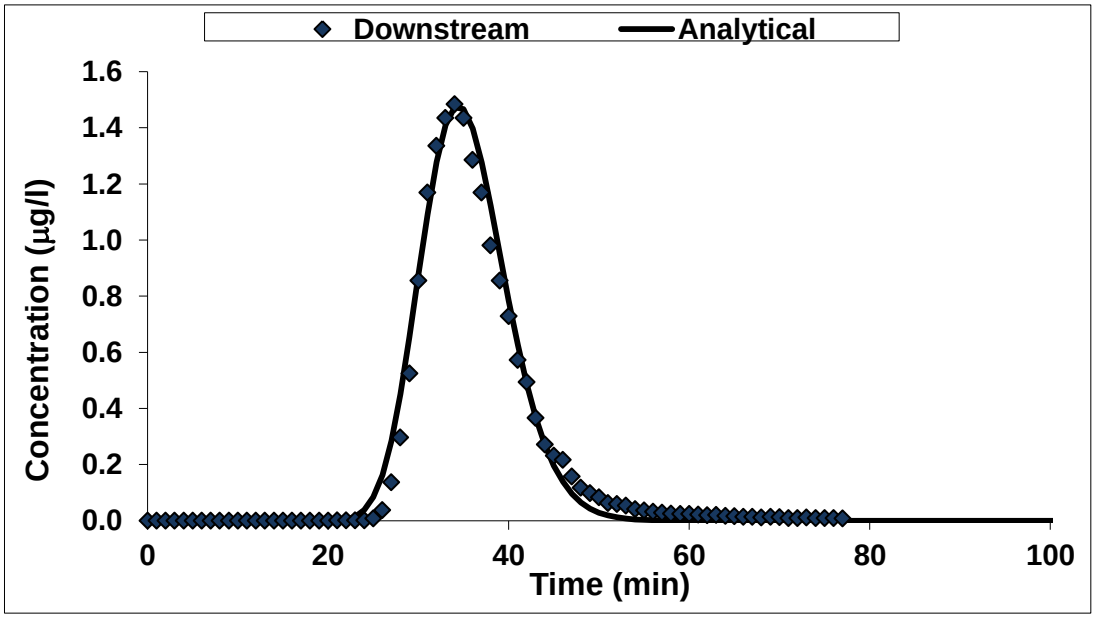

Figure 3.4 Example of the Analytical Solution output.

3.5.2 Comments

Since the method is based on a solution of the ADE, it is only valid if the evolution of the tracer is in the equilibrium zone (see section 2.4.2). There are three main sources

of error: errors in the concentration values that make up the concentration profile, errors induced by the advective zone and errors in the calculation. Similar to the Routing Procedure, the latter are mainly optimisation errors.

The main caveat on the method concerns the equilibrium zone because it assumes that this zone begins at the point of tracer release, whereas the initial transport of the tracer takes place in the advective zone (see section 2.4.1). The method was used to estimate the dispersion coefficient in the reach between the tracer release location and Site 3 and also in the reach between the tracer release location and Site 4. Neither of these is the same as the study reach (Site 3 – Site 4). Only the latter use of the method includes the study reach, so these results are more comparable with the results from the other three methods. In order to obtain a more directly comparable estimate of the dispersion coefficient for the study reach a weighted average approach was considered. This is described in section 5.3.

3.6 Stream flow rate

For each pair of temporal concentration profiles the stream flow rate was calculated using dilution gauging (Herschy, 1995). The method is based on the conservation of mass of a released tracer that has become well mixed in the flow. It relates the stream flow rate to the mass of tracer released and the area under an observed temporal concentration profile. Thus:

$$Q = \frac{M}{\int_{t_1}^{t_2} C(t)dt} \tag{3.18}$$

where Q is the stream flow rate, M is the mass of tracer, $C(t)$ is tracer concentration, t_1 is the start time of the concentration profile and t_2 is the finish time of the concentration profile. The denominator in the right-hand side of equation (3.18) represents the area under the profile, which was calculated using the trapezium rule, i.e.:

$$Area\ under\ the\ curve = \frac{\Delta t}{2}\sum_{i=1}^{N-1}(C_i + C_{i+1}) \tag{3.19}$$

where the symbols are the same as those defined in section 3.3.

There are two main sources of error: errors in the concentration values that make up the concentration profile and errors in the evaluation of the area under the profile.

3.7 Truncation of data

One of the aims of this research project was to discover the effect of truncating the tail (or trailing edge) of the observed temporal concentration profiles on the values of dispersion coefficient (and stream velocity) derived from the four methods described above. The main reason for investigating this is that the data in the tails is difficult to observe reliably because the data is often noisy and the tail may be elevated (see section 3.3.2). Also, previous work has shown that the method of moments can be disrupted by these issues but it is not known to what degree the other methods are affected by it. Hence by evaluating dispersion coefficients using both the original and the truncated data this issue could be clarified.

Yotsukura, Fischer and Sayre (1970) recognised a difficulty with the method of moments. Anticipating the problems of the "large contribution to the variance by the tails of the concentration distributions" they carried out truncation of the concentration data (when concentrations on the recession limbs of the curves reached 3 percent and 1 percent of the peak concentration) to resolve the problem. Although they didn't compare results with non-truncated data the 3 percent truncation produced lower variances than the 1 percent truncation and the truncated method of moments produced results that compared reasonably well with the routing procedure that was also used.

Truncated data was created by applying a truncation value of one percent of the peak concentration value to all concentration profiles. The truncation process produced slightly negative values at the beginning and ends of the concentration profiles: these values were set to zero and the concentration values that remained positive were identified as the truncated data. (further details in section 4.6)

An example of a standard (i.e. non-truncated) profile and the corresponding truncated profile are shown in Figures 3.5 and 3.6.

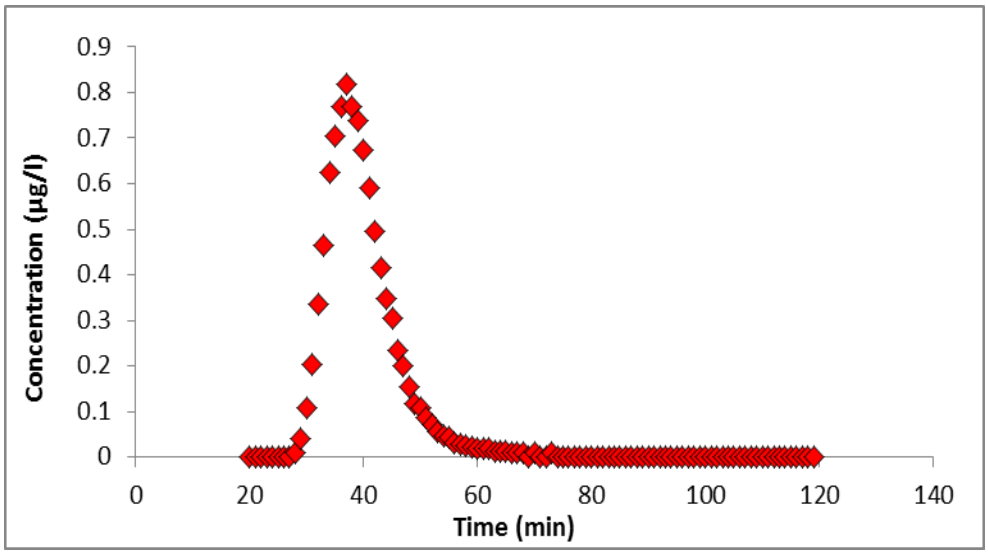

Figure 3.5 Example of a standard temporal concentration profile.

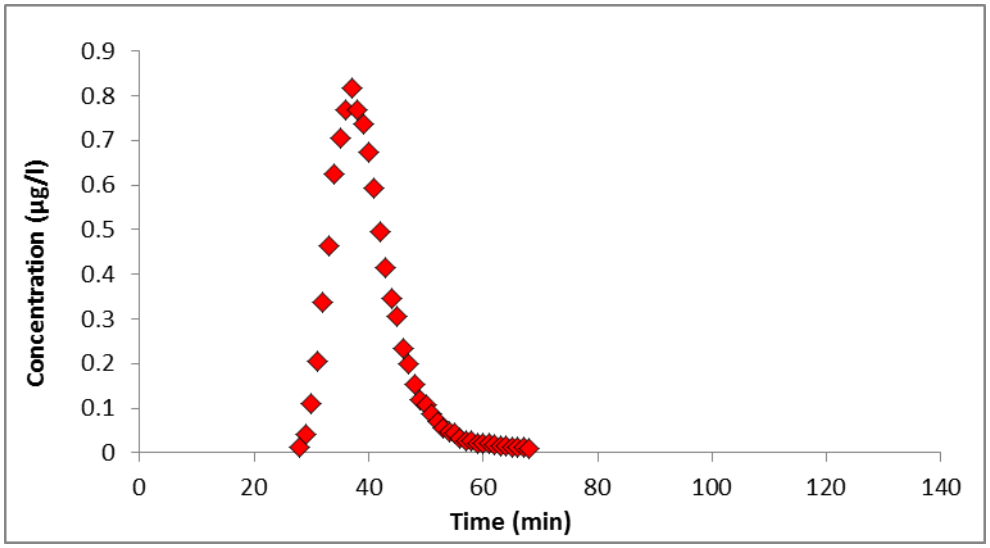

Figure 3.6 Example of a truncated temporal concentration profile.

3.8 Data interpolation

Short sampling intervals give a better defined temporal concentration profile but low flows require much longer sampling times. Once the peak has passed and it is estimated that only the tail is being sampled we do not require such high definition so the sampling interval can be increased in order to get as much of the tail as possible, this method is also useful if one has limited sampling equipment. Data interpolation

had to be carried out on experiments 9, 10 and 11 (lower flows): for example, increasing the time step from one minute to two minutes after about 80 minutes to extend the sampling time until a return to background levels had been estimated. After initial data analysis linear data interpolation was carried out from the point where the sampling time step would increase on the gathered concentration data, the procedure assumes the change between the two concentration values being interpolated is linear.

3.9 Summary

This chapter has described the four analysis methods used later to estimate dispersion coefficients from temporal solute concentration profiles observed at two locations downstream of a tracer release site. Advantages and disadvantages of the methods were discussed, leading to the introduction of two issues that are followed up later. Firstly, the effect of truncating the concentration profiles on the estimated dispersion coefficients. Whereas this is likely to improve the reliability of the Method of Moments, it is not clear what the effect is on the other methods (Peak Reduction, Routing Procedure and Analytical Solution). Secondly, a new weighted average approach for the Analytical Solution was devised to overcome the disadvantage that the method applies between the tracer release site and each observation location rather than between the two observation locations.

Chapter 4 Experimental work and data processing

4.1 Introduction

The experimental work was undertaken on a small stream called the Murray Burn, which flows through the Riccarton campus of Heriot-Watt University in Edinburgh. The work was built on a previous study undertaken several years ago (Burke, 2002) which looked at travel times of tracers: no dispersion coefficients were estimated by Burke. It was considered necessary for the new experiments to gather data from a wide range of flows in order to evaluate the dispersion coefficient over various flow conditions. It was decided to run tracer experiments on one of the reaches used by Burke (2002) extending between his Site 3 and Site 4. This reach is approximately uniform, and the basic reach characteristics reported by Burke (2002) are: length 184m, mean width 2.4m and mean slope 0.009. A map of the study site is shown in Figure 4.1.

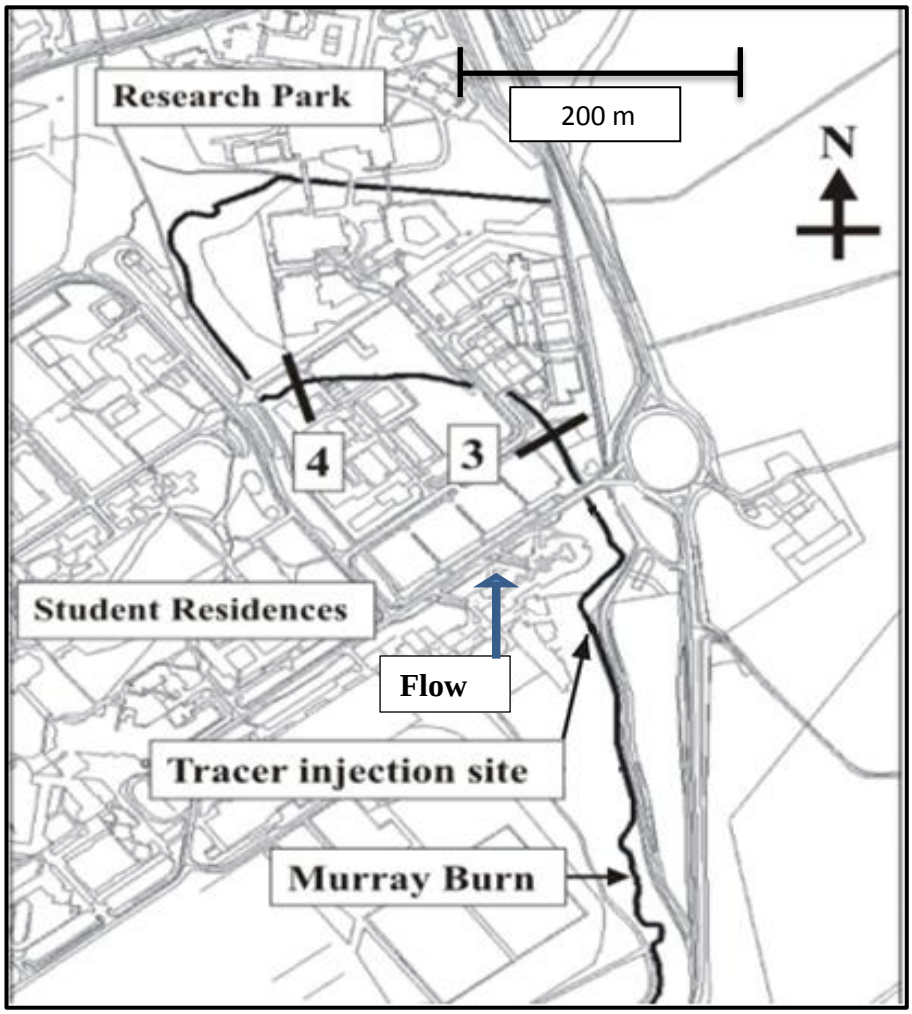

Figure 4.1 Map of study site. (main injection site shown)

Each experiment consisted of the sudden release of a known mass of tracer at one of two injection sites followed by the collection of water samples for later analysis at sites 3 and 4. The main injection site was 236m upstream of Site 3 and a secondary injection site was a further 64m upstream, above a waterfall. Permission was sought and obtained from the Scottish Environment Protection Agency (SEPA) to carry out the experiments, and Heriot-Watt University Health and Safety procedures were followed, e.g. at least two people were present at any site in the field when tasks were being undertaken. All activity at the three locations was undertaken to a common time base using synchronised stop watches.

Burke (2002) notes that when measuring conductivity (using salt as a tracer) in the Murray Burn that the background concentration would rarely return to the initial background level. This suggested that background levels of conductivity due to dissolved or suspended material may naturally fluctuate rather than be stable. Since such behaviour can affect the observation of the tail of a tracer concentration profile, an emphasis was placed on collecting water samples for long enough to ensure that all the tracer had passed the sampling sites.

The tracer used in the experiments was Rhodamine WT, which is a soluble, non-toxic, fluorescent dye. It has a good reputation in tracer hydrology having been used in a range of laboratory and field studies over many years (e.g. Wallis et al, 1989; Boxall et al, 2003). Two particular advantages are that it behaves conservatively (not undergoing physical, chemical or biological changes) over the time it is in the study reach (Smart & Laidlaw, 1977) and it can be measured to very low concentrations, which means that only very small amounts need to be used.

The following sections describe various details of the experimental work undertaken in the field and the laboratory followed by the data processing applied to create concentration profiles from the raw data.

4.2 Preparation of Rhodamine WT standards

In order to calibrate the fluorometer that was used to analyse the water samples collected in the experiments a series of standard Rhodamine WT solutions was required. These standards were prepared in the environmental chemistry laboratory of the School of Life Sciences at Heriot-Watt University, and all health and safety

procedures were followed as required. The concentration range of the standards was 0 – 5 μg/l.

The equipment used consisted of calibrated electronic balances (Chyyo electronic balance JP-3000w model), automatic pipettors with disposable tips (Finnpipette 1-5 ml; Thermo Electron micro pipette 200-1000 μl) and a range of glassware. All glassware was thoroughly cleaned and dried to ensure no false readings occurred by contamination or by extra weight from water on surfaces.

Firstly a 1 g/l Rhodamine WT stock solution was made by taking 5 g of manufactured Rhodamine WT 20% solution and then making it up to 1 litre with distilled water. Secondly, 2 ml of this 1 g/l solution was dissolved in 2 l of distilled water to create a 1 mg/l Rhodamine stock solution. Several high concentration standards were made from this 1 mg/l Rhodamine WT stock solution using the technique described below.

A new, clean standards bottle was placed on the electronic balance which was then zeroed. Then some 1 g/l Rhodamine WT solution was drawn by automatic pipettor to the volume needed and carefully dispensed to the beaker on the balance. A secondary check was made using the electronic balance reading (1 gramme weight being equivalent to 1 ml volume, assuming a density of 1000 g/l). Next the required volume of distilled water was added first by using graduated measuring cylinders until close enough to use the automatic pipettor to get the exact amount and finally for the last few drops using the automatic micro pipettor (again checked using the electronic balance). The glass standard bottle was then labelled with the concentration, volume and date. Pipettor tips were changed for each media change (i.e. adding Rhodamine WT solution or topping up the required amount of distilled water), and the same pipettors were used every time for consistency of results. All glassware was washed and thoroughly rinsed in distilled water, and the standard was stored in a covered cardboard box to prevent sunlight causing any photochemical decay during storage. Large volumes of standards were prepared because the sample used to calibrate the fluorometer was disposed of after use rather than being put back into the standard bottle and risk possible contamination.

Mid-range and low concentration standards were made in the same way, except that a lower concentration solution was used as the stock solution. Tables 4.1 and 4.2 show the range of standards made from each stock solution and examples of the volumes

used to make the standards. Appendix F shows the full serial dilution table for all standards.

Stock concentration	Standards made
1 mg/l	1-9 μg /l
1 μg /l	0.1-0.9 μg /l
0.1 μg /l	0.01-0.09 μg /l

Table 4.1: Summary of stock solutions used

Stock concentration	Volume (ml)	Standard concentration
1 mg /l	1.5 of 1 mg /l in 500 ml	3 μg /l
1 μg/l	150 of 1 μg/l in 500 ml	0.3 μg/l
0.1 μg/l	150 of 0.1 μg/l in 500 ml	0.03 μg /l

Table 4.2 Examples of dilutions

4.3 Tracer Experiments

4.3.1 Introduction

Thirteen tracer experiments were carried out over a period of fifteen months. For each one the mass of tracer released was based on an estimate of the flow rate in the stream, previous experience and a maximum concentration at the upper sampling location (Site 3). The stream flow rate estimate came from reading a stage board at the lower sampling location (Site 4) a few hours before the experiment was due to take place and the maximum concentration (2.5 μg/l) was set by SEPA.

A summary of the experiments is given in Table 4.3 from which it can be seen that the mass of tracer used ranged between 50 and 300 mg for stream flow rates between about 13 and 450 l/s, respectively. The flow rates shown were evaluated using dilution gauging (see section 3.6). The first two experiments were not successful in providing complete and well-resolved tracer concentration profiles, so they were not used in the subsequent analysis.

The tracer mass for release was made up from the 1 mg/l stock solution of Rhodamine WT from which the standards had been prepared. This was weighed into a cleaned and labelled glass bottle that was to be used for the tracer release.

Exp ID	Date	Tracer mass released (mg)	Flow rate at Site 4 (l/s)
Expt. 3	04/11/2009	100	147
Expt. 4	11/11/2009	50	84
Expt. 5	18/11/2009	100	97
Expt. 6	26/11/2009	200	385
Expt. 7	18/11/2009	100	41
Expt. 8	27/05/2010	75	44
Expt. 9	17/06/2010	50	37
Expt. 10	08/07/2010	50	17
Expt. 11	03/11/2010	150	150
Expt. 12	08/02/2011	300	436
Expt. 13	15/02/2011	150	148

Table 4.3 Summary data of the experiments

4.3.2 Tracer release

The main tracer release location was a few metres downstream from a waterfall of about 2m height: this area naturally had a lot of turbulence across the full width of the stream, which encouraged mixing. As far as possible the tracer release was carried out at the same point in the centre of the stream each time. However, at some of the higher stream flow rates the tracer release occurred closer to the bank, on the grounds of safety. The secondary tracer release location was used for experiments 12 and 13: this location was more easily accessible than the main release site and provided a longer distance for the tracer to become well mixed.

To release the tracer a bucket was dipped in the river collecting about 2 l of water, and the tracer was poured into it from its storage bottle. The bottle and cap were thoroughly rinsed into the bucket with another bucket containing stream water. At the

pre-arranged time for release (identified from a synchronised stop watch) the bucket of tracer was quickly poured into the stream and the bucket was quickly and repeatedly washed out with the stream water.

Although the majority of the data analysis was not expected to be significantly affected by small variations in the location and speed of tracer release, as far as was possible the tracer was released in the same way for each experiment. The most difficult aspect to replicate was rinsing the final traces of Rhodamine WT from the bucket. Indeed, the rinsing process meant that the final traces may have been released up to 10 seconds after the initial pouring, which may have extended the length of the tails on the profiles.

4.3.3 Collection of water samples

100ml glass medical flats were used for stream water sample collection. These were clean, numbered and had a site ID. Typically 100 sample bottles were available at each sampling site and the sampling interval was decided beforehand, based on the stream flow rate and the experience of earlier experiments. Ideally, the chosen sampling interval would lead to the observation of a complete and well-resolved tracer concentration profile, consisting of about 10 samples before the arrival of the tracer (used to estimate the background concentration) and sufficient samples to observe the whole tail of the profile. As far as possible water samples were taken from the same location point in the stream each time.

Water samples were collected from the stream bank using a long wooden pole with a quick- release sample bottle retainer. Firstly, an uncapped sample bottle was clipped to the pole, then at the appropriate time (identified using a synchronised stopwatch) the sample was taken by submerging the sample bottle in the stream, and finally the sample bottle was unclipped, capped and stored.

Typically, sampling began at Site 3 about 10 minutes after tracer release and at Site 4 about 20 minutes later, but this varied according to the stream flow rate. Since the same number of sample bottles was available at both sampling locations, but the durations of the upstream and downstream concentration profiles were different, a larger sampling interval was sometimes used at the downstream sampling location. In most of the experiments the sampling interval at a site was constant, but in three of the

experiments (9, 10 & 11) the sampling interval was increased towards the end of the experiment to ensure that the whole tail was observed.

Several errors were inevitably present in the sampling. For example the time taken to fill the sample bottle was not always the same and mistakes occurred particularly when operating at a high sampling frequency. With two people working together, 20 seconds was the smallest sampling interval that was possible. If a bottle was dropped, however, there was no time to recover the situation at such a short sampling interval, so the occasional sample was missed. Other minor fumblings (e.g. selecting the wrong bottle) occasionally led to a sample being mis-timed by a few seconds. Although notes were kept of such accidents, they couldn't be recorded until the end of the sampling, if the sampling rate were high, so there was scope for errors in the recording of such incidents. For a few of the profiles, the design of the sampling start time wasn't accurate leading to either a few background samples being collected or even missing the start of the rise in concentration.

4.4 Operation of the Turner Designs Fluorometer

4.4.1 Introduction

A Turner Designs model 10 Fluorometer was used to carry out the fluorescence analysis of the water samples, see Figure 4.2. The fluorescent nature of Rhodamine WT means that its molecules fluoresce when excited by light of a particular wavelength, i.e. the exitation light is almost instantly emitted at a longer wavelength. For use with Rhodamine WT the Turner Designs fluorometer is configured to shine green light on the sample and to detect the red light emitted. The amount of red light emitted is directly proportional to the concentration of the dye in the sample, up to about 100 parts per billion (100 μg/l). The use of the fluorometer's controls is described below, where necessary. The most important feature of the fluorometer is its four sensitivity ranges. The lowest concentrations are measured on the highest sensitivity range (named x31.6) and the highest concentrations are measured on the lowest sensitivity range (named minimum sensitivity or MS). Two intermediate ranges (x10 and x3.16) are also available. This allows a large range of concentrations to be measured, whilst enabling analogue panel meter readings in the lower third of the scale to be avoided. For example, instead of a reading being around 2 on the x3.16

sensitivity range, it can be more accurately read by changing to the x10 sensitivity range where the reading will be around 6.3.

Figure 4.2 Turner Designs model 10 Fluorometer

4.4.2 Use and initial set-up

The fluorometer was turned on at least an hour before being used: this allowed the flourometer's lamp to be in a steady state, ready for use, and for the instrument's electronic circuits to warm up to normal operating temperature. The fluorometer was calibrated using a set of Rhodamine WT standards (see section 4.2) before a set of water samples was analysed, and the calibration was checked at the end. In order to ensure high quality sample analysis the temperature of the sample and the standards should be the same. Therefore, the samples and standards were stored overnight in the temperature controlled room in which the analysis took place. During the analysis a few temperature readings were taken to check that the laboratory temperature was stable during the analysis.

Initial set-up of the fluorometer involved adjusting it so that it was operating in the range of concentrations expected in the samples. This was estimated to be 0 – 5 μg/l. Following the instruction manual, a 5 μg/l standard and distilled water blanks were used to adjust the instrument's sensitivity such that full scale deflection (a reading close to 10) on the minimum sensitivity range was achieved for the 5 μg/l standard.

4.4.3 Calibration and analysis of samples

Calibration of the fluorometer consisted of recording the reading for each of the standard solutions, doing them in order of increasing concentration. Firstly, the maximum sensitivity range was selected. Then an amount of the standard was poured into a boiling tube, washed around and then disposed of. Next a larger amount of the same standard was put into the tube, which was inserted in the sample holder and the light shield put in place. Then the reading was taken and recorded: if feasible, other sensitivity ranges were selected and readings recorded. After the readings had been recorded the sample was disposed of and the process repeated for the remaining standards. The washing around was to ensure no contamination from the previous standard.

There was a delay of several seconds after placing the light shield or changing the sensitivity range before the output displayed on the panel meter settled down. So it was important to wait until a steady reading was displayed. However, the signal was noisy (particularly on the higher sensitivity ranges) so it was sometimes difficult to judge when it had become steady. To help overcome this difficulty the output signal was logged and displayed graphically on a laptop computer. From this it was much easier to consistently judge when to take the reading.

Another issue to be aware of was that if a standard were left in the instrument for too long it would warm up and the reading would reduce as Rhodamine WT has a temperature coefficient of -2.6% / degrees C; therefore the concentration reading will reduce2.6% for every degree C rise in temperature. Although it is unlikely that a standard would be in the instrument for long enough for this effect to be significant, the use of the laptop display of the instrument's reading helped to adopt a standard procedure in which all standards spent approximately the same length of time in the instrument before a reading was made.

The same procedure was used when analysing the water samples, except that a reading was only recorded for one of the sensitivity ranges – the one which gave the largest panel meter deflection.

4.4.4 Estimation of calibration factor

For each batch of analysed water samples a calibration factor was derived from the analysis of the calibration standards. Since, for the range of concentrations encountered in the experiments, there was a linear response of the fluorometer to increasing Rhodamine WT concentrations a graph of Rhodamine WT concentration against fluorometer output gave a straight line. The slope of this line was used to obtain the calibration factor that was used to calculate the Rhodamine WT concentration in the water samples. The first stage in this was to convert all the fluorometer readings for the standards to the MS range by dividing the reading by the range multiplier (31.6 for the x31.6 range; 10 for the x10 range; 3.16 for the x3.16 range; 1 for the MS range). An example of this process is given in Table 4.4 and the corresponding calibration graph is shown in Figure 4.3.

Clearly the response is linear. The slope of the response was evaluated by fitting a linear trend, giving for this example a calibration factor of 0.5099 with a coefficient of determination of 0.9996. It was found that the calibration factor varied over the duration of the research, but the response was always linear with very high coefficients of determination.

Calibration Standard (μg/l)	Sensitivity Range	Fluorometer Reading	Equivalent MS Reading
0.02	x31.6	1.2	0.0379
0.04	x31.6	1.2	0.0379
0.06	x31.6	2.1	0.0664
0.08	x31.6	3.4	0.1075
0.1	x31.6	4.5	0.1423
0.08	x10	1.1	0.1100
0.1	x10	1.4	0.1400
0.2	x10	3.6	0.3600
0.4	x10	8.9	0.8900
0.2	x3.16	1.1	0.3479
0.4	x3.16	2.8	0.8854
0.6	x3.16	3.7	1.1700
0.8	x3.16	5.3	1.6760
1	x3.16	6.3	1.9922
0.6	MS	1.1	1.1000
0.8	MS	1.6	1.6000
1	MS	2.0	2.0000
2	MS	3.9	3.9000
3	MS	5.9	5.9000
4	MS	7.8	7.8000
5	MS	9.8	9.8000

Table 4.4 Example of readings for calibration standards and conversion to MS range.

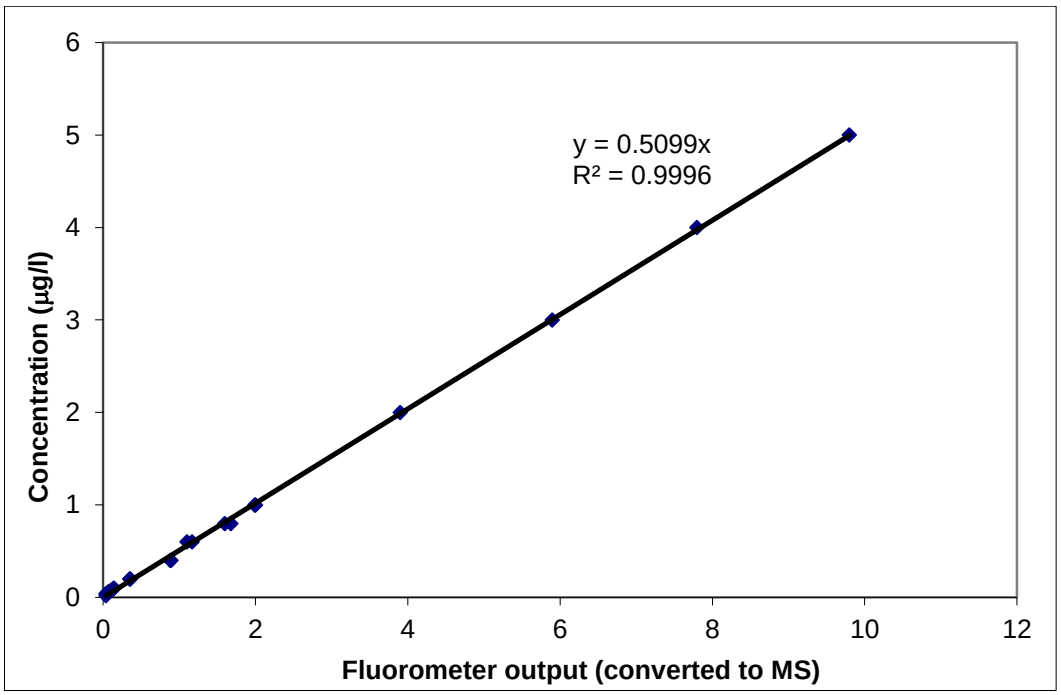

Figure 4.3: Example of fluorometer calibration graph.

The method of converting all readings for the standards to the MS sensitivity range relies on the four sensitivity ranges being accurately aligned with each other. This can be examined by comparing the converted readings of the standards taken on different sensitivity ranges. For example, in Table 4.4 the 0.1 µg/l standard has converted readings of 0.1423 and 0.1400, corresponding to readings taken on the x31.6 and x10 sensitivity ranges, respectively. Looking at several similar examples in the table suggests that, overall, the method was justified. Alternatively, each sensitivity range could be calibrated independently, but this would require a greater number of standards being made up in order to have 4 or 5 calibration points for each sensitivity range.

4.5 Identification of background signal

A stream's background fluoresence signal is caused by naturally occurring material. Baker (2002) suggests this natural fluorescence can be produced by bacteria or come from local in situ minerals, rural pollution or dissolved organic matter. In the absence of any Rhodamine WT, stream water gives a very small reading when analysed in the fluorometer. This signal needs to be removed from the fluorescence outputs of all the water samples. However, the signal tends to fluctuate due to natural variations in the stream chemistry. Therefore several (nominally 10) water samples were collected at each sampling site before the tracer arrived, and the average fluorometer reading from these samples was used as the background signal. Care was taken not to include a

sample that might have been the start of the rise of the concentration due to the arrival of the tracer. Although the average (over both sites and all experiments) number of samples available for background evaluation was about 7, occasionally the design of a tracer experiment failed to capture any water samples before the arrival of the tracer. In such cases samples from the end of the experiment were used to estimate the background signal (provided it was clear that all the tracer had passed the sampling location). If appropriate, a combination of samples from the start and the end of the experiment were used.

4.6 Removal of background signal and application of calibration factor

Temporal concentration profiles were created from the fluorometer readings of the water samples in the following way. Firstly, all water sample fluorometer readings were converted to the MS range by dividing by the range multiplier. Then the estimated background signal (estimated from the beginning of a consistent rise in values) (also converted to the MS range) was subtracted from the converted readings. Next, these net values were multiplied by the calibration factor to give concentrations. Finally, all concentrations before the start of the profile (identified by the steep rise of concentration) were set to zero.

4.7 Missing data

If a planned water sample had not been collected the missing concentration value was estimated by linear interpolation of the observed concentrations from the previous and following samples.

4.8 Data scaling

In the absence of any lateral inflows to the study reach, the small duration of travel time in regard to dye adsorption and assuming complete mixing of the tracer was achieved upstream of Site 3, the areas under the upstream and downstream concentration profiles should be the same for a conservative tracer. However, the study reach does receive lateral inflows (see section 5.2), so that the downstream concentrations are lower than they would be if the extra dilution from the lateral inflows were absent. To correct for this the concentrations at the upstream site were linearly scaled by the ratio of the areas under the two profiles.

4.9 Data interpolation

The majority of the concentration profiles contained equally spaced data, but in a few of the longer profiles the time step was increased towards the end of the profile in order to capture the whole profile. Whereas this had no effect on the Reduction of Peak method, some minor adjustments were made for the other three dispersion coefficient calculations. For the Routing Procedure and the Analytical Solution the more coarsely sampled data was linearly interpolated to the finer sampling interval used earlier in the profile. For the Method of Moments, the calculation was split into two parts: one for the finer sampled portion and the other for the coarser sampled portion. The contribution to the moments from each part were calculated separately and then added.

4.10 Summary

This chapter has described the design and execution of the tracer experiments undertaken to provide the data used in the estimation of dispersion coefficients. Procedures in the field and laboratory were covered, including, for example, the collection of water samples and the operation of the sample analysis equipment. Aspects of the initial data processing that was undertaken were explained, for example the removal of the background signal and data scaling.

Chapter 5 Results and Discussion

5.1 Introduction

This chapter presents the results of the analysis of the temporal concentration profiles. Firstly, the stream flow rates are considered, followed by the velocities and the dispersion coefficients from the four methods described in Chapter 3 using standard and truncated data. The chapter finishes with a discussion based around a comparison of the four sets of dispersion coefficients, the effect of truncating the concentration profiles and how the results compare with published data from other small streams. Profiles of all experiments are shown in Appendix B.

5.2 Stream flow rate

For each experiment the stream flow rate was calculated for both sampling locations using dilution gauging (see section 3.6). The results are presented in Table 5.1.

Tracer experiment	3	4	5	6	7	8	9	10	11	12	13
Site 3 (l/s)	135	83	93	371	38	40	33	14	145	431	143
Site 4 (l/s)	147	84	97	385	41	44	37	17	150	436	148

Table 5.1: Stream flow rates for each site for all experiments

Stream flow rate appears to be a little larger at the downstream site (Site 4) than at the upstream site (Site 3) in all the experiments. The average increase across all the experiments is 7.3%. The most likely explanation for this increase is drainage from the surrounding land, which was observed to occur through several pipes and small channels in the study reach, see Figure 5.1. In general these inflows varied between the experiments, and some of them were zero during low flow periods. However, the small channel marked by the left-hand arrow in Fig 5.1 appeared to be running all the time, but not necessarily at the same rate.

Figure 5.1 Examples of sources of land drainage upstream of Site 4 (looking downstream): arrows show location of pipes and small channels.

Another possible reason for the increase in stream flow rate is that some tracer has been lost in the study reach. If this happens the area under the downstream concentration profile will be smaller than the area under the upstream profile, creating the impression that the flow rate has increased. However, Rhodamine WT has a reputation for behaving conservatively over the short residence times of the tracer in the study reach in these experiments, so it seems unlikely that tracer loss, due to e.g. photo-chemical decay or adsorption on to sediments, is a major factor.

For the purposes of quantifying the stream flow rate for each experiment, the flow at Site 4 was used. Unless stated otherwise, any stream flow rates presented in this thesis are those obtained using the data from Site 4. There are two main advantages in using the data from Site 4 compared to using the data from Site 3. Firstly, at the higher

flows it is possible that the tracer may not have been completely mixed at Site 3, so flow rates from Site 4 may be more reliable because there is a greater time for mixing of the tracer to be achieved. Secondly, the drainage inflows to the study reach may contribute to the dispersion, so it is consistent to include them in the estimate of the flow rate in the study reach.

5.3 Some preliminary issues

The data analysis methods used are based on the assumption that tracer mass is conserved in the experiments. Since the presence of lateral inflow in the study reach introduces an apparent loss of tracer mass, the data was corrected to prevent the results of velocity and dispersion coefficient from being affected. This was achieved for each experiment by linearly scaling the upstream concentration profile so that the areas under both upstream and downstream profiles were the same.

The results from the optimisation of the analytical solution needed some consideration before being used. Unlike the results from the other three analysis methods it did not give results that directly represented the study reach. Instead results were obtained for two related reaches: the reach between the tracer release site and Site 3 (reach A), and the reach between the tracer release site and Site 4 (reach B). Representative results for the study reach were obtained using a weighted average approach. In this it was assumed that results for reach B could be expressed as the following weighted average of results for reach A and for the study reach:

$$C_B = \frac{(C_A t_A + C_{SR} t_{SR})}{(t_B)} \tag{5.1}$$

where *C* is the coefficient being evaluated (velocity or dispersion), t is the travel time for a reach (reach length divided by reach velocity) and the subscripts define the reaches: *SR* representing the study reach and A and B having been defined above. Hence the required coefficients were calculated by re-arranging equation (5.1):

$$C_{SR} = \frac{(C_B t_B - C_A t_A)}{(t_{SR})} \tag{5.2}$$

A similar weighted average analysis using the reach length as the weighting parameter instead of the reach travel time was also considered.

Results for velocity and dispersion coefficient are presented and discussed in the next two sections, and are illustrated with various charts. Accompanying numerical values are provided in tables, which are presented in Appendix E.

5.4 Velocity

5.4.1 Reduction of peak

Figure 5.2 shows the results from all the tracer experiments plotted against stream flow rate. As would be expected velocity increases with increasing stream flow rate. There is no difference between standard and truncated results because truncating the concentration profiles has no effect on the concentration values around the peaks of the profiles. Numerical values are given in Table 5.2.

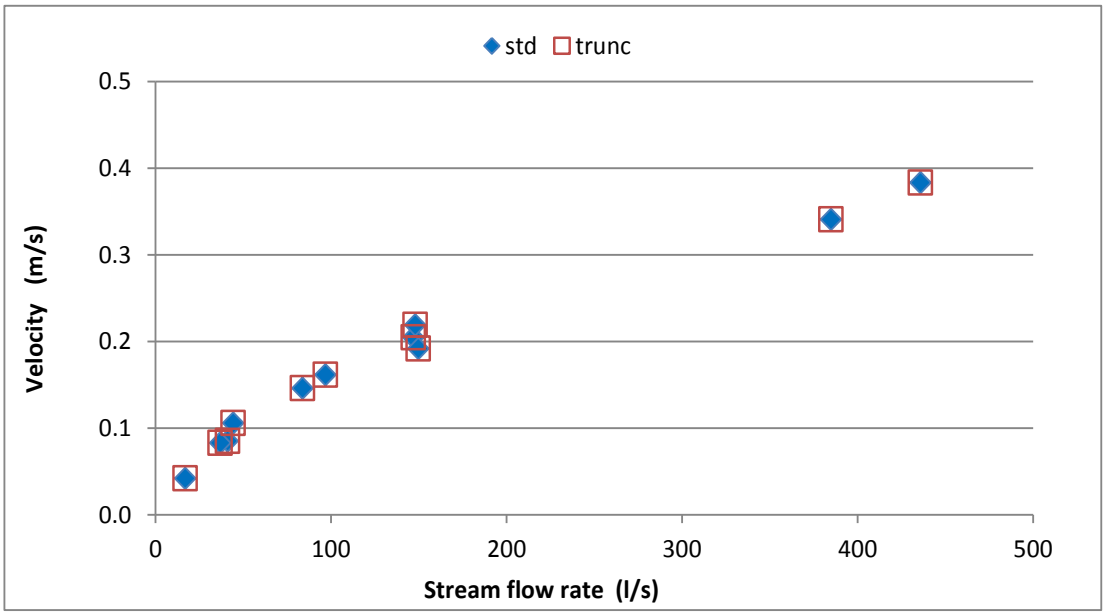

Figure 5.2 Variation of velocity with stream flow rate: Reduction of Peak Analysis (legend: std – standard data; trunc – truncated data)

5.4.2 Method of moments

Figure 5.3 shows the results from all the tracer experiments plotted against stream flow rate. As with the previous results the velocity increases with increasing stream flow rate. There are some small differences between standard and truncated results, however, apart from Experiment 8 where the percentage difference is about 12% the percentage differences are less than 5%. The standard velocities are larger than the

truncated velocities for 5 experiments and the standard velocities are smaller than the truncated velocities for 6 experiments. Numerical values are given in Table 5.3.

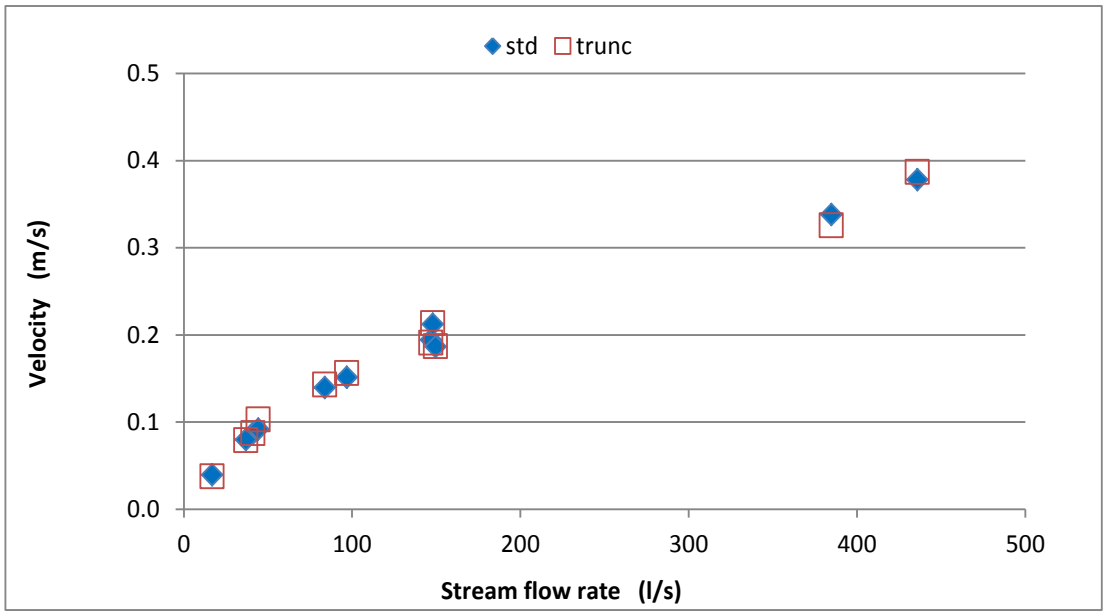

Figure 5.3 Variation of velocity with stream flow rate: Method of Moments Analysis

5.4.3 Routing procedure

Figure 5.4 shows the results from all the tracer experiments plotted against stream flow rate. Again the velocity increases with increasing stream flow rate. There is very little difference between standard and truncated results. Apart from Experiment 3 for which the percentage difference is about 6%, the other percentage differences are less than 1%. The standard velocities are larger than the truncated velocities for 4 experiments and the standard velocities are smaller than the truncated velocities for 7 experiments. Numerical values are given in Table 5.4, fitted and observed profiles are shown in Appendix C.

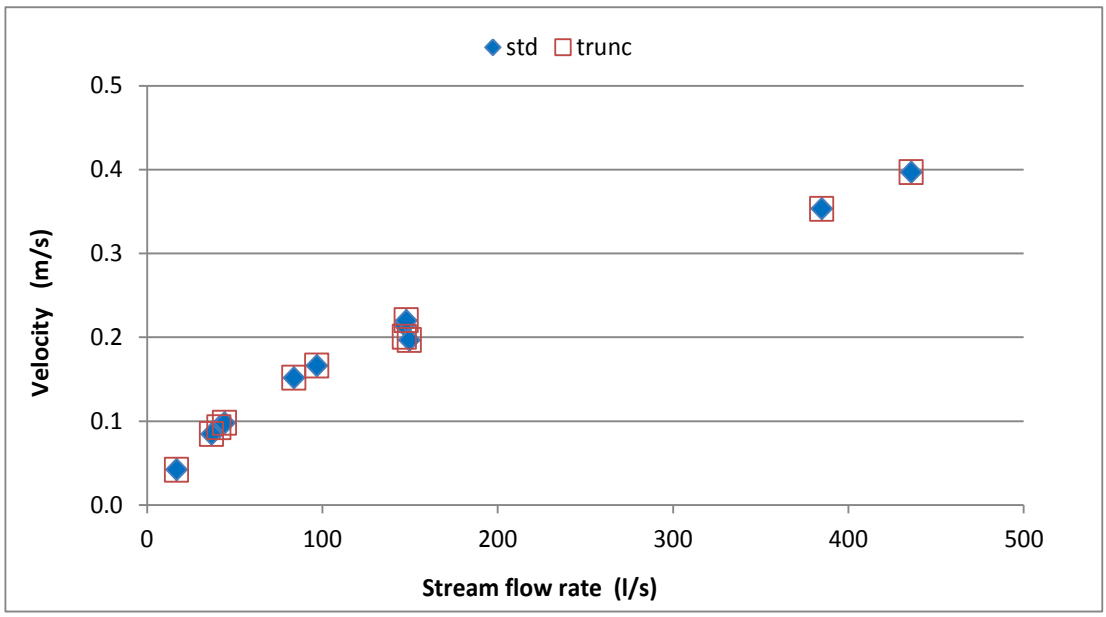

Figure 5.4 Variation of velocity with stream flow rate: Routing Procedure Analysis

5.4.4 Analytical solution

Figure 5.5 shows the standard results from all the tracer experiments for Reach A, Reach B and the Study Reach. In all cases the velocity for Reach A is the largest, followed by the velocity for Reach B followed by the Study Reach (evaluated as a weighted average of the other two, as described in Section 5.3). This trend reflects the slightly steeper nature of the stream in the upper part of the experimental area compared to the lower part. The same pattern (and very similar values) was found for the truncated data velocities. Figure 5.6 shows the weighted average results from all the tracer experiments plotted against stream flow rate. As before, the velocity increases with increasing stream flow rate. Apart from two experiments (8 and 9) for which the percentage difference between standard and truncated results is about 1.5%, the other percentage differences are less than 1%. The standard velocities are larger than the truncated velocities for 6 experiments and the standard velocities are smaller than the truncated velocities for 5 experiments. Numerical values are given in Tables 5.5 and 5.6, fitted and observed profiles are shown in Appendix D.

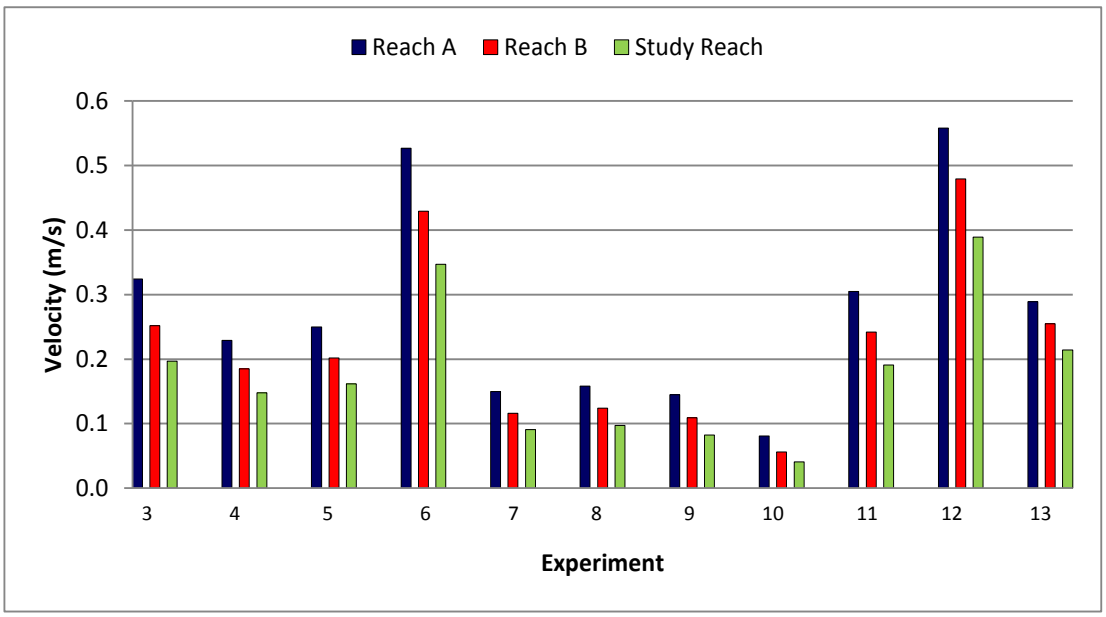

Figure 5.5 Comparison of 3 different velocity estimates: Analytical Solution Analysis using standard data

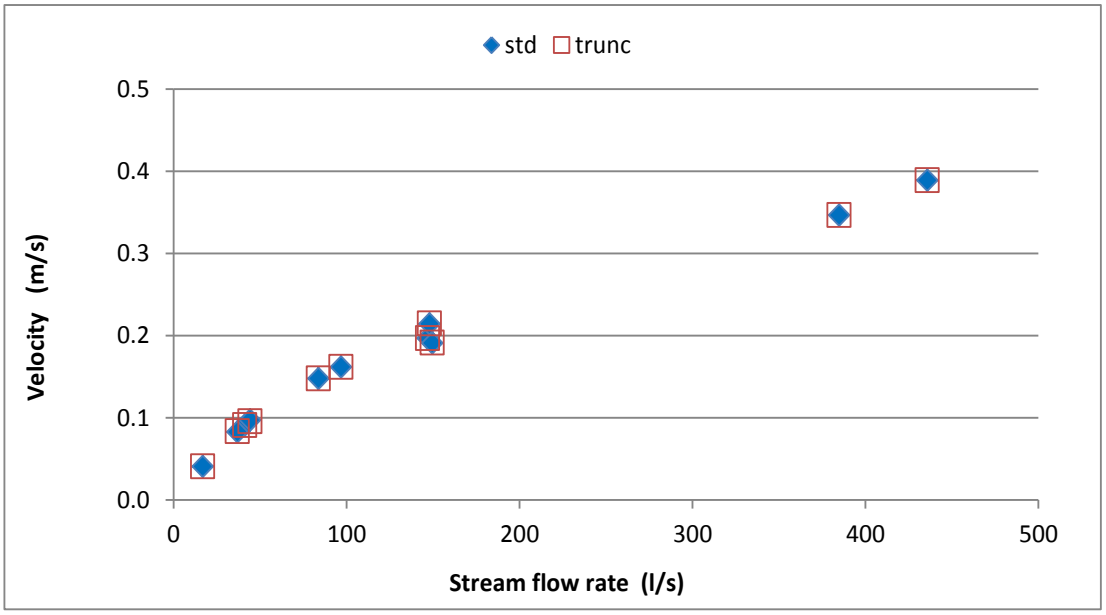

Figure 5.6 Variation of velocity with stream flow rate: Analytical Solution Analysis

5.4.5 Discussion

Figures 5.7 and 5.8 compare the velocity results from all four methods for standard and truncated data, respectively. Generally, there is excellent agreement between all four methods and between the two types of data (as already noted in the previous 4 sub-sections). It is noticeable that for the majority of the experiments, the Routing Procedure gives the highest velocity and the Method of Moments gives the lowest

velocity, with the percentage difference between these two methods being between +3% and +10% for the standard data. For the truncated data these percentage differences are lower for 6 experiments, higher for 4 experiments and the sign is reversed for one experiment (5% becoming -5%, Experiment 8). Experiment 6 shows the largest percentage difference (+13%).

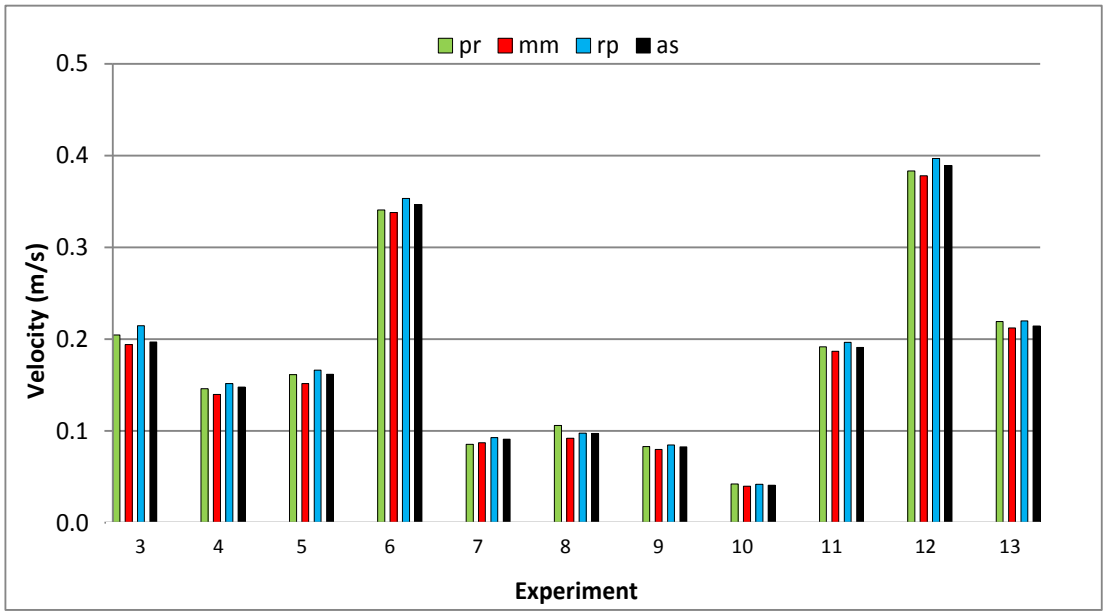

Figure 5.7 Comparison of velocities from four analysis methods using standard data (legend: pr – peak reduction; mm – method of moments; rp – routing procedure; as – analytical solution)

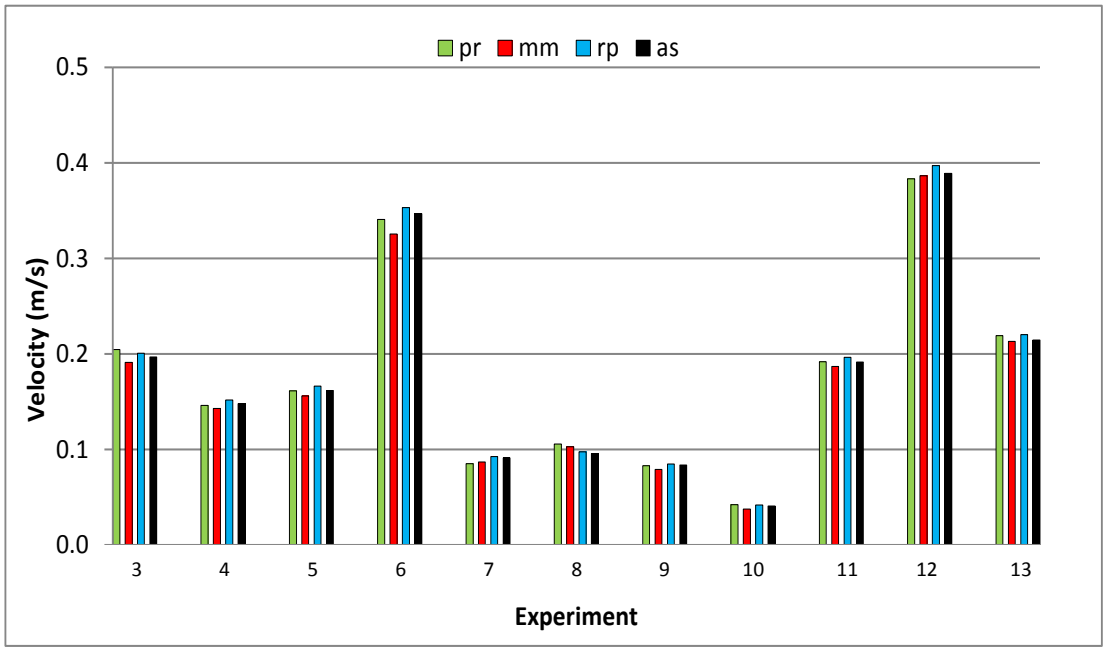

Figure 5.8 Comparison of velocities from four analysis methods using truncated data

It is clear that the weighted average approach for the Analytical Solution method is a satisfactory method for using this approach. Comparing Figures 5.5 and 5.7 shows that the weighted average results are more consistent with the other three analysis methods results than are either of the original results (i.e. Reach A or Reach B). Similarly, using the time difference of the peak concentration (for the Peak Reduction method) gives a good estimate of the velocity. Previous work suggests the peak velocity is closely related to the centroid velocity, i.e. the velocity derived from the time difference of the centroids of the concentration profiles in the Method of Moments (Burke, 2002; Wallis 2005), so the consistency of the results from those two methods is expected.

Figure 5.9 shows the same results as Figure 5.7, but also includes alternative results for the Analytical Solution method using standard data in which the weighted average values were based on reach length rather than reach travel time. Clearly, the former approach gives results which are always smaller than the latter approach: also they are less consistent with the results from the other three analysis methods. Hence using reach travel time as the weighting parameter appears to be better than using the reach length. A similar conclusion was found for the truncated data.

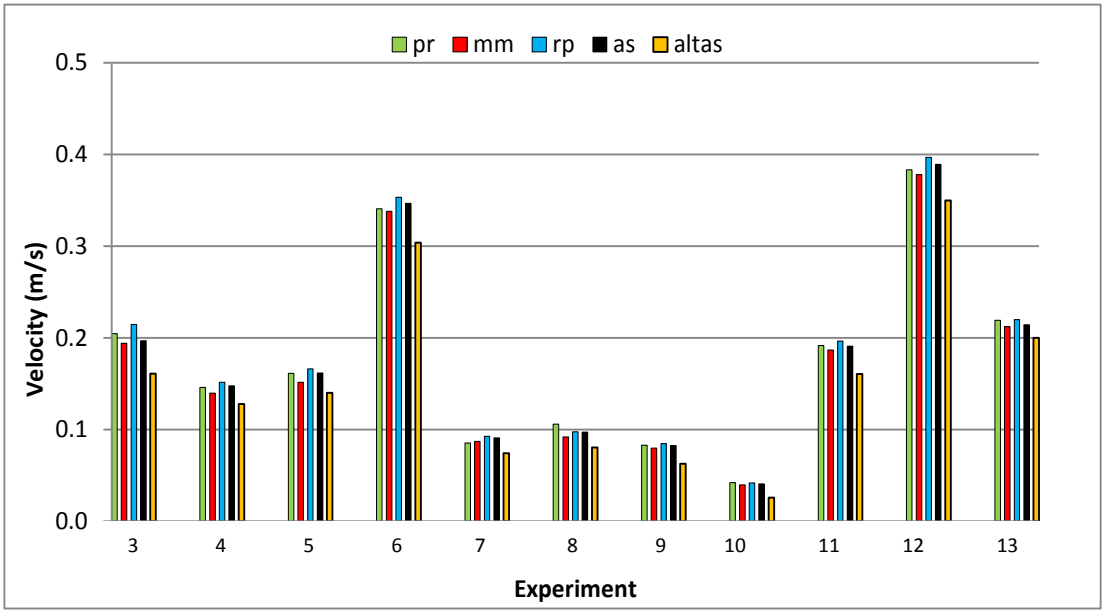

Figure 5.9 Comparison of alternative Analytical Solution velocities (altas in legend) with other analysis methods using standard data

The good agreement between the 4 analysis methods is also shown in Figures 5.10 and 5.11 for standard and truncated data analysis where the variation of velocity with

stream flow rate shows an increasing, smooth, non-linear trend. The relatively large difference between the Routing Procedure and Method of Moments results for Experiment 6 (stream flow rate 385.2 l/s) noted above is evident on Figure 5.11.

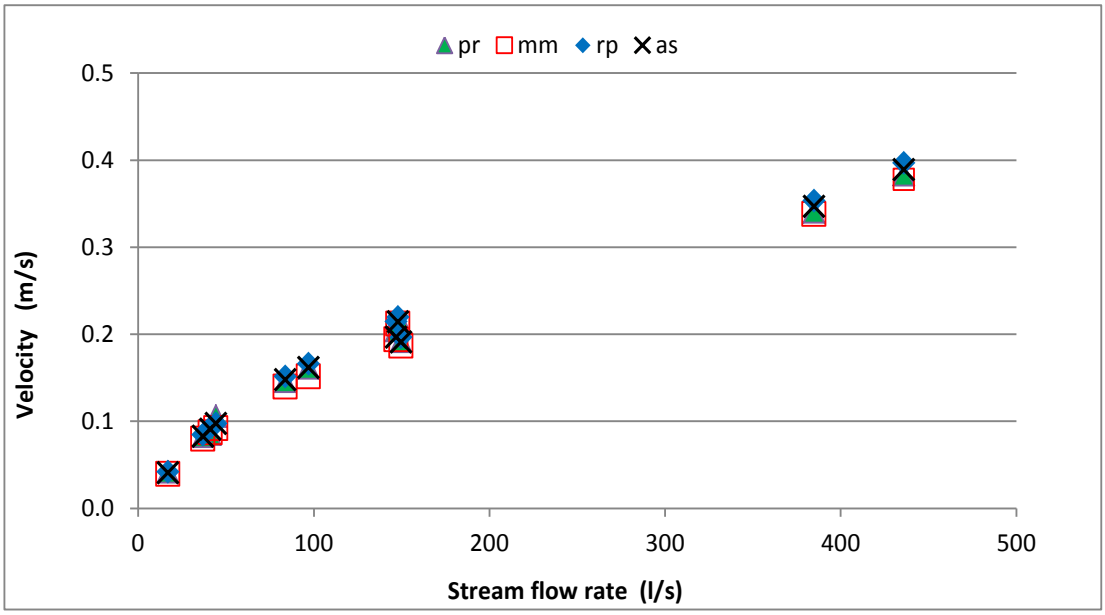

Figure 5.10 Comparison of velocity with stream flow rate: four analysis methods using standard data

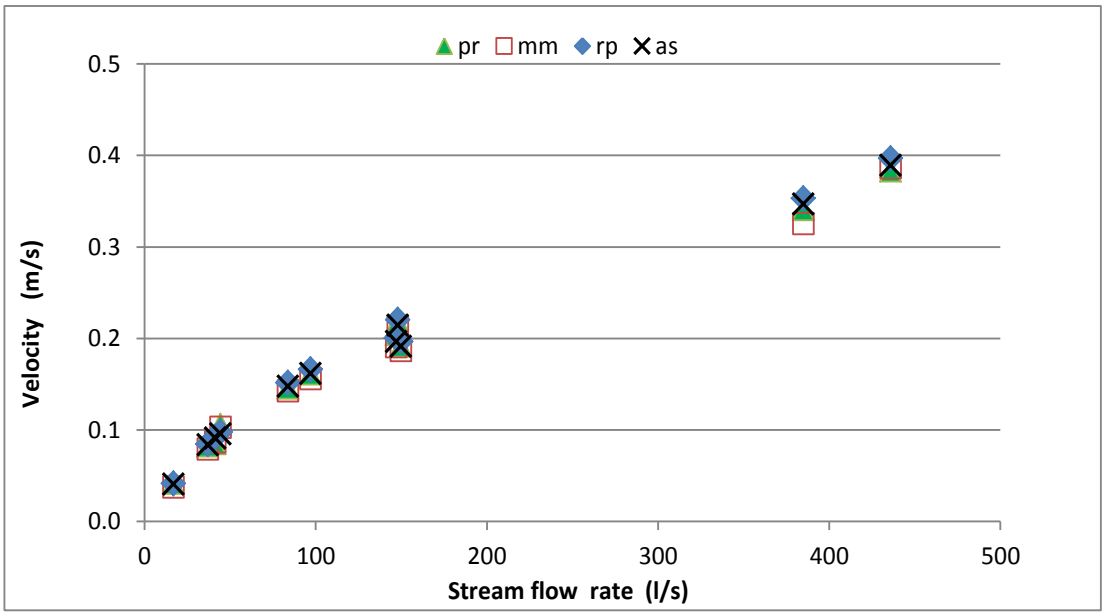

Figure 5.11 Comparison of velocity with stream flow rate: four analysis methods using truncated data

5.5 Dispersion coefficient

5.5.1 Reduction of peak

Figure 5.12 shows the results from all the tracer experiments plotted against stream flow rate. As would be expected the dispersion coefficient increases with increasing stream flow rate. There is no difference between standard and truncated results because truncating the concentration profiles has no effect on the concentration values around the peaks of the profiles. Numerical values are given in Table 5.7.

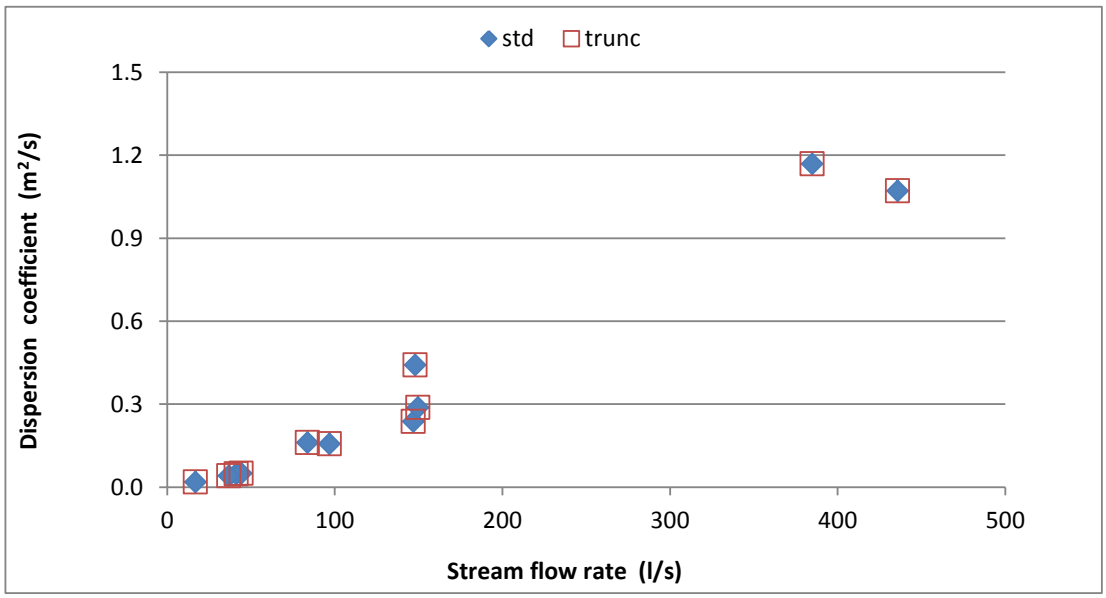

Figure 5.12 Variation of dispersion coefficient with stream flow rate: Reduction of Peak Analysis

5.5.2 Method of moments

Figure 5.13 shows the results from all the tracer experiments plotted against stream flow rate. As with the previous results the dispersion coefficient increases with increasing stream flow rate. There are significant differences between standard and truncated results. The standard dispersion coefficient values are larger than the truncated dispersion values for seven experiments (differences being between +10% and +63%) and the standard dispersion coefficients are a little smaller than the truncated velocities for three experiments (differences being between -15% and -49%). Experiment 3 analysis returned a negative value with the standard data, this was caused by the variance of the downstream concentration profile being less than the variance of the upstream concentration profile. This occurred because the tail at Site 3

was excessively long (see Appendix B), which resulted from only a poor estimate of the background being used. This value was set to zero because a negative dispersion coefficient has no physical meaning. Numerical values are given in Table 5.8.

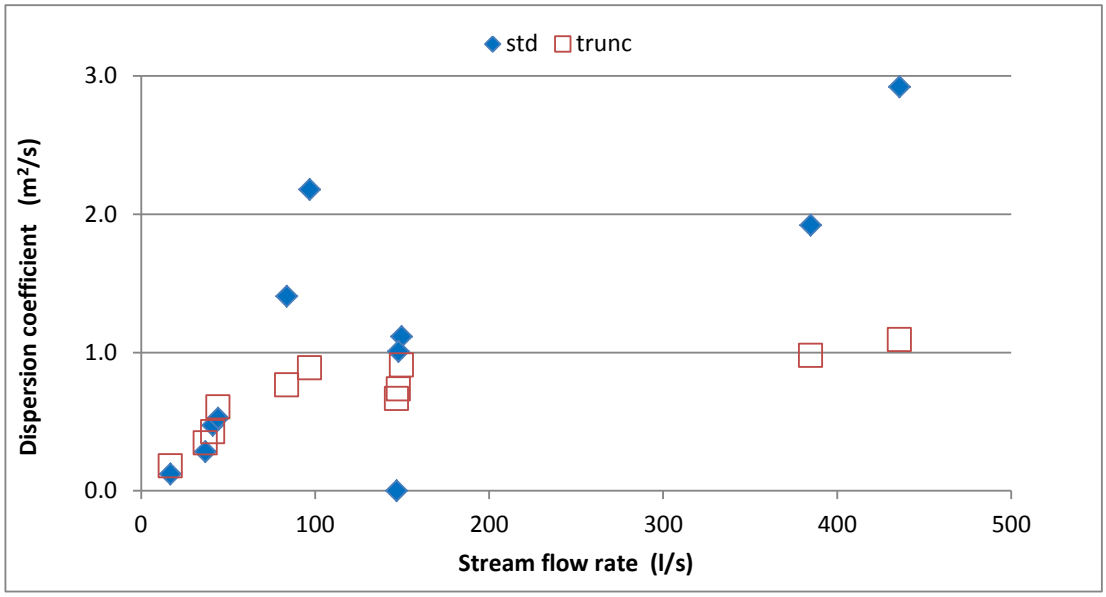

Figure 5.13 Variation of dispersion coefficient with stream flow rate: Method of Moments Analysis

5.5.3 Routing procedure

Figure 5.14 shows the results from all the tracer experiments plotted against stream flow rate. Again the dispersion coefficient increases with increasing stream flow rate. There is little difference between standard and truncated results (percentage differences being less than 4%) apart from Experiment 3 for which the percentage difference is about 18%. Truncated data values were larger than standard data values for 8 experiments, they were equal for 1 experiment and they were smaller for 2 experiments. Numerical values are given in Table 5.9, fitted and observed profiles are shown in Appendix C.

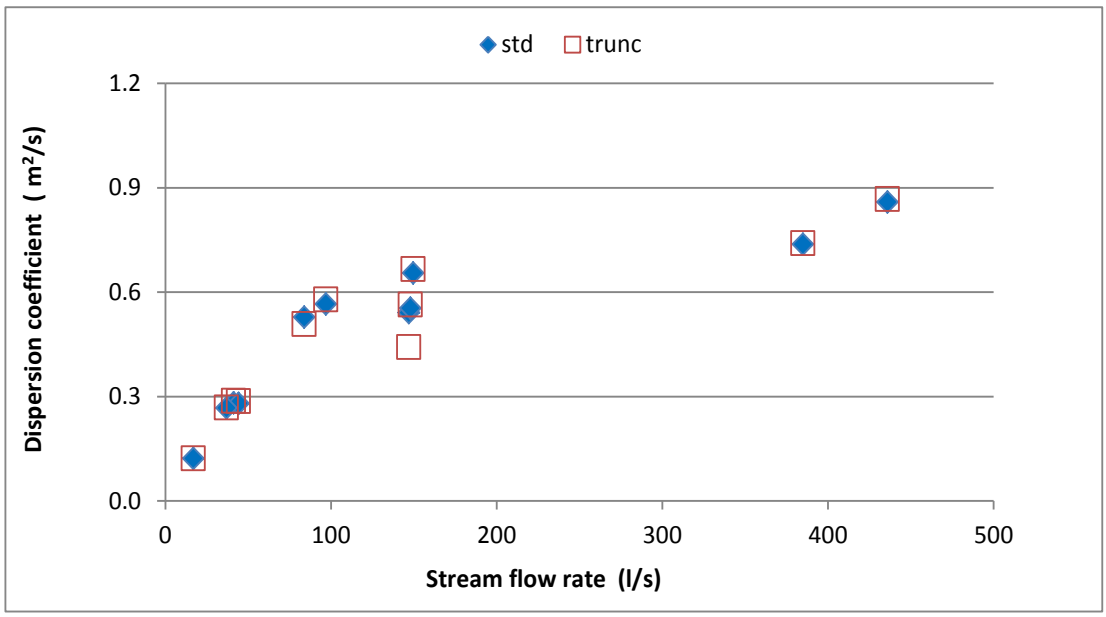

Figure 5.14 Variation of dispersion coefficient with stream flow rate: Routing Procedure Analysis

5.5.4 Analytical solution

Figure 5.15 shows the results of all the tracer experiments using standard data for Reach A, Reach B and the Study Reach. The results fall into two groups. For stream flow rates between 17 l/s and 97l/s (Experiments 4, 5, 7, 8, 9 & 10) the values increase in the order of Reach A, Reach B and the Study Reach. In contrast, for stream flow rates between 147l/s and 436l/s (Experiments 3, 6, 11, 12 & 13) the values decrease in the order of Reach A, Reach B and the Study Reach. It is not clear why the results show a different behaviour for these two flow ranges: nor is there any obvious physical explanation for the trends. Unlike the velocity results (section 5.4.4), where the smaller channel slope of the Study Reach explained a clear trend, the relationship between dispersion and hydraulic variables is not so simple. Nevertheless, the logic of using a weighted average approach remains. The same pattern (and very similar values) was found for the truncated data dispersion coefficients. Numerical values are given in Tables 5.10 and 5.11, fitted and observed profiles are shown in Appendix D.

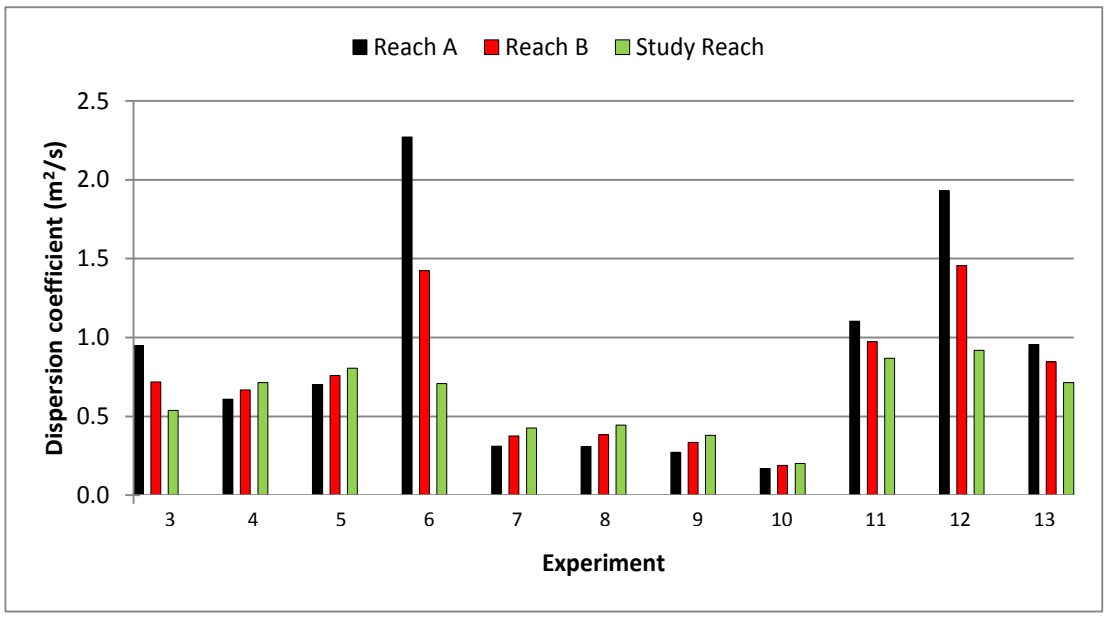

Figure 5.15 Comparison of 3 different dispersion coefficient estimates: Analytical Solution Analysis using standard data

Figure 5.16 shows the weighted average results (i.e. the Study Reach values) from all the tracer experiments plotted against stream flow rate. As before, the dispersion coefficient increases with increasing stream flow rate. The standard dispersion coefficients are larger than the truncated ones for 7 experiments (differences being between +3% and +10% for 6 of these, with one being significantly larger (+16%)) and the standard dispersion coefficients are smaller than the truncated ones for 4 experiments (differences being less than -2%).

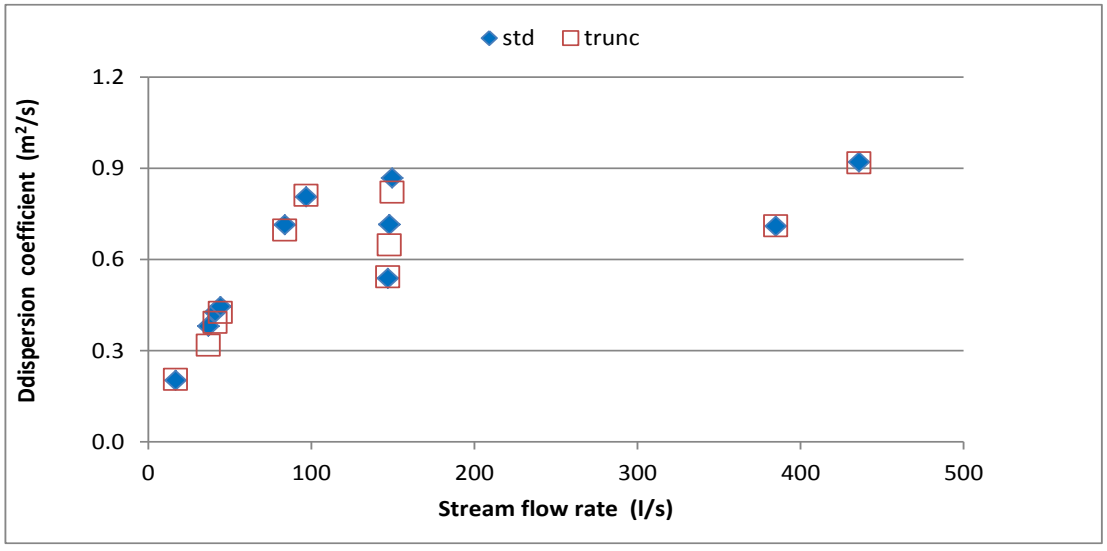

Figure 5.16 Variation of dispersion coefficient with stream flow rate: Analytical Solution Analysis

5.5.5 Discussion

Figures 5.17 and 5.18 compare the dispersion coefficient results from all four methods for standard and truncated data, respectively. Generally, there is quite a lot of variation between all four methods and some variation between the two types of data. The most noticeable difference is between the method of moment results for standard and truncated data (as noted in section 5.5.2). Of these, the truncated data results are generally more consistent with the results from the other three methods than are the standard data results. Difficulties with the method of moments has been reported by other workers (see, e.g. Fischer, 1968; Yotsukura et al, 1970; Rutherford, 1994), and can be attributed to the presence of poorly observed concentration profile tails. Either a missing tail (leading to underestimation of profile variance) or an unusually long tail (leading to overestimation of profile variance, as with the Site 3 data in Experiment 3) can cause problems. It is clear that the data truncation employed has significantly improved the quality of the method of moments results. Truncation of long tails has been carried out by other workers to be applied to various methods including the method of moments (Elder, 1959; Godfrey and Frederick, 1963; Fischer, 1968; Yotsukura et al, 1970). The methods used for truncation varied from "chosen, entirely by eye" (Fischer, 1970) to a percentage of the peak. For this study, truncated data was created by applying a truncation value of one percent of the peak concentration value to all concentration profiles. It is interesting to observe that Experiment 3 was also the only experiment for which truncating the data gave significantly different results with the Routing Procedure (section 5.5.3). Truncating had no effect on the Peak Reduction results (section 5.5.1), whilst the Analytical Solution results (section 5.5.4) were generally affected a little more than the Routing Procedure results. Overall, therefore, truncating the data has no serious negative consequences and is certainly beneficial for the method of moments.

A closer look at the truncated results in Figure 5.18 shows that the Peak Reduction method significantly underestimates the dispersion coefficient at low flows, but gives results that are more consistent with those from the other three methods at high flows. In general, the Method of Moments gives the largest results and the Routing Procedure results are always smaller with the former being between 20% and 50% larger. Interestingly, Rowinski et al (2007) found that the Method of Moments gave consistently larger dispersion coefficients than the same Routing Procedure in a study on a large river, with differences ranging between 6% and 54%. Comparing Figures

5.15 and 5.17 provides a little evidence that the weighted average approach for the Analytical Solution method is beneficial, but the matter is less clear than it is for velocities.

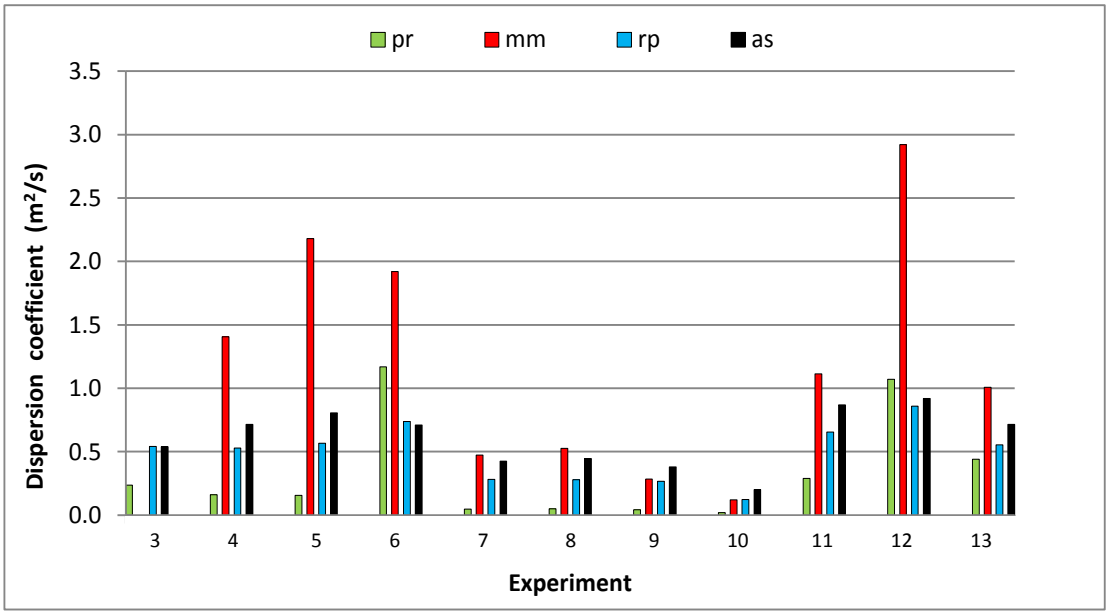

Figure 5.17 Comparison of dispersion coefficients from four analysis methods using standard data

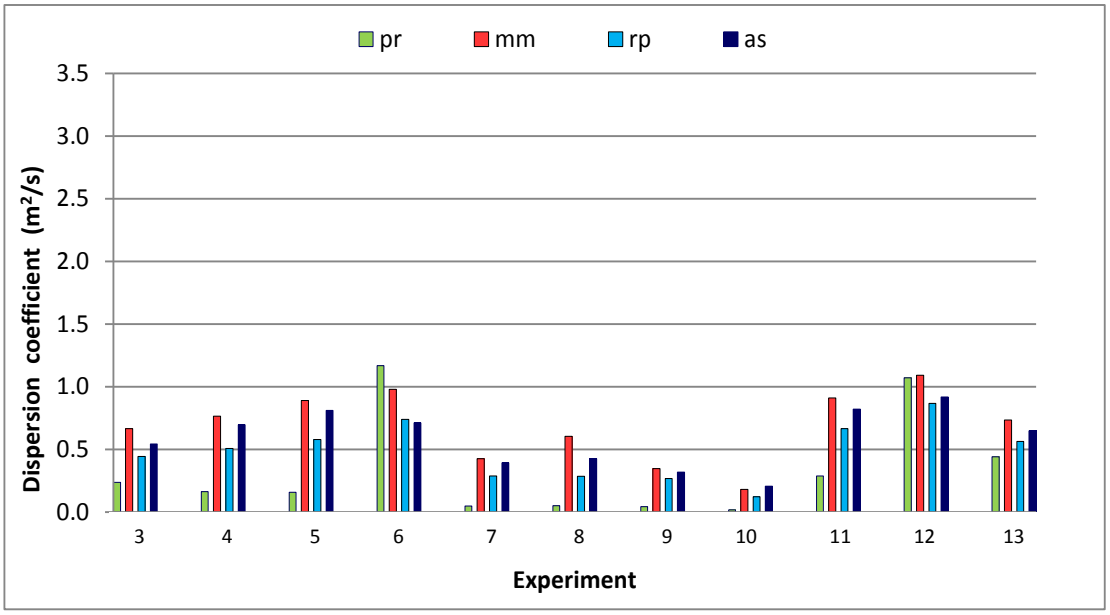

Figure 5.18 Comparison of dispersion coefficients from four analysis methods using truncated data

Figure 5.19 shows the same results as Figure 5.18, but also includes alternative results for the Analytical Solution method using truncated data in which the weighted average

values were based on reach length rather than reach travel time. The latter are smaller than the former for 5 experiments (differences being between 9% and 52%) and are larger than the former for 6 experiments (differences being between 2% and 8%). Interestingly, this division of the experiments is exactly the same as the division noted in section 5.5.4 and suggests a difference between low and high flow rates. Unlike the velocity results no clear preference for the weighting parameter is immediately obvious. However, some light is thrown on the issue if the two weighted average results are compared against a representative result derived from the other three analysis methods. Defining the latter as the average of the Method of Moments result and the Routing Procedure result, then the difference between it and each weighted average result gives a measure of consistency for each weighted average approach. In 9 of the 11 experiments there was a greater difference for the reach length weighted average results than for the time weighted average results. On this basis, therefore, there is some justification for preferring the time weighted average approach. The Peak Reduction results were not used in this analysis because, as noted above, the method seems to underestimate the dispersion coefficient at low flows. The same comparison for the standard data dispersion coefficients gave the same conclusion, but due to the potentially unreliable nature of the Method of Moments results, the comparison was based only on the Routing Procedure results.

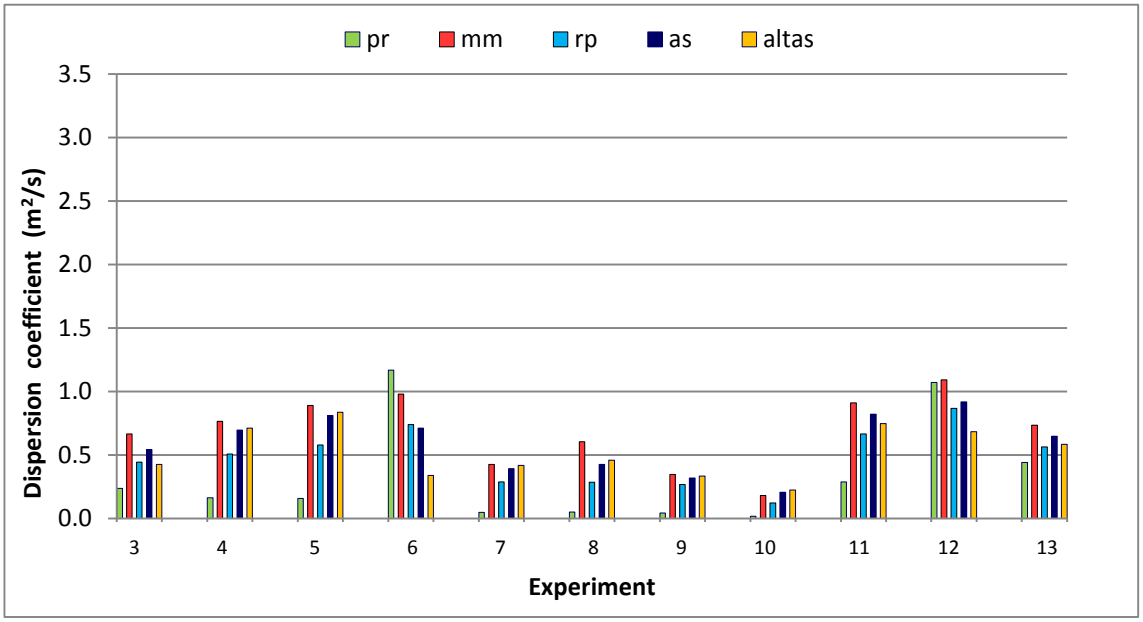

Figure 5.19 Comparison of alternative Analytical Solution dispersion coefficients with other analysis methods using truncated data

Figure 5.20 shows the variation of dispersion coefficient with stream flow rate from all four methods using truncated data and reveals increasing trends for all methods (as previously identified), but there is considerable scatter. A clearer picture is given in Figure 5.21 where power law trends are fitted to the data. Power laws have been suggested by previous studies, see e.g. Rutherford, 1994; Deng et al, 2001; Wallis and Manson, 2004. The trends expose a rather different relationship for the Peak Reduction method compared to the other three, and the tendency for the Method of Moments and the Routing Procedure to give the largest and smallest values, respectively, is evident. It is interesting to note that the peak reduction power trend produces the best R^2 value but has the opposite profile shape compared to the other three methods with lesser but consistent R^2 values.

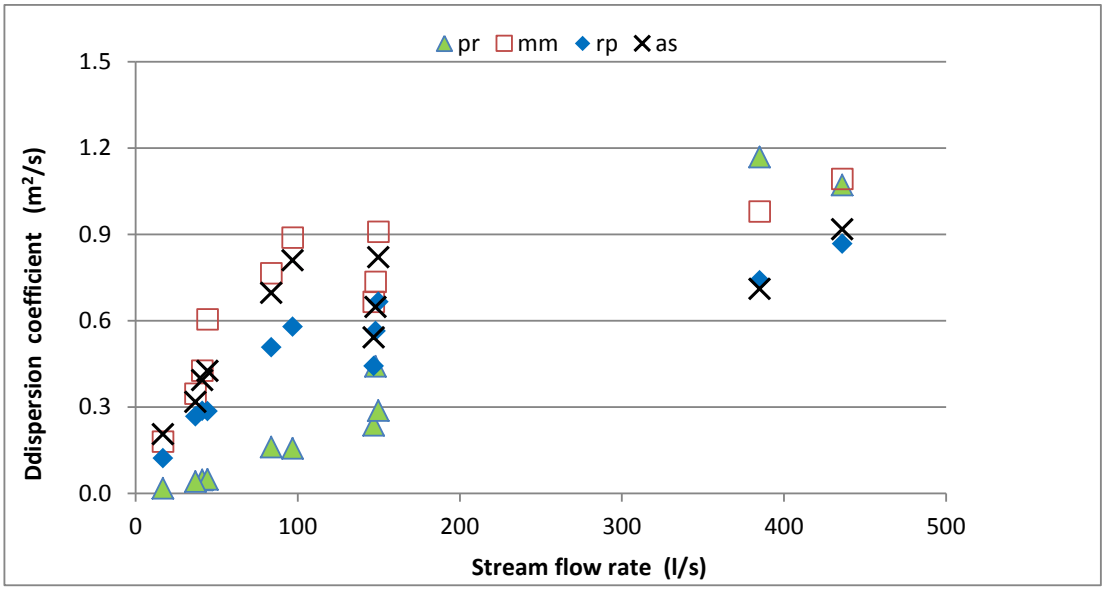

Figure 5.20 Comparison of dispersion coefficient with stream flow rate: four analysis methods using truncated data; individual results

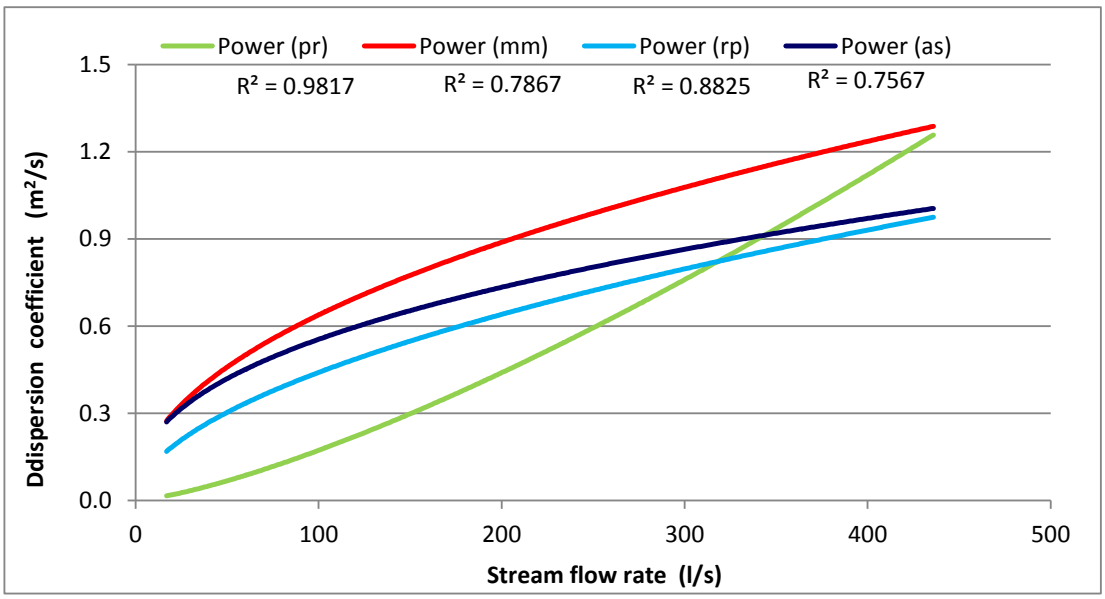

Figure 5.21 Comparison of dispersion coefficient with stream flow rate: four analysis methods using truncated data; power law trends

Figure 5.22 attempts to characterise the dispersion coefficient in the study reach by showing the average of the results from three of the analysis methods using truncated data. Here results from the truncated data are preferred to those from the standard data for the reason given earlier in this section. Peak Reduction results weren't used because they appear to be inconsistent with the other results. Overall, the coefficient lies in the range 0.15 m^2/s to 1 m^2/s, which is consistent with recent results from studies in nearby reaches of the Murray Burn. For example: Wallis and Manson (2005) calibrated their DISCUS numerical model of the ADE to a reach about 250m upstream of the study reach finding dispersion coefficients in the range of 0.4 m^2/s to 2.0 m^2/s; Wallis et al (2007) used a calibrated neural network to estimate dispersion coefficients in the same reach reporting values in the range 0.3 m^2/s to 2.1 m^2/s; and Silavwe (2009), applying three routing procedures to that reach, found values in the range 0.2 m^2/s to 2.1 m^2/s. For all these studies, which used an earlier set of tracer data (Burke, 2002), the stream flow rate was between 14 l/s and 535 l/s, which is similar to the flow range in the current study.

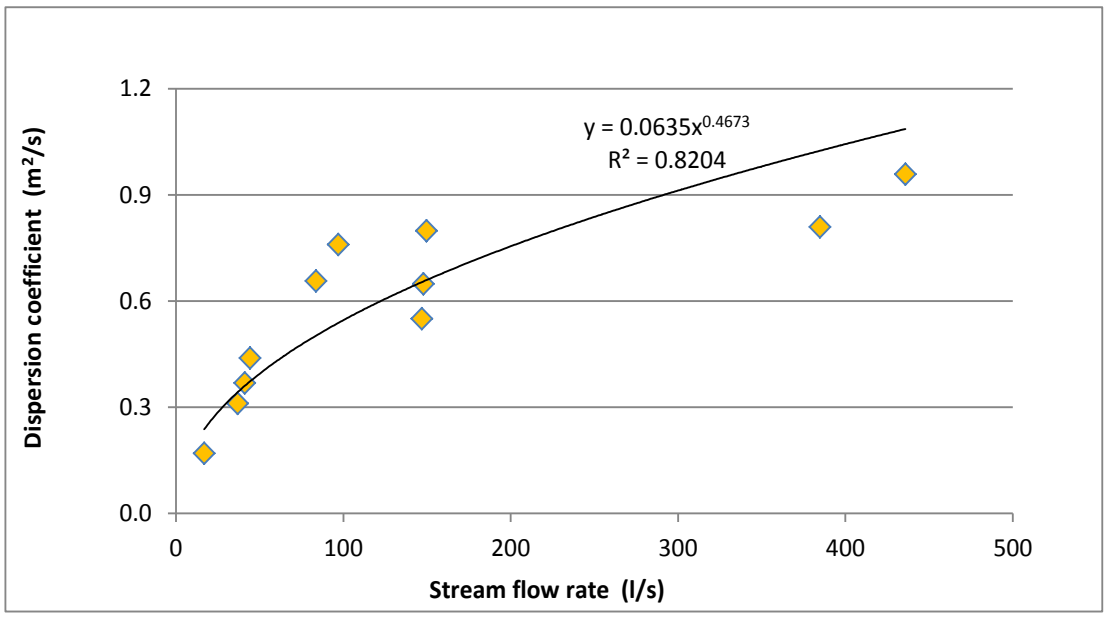

Figure 5.22 Variation of dispersion coefficient with stream flow rate: average of three analysis methods using truncated data

As noted in Chapter 2 there are very few published data on dispersion coefficients in small streams with which to compare these dispersion coefficients from the Murray Burn. However, a review of published work found two sources. Firstly, Sukhodolov et al (1997) reported dispersion coefficients between 0.16 m^2/s and 2.76 m^2/s; secondly, Singh and Beck (2003) reported values between 0.38 m^2/s and 1.45 m^2/s. In all of these cases stream flow rates were less than 1000 l/s. Clearly, the new Murray Burn results presented in this thesis (and the earlier Murray Burn results) are consistent with these earlier findings.

Figures 5.23 shows how the new Murray Burn results fit into the relationship between dispersion coefficients and stream flow rates previously shown in Chapter 2. The previously unpublished results in Silavwe (2009) are also shown, these being representative of the results from the earlier studies on the Murray Burn. Silavwe used Fischer's routing procedure to analyse tracer data (Burke, 2002) collected for a study of travel times (no dispersion coefficients were evaluated).

It is clear that the Murray Burn data fits well into the overall pattern of dispersion coefficients increasing with increasing stream flow rate. Additionally, the Murray Burn data makes an important contribution to our knowledge of dispersion in small streams by augmenting the relatively few data points at stream flow rates less than 1000 l/s.

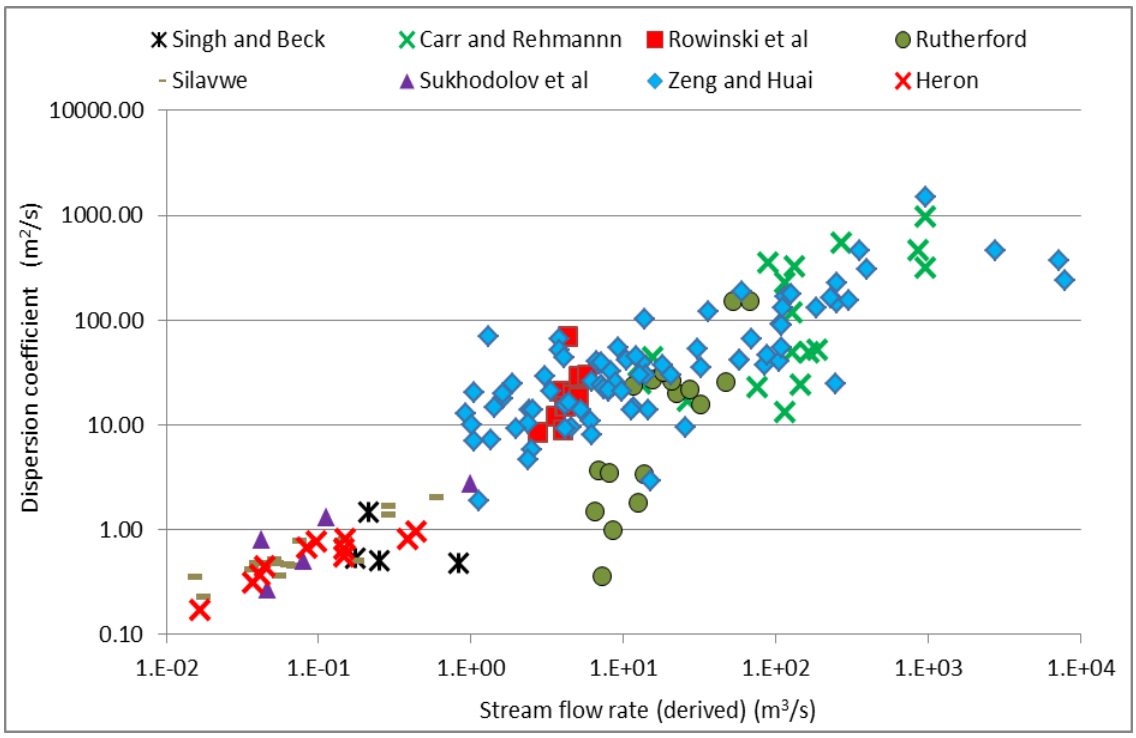

Figure 5.23 Variation of dispersion coefficient with stream flow rate: new and existing data

Although Figure 5.23 displays a clear trend it does not demonstrate how dispersion might be related to common hydraulic variables such as velocity and depth. Since such variables vary over several orders of magnitude in natural watercourses, presenting the data non-dimensionally may have some advantages. Following Rutherford (1994), Figures 5.24 and 5.25 show two non-dimensional plots. In both figures the horizontal axis shows a non-dimensional velocity (cross-sectional average velocity divided by shear velocity). In Figure 5.24 the non-dimensional dispersion coefficient on the vertical axis is obtained by dividing the dispersion coefficient by the product of depth and shear velocity. Since the width of a river is an important variable in generating longitudinal dispersion, Figure 5.25 shows the result of using the width rather than the depth as a length scale.

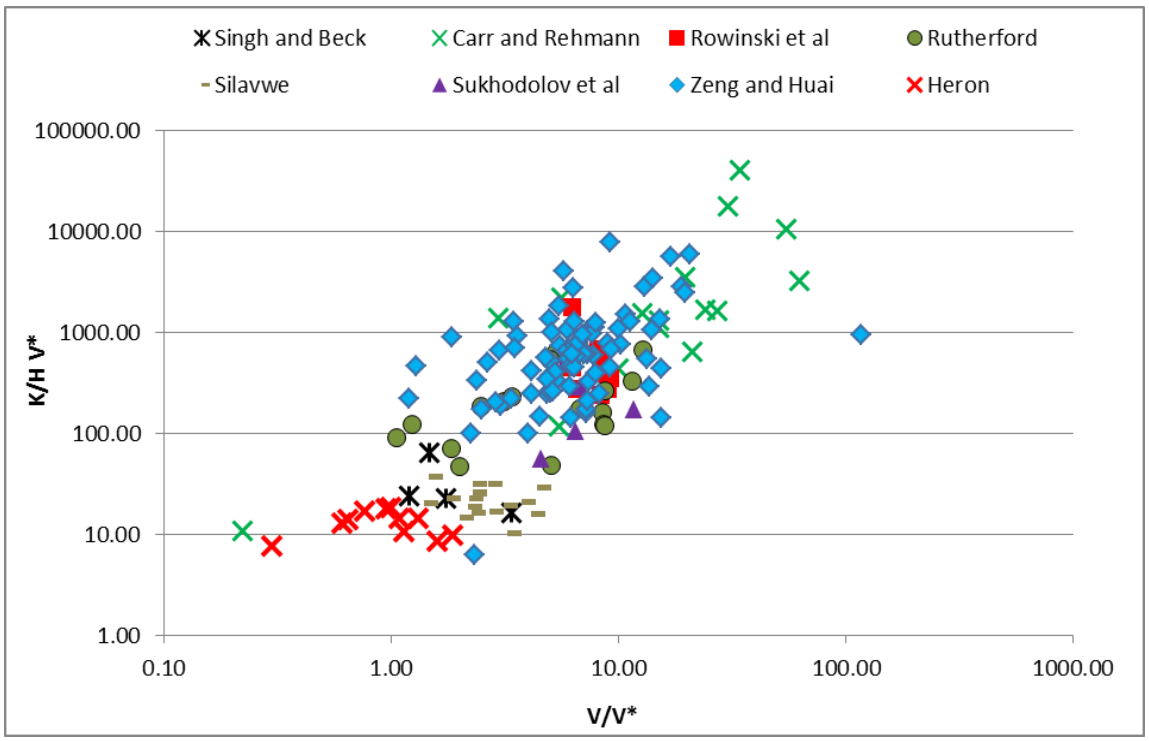

Figure 5.24 Variation of non dimensional dispersion coefficient using river depth as the length scale

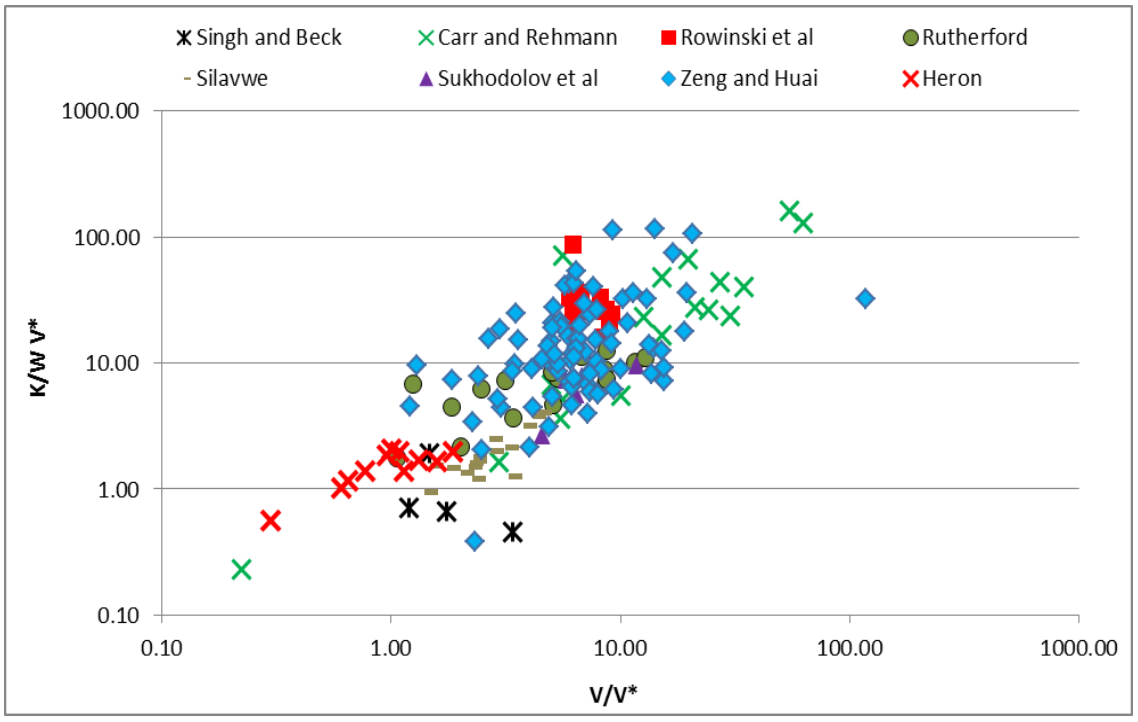

Figure 5.25 Variation of non dimensional dispersion coefficient using river width as the length scale

Both figures show a strong positive correlation between the non-dimensional quantities. It is interesting that most of the data fall into a two order of magnitude range of non-dimensional velocity, which contrasts with the six order of magnitude range of the stream flow rates. Similarly, in Figure 5.25 the non-dimensional dispersion coefficient occupies about a two order of magnitude range compared to a three order magnitude range in Figure 5.24, while the original dimensional dispersion coefficients extend over about four orders of magnitude.

5.5.6 Errors

It is difficult to evaluate the consequences of experimental and analysis errors on the final results because the sizes of the error in each stage of the procedures are not known. Also, the sources of errors vary between the four analyses used (see Chapter 3). Errors in the concentration values are common to all methods, however, and were minimised by the adoption of good practices in the collection, handling and analysis of the samples, as described in Chapter 4.

Calculation errors in the stream flow rates were minimised by collecting complete and well-resolved concentration profiles. Thus the numerical integration used to calculate the area under the profile was reliable. Herschy (1995) suggests that errors in dilution gauging are typically 5%. Some issues concerning errors in the dispersion coefficients obtained from the four analysis methods are given below.

The main calculation error in the Reduction of Peak method comes from using only two data points to estimate the slope of the line in the plot. Certainly, a more reliable estimate of this slope would be obtained by having several data points. Although this was not considered in the design of the experimental work, it would have been feasible to have measured the region around the peak of the concentration profile at, say, two intermediate locations. Since the estimates of velocity from all four methods were very consistent with each other, no significant error was introduced by using the velocity estimate from the method of moments when evaluating he cross-sectional area for use in equation 3.5. Finally, the possibility of a peak concentration occurring between two observed concentrations was minimised by collecting well-resolved profiles.

The main calculation error in the Method of Moments comes from the numerical integration used to calculate the moments of the concentration profiles. As highlighted

in Chapter 3, the major issue here is the difficulty of reliably estimating the end of the concentration profile. Although collecting complete and well-resolved profiles is essential, and was generally achieved, the dispersion coefficients are very sensitive to the length of the tail on the profiles. This was illustrated by the results from Experiment 3 (Section 5.5.2). Furthermore, the analysis of truncated data (to a large extent eliminating the issue) provided more robust results. Similar to the Reduction of Peak method, having estimates of the moments of concentration profiles at some intermediate locations in the experimental reach would have been helpful, although collecting these additional complete profiles was not feasible. This would have allowed more reliable estimates to have been made of the rates of change of the profile moments along the reach (equations 3.14 & 3.15), from which the velocity and dispersion coefficients were estimated.

The main calculation error in the Routing Procedure comes from fitting the simulated downstream concentration profile to the corresponding observed profile. This was minimised by using an optimisation method which identified the best fit in an objective manner. The "frozen cloud" assumption is inherent in the particular routing procedure used. Although this has been identified as a potentially significant source of error (Singh & Beck, 2003), Rutherford (1994) suggests that it is not a significant issue.

The main calculation error in the Analytical Solution comes from fitting the simulated downstream concentration profile to the corresponding observed profile. This was minimised by using an optimisation method which identified the best fit in an objective manner. Since the reach over which the solution is applied (extending between the tracer release site and a sampling site) includes the advective zone, the results are likely to be unreliable to some extent. However, one of the outcomes of this work was the investigation of a new approach (Section 5.3). This allowed more robust results to be achieved by adopting a weighted-average approach that used results from initially applying the method to concentration profiles observed at Site 3 and at Site 4.

5.5.7 Summary

This chapter has presented and discussed the results of the four data analysis methods described in Chapter 3. Flow velocities were consistent between all four methods and truncating the concentration profiles had very little effect. Some important differences between the dispersion coefficients from the four methods were found. Truncating the

concentration profiles had a beneficial effect on the Method of Moments and had no significant negative effect on the other methods used. Using a weighted average approach based on travel time with the Analytical Solution produced velocity results that were more consistent with those from the other methods. In contrast, dispersion coefficient results were not similarly more consistent. The dispersion coefficient values were consistent with the few previously published results for similar sized streams and strengthen our knowledge of solute transport in such watercourses.

Chapter 6 Conclusions

The thesis has described the execution of tracer experiments in the Murray Burn and the subsequent analysis of the data collected. The aim of the work is to improve our knowledge of the solute dispersion characteristics of small streams. Specific objectives were to:

- Carry out tracer experiments to determine dispersion coefficients (and flow velocities) for the Murray Burn over a wide range of stream flow rates
- Use four methods of estimating dispersion coefficients (Peak Reduction, Method of Moments, Routing Procedure, Analytical Solution) with the tracer data and compare the results
- Determine the influence of long tails (on the concentration profiles) on the results by repeating the data analysis using truncated profiles and comparing the results with the original analysis
- Compare the dispersion coefficients with previous unpublished results from a nearby reach of the Murray Burn and with published data from other streams
- To augment the very small number of published dispersion coefficients for small streams (defined as streams with stream flow rate less than 1000 l/s)

The following primary conclusions have been drawn.

- Eleven successful experiments were completed, yielding complete and well resolved temporal concentration profiles at two locations over a stream flow rate range of 17 l/s to 436 l/s
- Estimates of flow velocities from the four analysis methods gave very consistent results
- Estimates of dispersion coefficients from the four analysis methods were generally consistent but some important differences were found
- The influence of long tails on the concentration profiles was investigated by truncating the profiles at the 1% peak concentration level: the influence on velocities was negligible for all four analysis methods; the influence on dispersion coefficients was greater, but was only significant for the Method of Moments

- Overall, truncating the profiles is recommended
- The new dispersion coefficients obtained for the Murray Burn were in the range 0.15 m^2/s to $1m^2/s$ and were consistent with previous results from a nearby reach of the Murray Burn
- The dispersion coefficients for the Murray Burn (new and previous) augment our knowledge of dispersion in small streams by complimenting the previously published sparse data for stream flow rates less than 1000 l/s
- The dispersion coefficients from the Peak Reduction method were inconsistent with the results from the three other methods at the lower stream flow rates. Also the relationship with stream flow rate was rather different.
- A new weighted average approach for the Analytical Solution method yielded velocity results that were clearly more consistent with the results from the other analysis methods than were the initial results. Weighting according to travel time was preferred to weighting according to reach length.
- The dispersion coefficients from the Analytical Solution method showed fewer consistent patterns than the corresponding velocity results. For example, when comparing the initial results with the weighted average results lower stream flow rate results behaved differently than higher stream flow rate results. Also the weighted average results were not always clearly more consistent with the results from the other analysis methods than were the initial results. Nevertheless weighting according to travel time was preferred to weighting according to reach length.

6.1 suggestions for further work

This work used a one percent of peak value as the basis for data truncation. It may be worthwhile increasing this value incrementally to determine an acceptable upper range to apply that maintains reliable results. Application of the weighted average approach with the Analytical Solution method needs to be expanded to other rivers to find out if its merits are widely found. This project has begun to address what is a large gap in our knowledge of small streams, it was found that in the UK there is no database of small streams, no agency knows the extent of zero to first order streams, and in fact no UK agency has an official stream classification system. In other countries that record small streams they are considered to constitute up to 75% of all headwater in catchments. The UK may have more, we don't know: further work could be carried

out to map, quantify and categorise streams and to carry out tracer tests to fill in much needed data on small streams: this is needed to improve the models used for the estimation of dispersion coefficients which has relied on datasets from a few mostly larger rivers whilst ignoring the majority of water courses which would be categorised as small streams. Whilst the goal of one model to fit all may be impossible, we can improve our estimates of dispersion coefficients by having datasets which are more representative of our river networks.

Appendix A. Table for figure 2.1

River	Width	Depth	Velocity	disp coeff	Flow
Zeng and Huai (2014)	m	m	m/s	m2/s	m3/s(derived)
This data from was Nordin and Sabol (1974)					
Antietam creek, MD a	12.80	0.30	0.42	17.50	1.61
Antietam creek, MD a	24.08	0.98	0.59	101.50	13.92
Antietam creek, MD a	11.89	0.66	0.43	20.90	3.37
Antietam creek, MD a	21.03	0.48	0.62	25.90	6.26
Antietam creek, MD b	15.80	0.39	0.32	9.29	1.97
Antietam creek, MD b	19.80	0.52	0.43	16.26	4.43
Antietam creek, MD b	24.40	0.71	0.52	25.55	9.01
Monocacy river MD a	48.70	0.55	0.26	37.80	6.96
Monocacy river MD a	92.96	0.71	0.16	41.40	10.56
Monocacy river MD a	51.21	0.65	0.62	29.60	20.64
Monocacy river MD a	97.54	1.15	0.32	119.80	35.89
Monocacy river MD a	40.54	0.41	0.23	66.50	3.82
Monocacy river MD b	35.10	0.32	0.21	4.65	2.36
Monocacy river MD b	36.60	0.45	0.32	13.94	5.27
Monocacy river MD b	47.50	0.87	0.44	37.16	18.18
Susquehanna river a	203.00	1.35	0.39	92.20	106.88
Conococheague river GA a	42.21	0.69	0.23	40.80	6.70
Conococheague river GA a	49.68	0.41	0.15	29.30	3.06
Conococheague river GA a	42.98	1.13	0.63	53.30	30.60
Chattahoochee river GA a	75.59	1.95	0.74	88.90	109.08
Chattahoochee river GA a	91.90	2.44	0.52	166.90	116.60
Salt creek NE a	32.00	0.50	0.24	52.20	3.84
Salt creek NE c	167.00	0.20	0.47	43.20	15.70
Difficult run VA a	14.48	0.31	0.25	1.90	1.12
Bear creek CO a	13.72	0.85	1.29	2.90	15.04
Little Pincy creek MD a	15.85	0.22	0.39	7.10	1.36
Bayou Anacoco LA a	17.53	0.45	0.32	5.80	2.52
Bayou Anacoco LA b	19.80	0.41	0.29	13.94	2.35
Bayou Anacoco LA a	25.91	0.94	0.34	32.52	8.28
Bayou Anacoco LA a	36.58	0.91	0.40	39.48	13.32
Bayou Anacoco LA a	20.00	0.42	0.29	13.90	2.44
Comite river LA a	15.70	0.23	0.36	69.00	1.30
Comite river LA a	13.00	0.26	0.31	7.00	1.05
Copper creek VA a	18.29	0.38	0.15	20.17	1.04
Copper creek VA a	19.61	0.84	0.49	20.82	8.07
Copper creek VA a	16.76	0.47	0.24	24.62	1.89
Copper creek VA b	15.90	0.49	0.21	19.52	1.64
Copper creek VA b	18.30	0.84	0.52	21.40	7.99
Copper creek VA b	18.60	0.39	0.14	9.85	1.02
Coachella canal CA b	24.40	1.56	0.67	9.57	25.50

Clinch river VA a	48.46	1.16	0.21	14.76	11.80
Clinch river VA a	28.65	0.61	0.35	10.70	6.12
Clinch river VA a	57.91	2.45	0.75	40.49	106.41
Clinch river VA a	53.24	2.41	0.66	36.93	84.68
Clinch river TN b	46.90	0.86	0.28	13.93	11.29
Clinch river TN b	59.40	2.13	0.86	53.88	108.81
Clinch river TN b	53.30	2.09	0.79	46.45	88.00
Clinch river VA b	36.00	0.58	0.30	8.08	6.26
Powell river TN a	36.78	0.87	0.13	15.50	4.16
Powell river TN b	33.80	0.85	0.16	9.50	4.60
Comite river LA a	16.00	0.43	0.37	13.90	2.55
Bayou Bartholomew LA a	33.38	1.40	0.20	54.70	9.35
Amite river LA a	21.34	0.52	0.54	501.40	5.99
Amite river LA a	37.00	0.81	0.29	23.20	8.69
Amite river LA a	42.00	0.80	0.42	30.20	14.11
Tickfau river LA a	14.94	0.59	0.27	10.30	2.38
Tangipahoa river LA a	31.39	0.81	0.48	45.10	12.20
Tangipahoa river LA a	29.87	0.40	0.34	44.00	4.06
Red river LA a	253.59	1.62	0.61	143.80	250.60
Red river LA a	161.54	3.96	0.29	130.50	185.51
Red river LA a	152.40	3.66	0.45	227.60	251.00
Red river LA a	155.14	1.74	0.47	177.70	126.87
Sabine river LA a	116.43	1.65	0.58	131.30	111.42
Sabine river LA a	160.32	2.32	1.06	308.90	394.26
Sabine river TX a	14.17	0.50	0.13	12.80	0.92
Sabine river TX a	12.19	0.51	0.23	14.70	1.43
Sabine river TX a	21.34	0.93	0.36	24.20	7.14
Sabine river TX b	35.10	0.98	0.21	39.48	7.22
Mississippi river LA a	711.20	19.94	0.56	237.20	7941.54
Mississippi river MO a	533.40	4.94	1.05	457.70	2766.75
Mississippi river MO a	537.38	8.90	1.51	374.10	7221.85
Missouri river LA a	180.59	3.28	1.62	1486.45	959.58
Missouri river LA b	182.90	2.23	0.93	464.52	379.32
Missouri river LA b	201.20	3.56	1.27	836.13	909.67
Nooksack river WA a	64.01	0.76	0.67	34.84	32.59
Nooksack river WA a	86.00	2.93	1.20	153.00	302.38
Wind/Bighorn river WY a	44.20	1.37	0.99	184.60	59.95
Wind/Bighorn river WY a	85.34	2.38	1.74	464.60	353.41
Wind/Bighorn river WY a	59.44	1.10	0.88	41.81	57.54
Wind/Bighorn river WY a	68.58	2.16	1.55	162.58	229.61
Wind/Bighorn river WY b	67.10	0.98	0.88	41.81	57.87
Minnesota river a	80.00	2.74	0.03	22.30	7.45
Minnesota river a	80.00	2.74	1.14	24.90	249.89
White river a	67.00	0.55	0.35	30.20	12.90
John Day river OR a	24.99	0.58	1.01	13.94	14.64
John Day river OR a	34.14	2.47	0.82	65.03	69.15

Elkhorn river b	32.60	0.30	0.43	9.29	4.21
Elkhorn river b	50.90	0.42	0.46	20.90	9.83
Sukhodolov et al (1997)	W	D	V	DC	
Ikel 2	7.30	0.11	0.14	1.30	0.11
Byk 4	2.60	0.14	0.22	0.50	0.08
Botna 6	2.10	0.10	0.22	0.27	0.05
Kogilnik 10	5.20	0.29	0.66	2.76	1.00
Salchea 12	2.20	0.06	0.32	0.81	0.04
Carr and Rehmannn (2007)	W	D	V	DC	
Big Blue River	75.00	1.60	0.22	17.00	26.40
Embarrass River	30.00	1.10	0.38	35.90	12.54
Illinois River, Henry III	158.00	4.30	0.19	48.90	129.09
Illinois River, Henry III	232.00	3.40	0.24	52.00	189.31
Illinois River, Kingston III	202.00	4.60	0.18	49.10	167.26
Illinois River, Kingston III	194.00	6.30	0.22	537.70	268.88
Illinois River, Marseilles III	183.00	5.70	0.11	13.30	114.74
Kanawha River	259.00	3.30	0.17	24.20	145.30
Missouri river Decatur Neb	230.00	3.50	1.08	455.10	869.40
Missouri river Omaha Neb	176.00	3.40	1.61	966.20	963.42
Missouri river Sioux City Neb	229.00	3.40	1.24	309.80	965.46
New River	102.00	4.40	0.17	22.40	76.30
Salt Creek	167.00	0.20	0.47	43.20	15.70
Sangamon River	27.00	1.10	0.44	24.60	13.07
Yampa River	78.00	1.20	1.42	325.60	132.91
Yampa River	300.00	0.30	1.00	349.60	90.00
Yampa River	300.00	0.40	0.97	227.70	116.40
Yampa River	76.00	1.20	1.41	116.40	128.59
Rowinski et al (2006)					
Narew river Poland	w	d	V	dc	m3/s(derived)
Reach 1-2	9.70	0.75	0.38	8.50	2.75
2-3	11.60	0.79	0.40	12.00	3.64
3-4	12.80	0.84	0.37	9.00	4.01
4-5	15.20	0.75	0.35	21.00	3.93
5-6	13.20	0.83	0.37	15.00	4.10
6-7	11.40	1.09	0.34	15.00	4.16
7-8	17.70	0.87	0.28	70.00	4.36
8-9	16.90	0.94	0.29	21.00	4.65
9-10	17.40	0.74	0.36	19.00	4.64
10-11	17.00	0.94	0.32	29.00	5.07
11-12	19.90	0.89	0.29	18.00	5.12
12-13	18.00	1.07	0.30	30.00	5.82
Singh and Beck (2003)					

Reach					
Calder-1	6.40	0.19	0.142	0.54	0.17
Calder-2	6.40	0.19	0.207	0.50	0.25
Calder-3	6.40	0.19	0.175	1.45	0.21
Calder-4	8.10	0.23	0.442	0.48	0.82
Rutherford (1994)	Width	Depth	Velocity	Disp coeff	flow derived
Punehu	5.00	0.28	0.26	7.20	0.36
Kapuni	9.00	0.30	0.37	8.40	1.00
Kapuni	10.00	0.35	0.53	12.40	1.86
Manganui	20.00	0.40	0.19	6.50	1.52
Waiongana	13.00	0.60	0.48	6.80	3.74
Stony	10.00	0.63	0.55	13.50	3.47
Waiotapu	11.40	0.75	0.41	8.00	3.51
Manawatu	59.00	0.72	0.37	32.00	15.72
Manawatu	63.00	1.00	0.32	22.00	20.16
Manawatu	60.00	0.95	0.46	47.00	26.22
Tarawera	25.00	1.21	0.73	27.00	22.08
Tarawera	20.00	1.92	0.62	11.50	23.81
Tarawera	25.00	1.38	0.77	20.50	26.57
Tarawera	25.00	1.40	0.78	15.50	27.30
Tarawera	25.00	1.57	0.83	18.00	32.58
Waikato	85.00	2.60	0.69	52.00	152.49
Waikato	120.00	2.00	0.64	67.00	153.60

Appendix B. Temporal concentration profiles

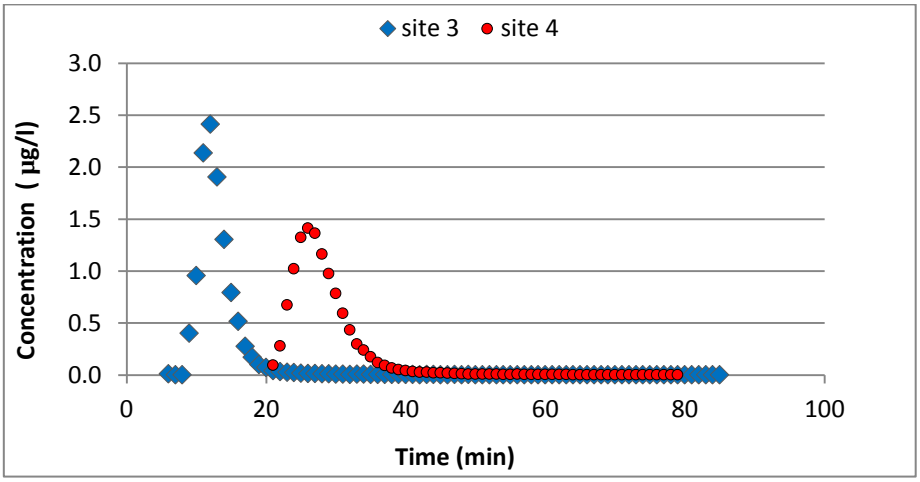

Experiment 3: Temporal concentration profiles

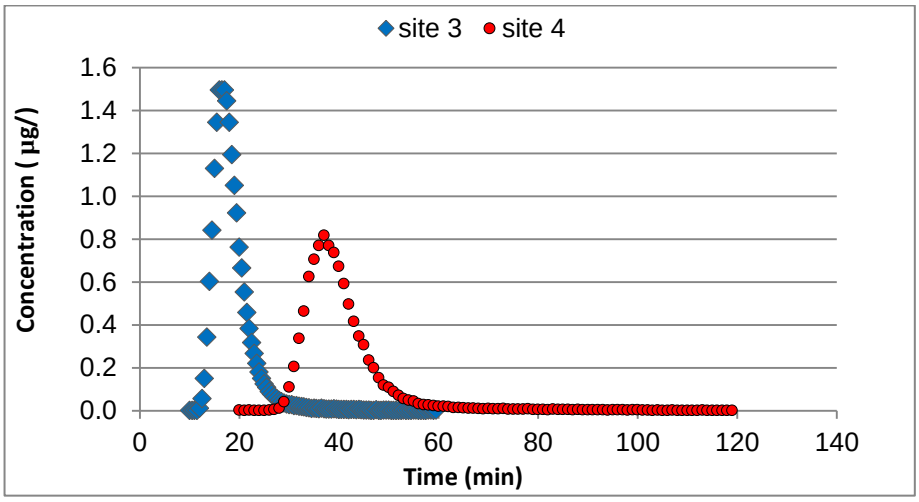

Experiment 4: Temporal concentration profiles

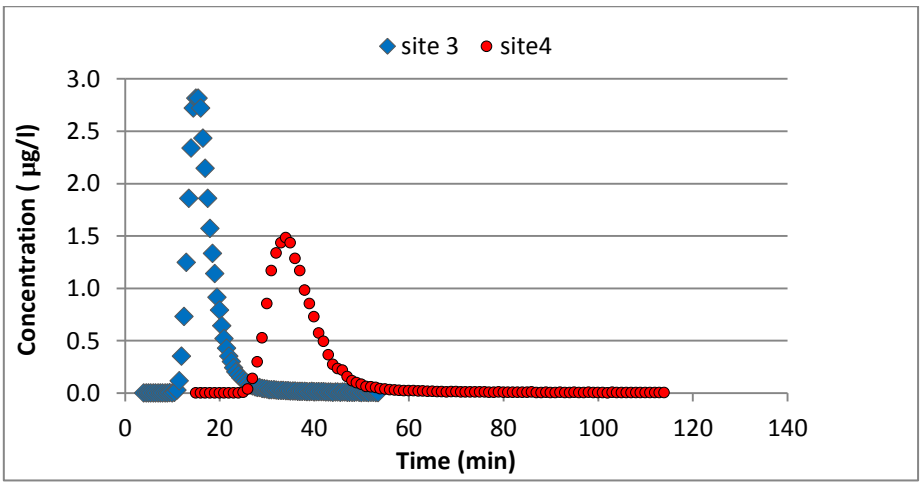

Experiment 5: Temporal concentration profiles

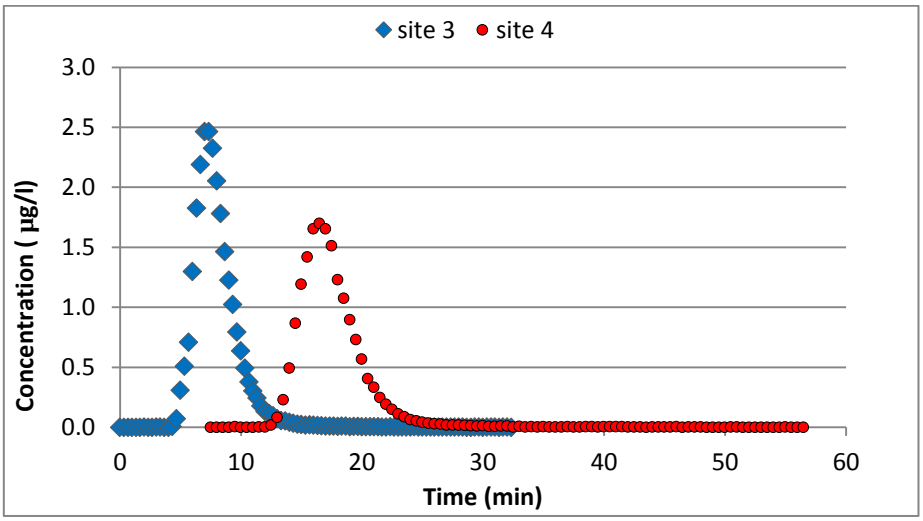

Experiment 6: Temporal concentration profiles

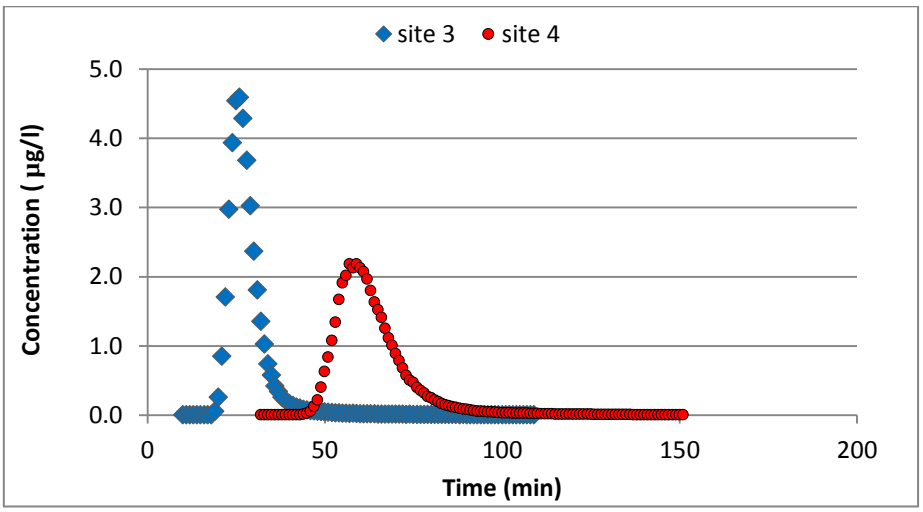

Experiment 7: Temporal concentration profiles

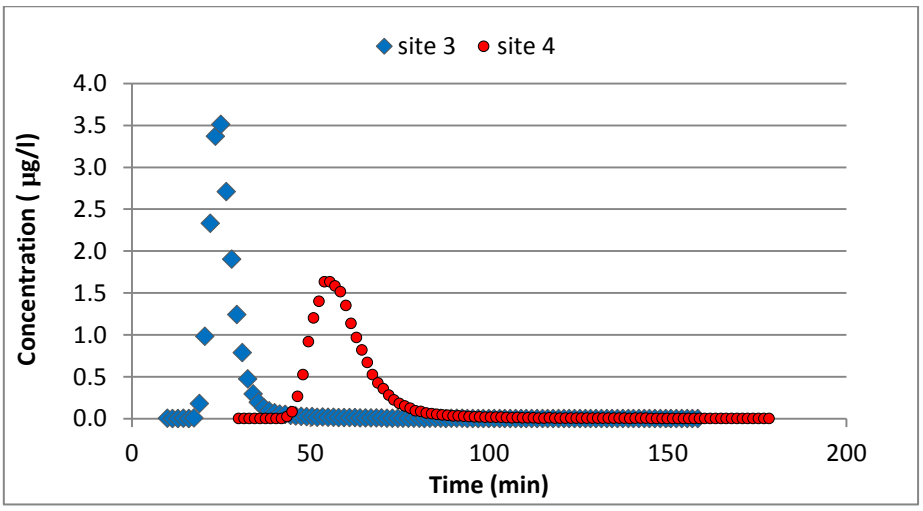

Experiment 8: Temporal concentration profiles

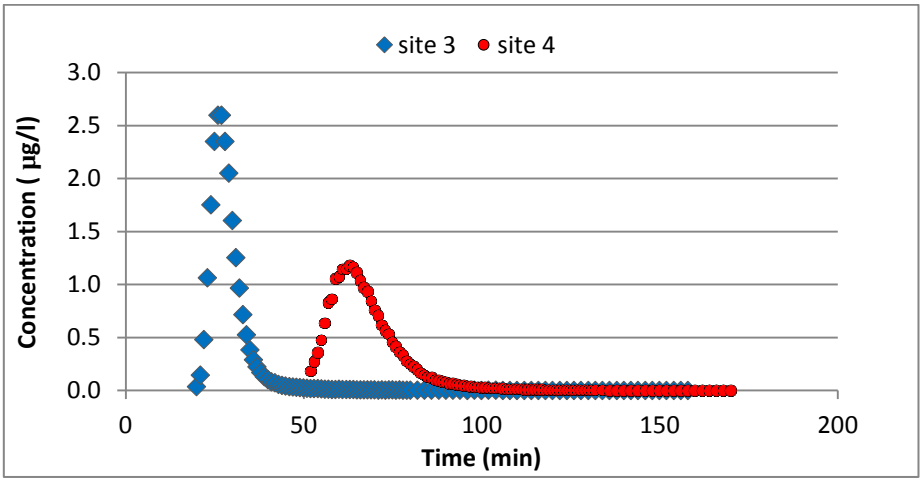

Experiment 9: Temporal concentration profiles

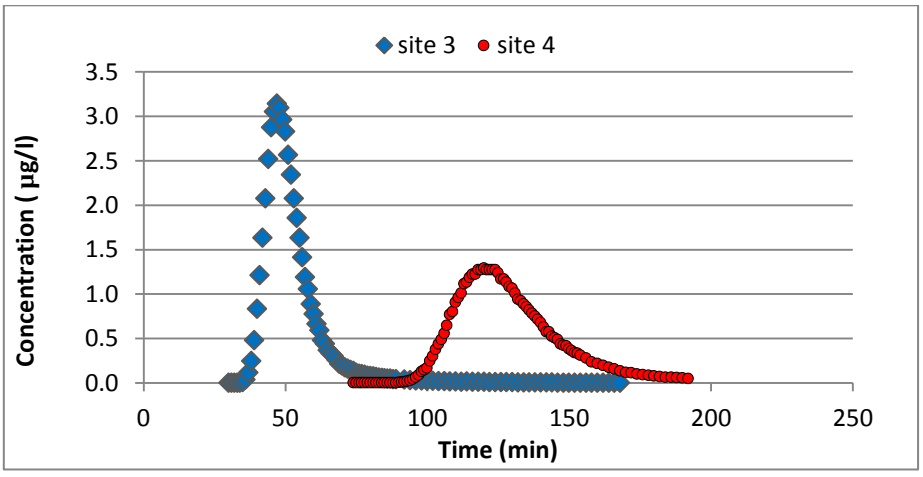

Experiment 10: Temporal concentration profiles

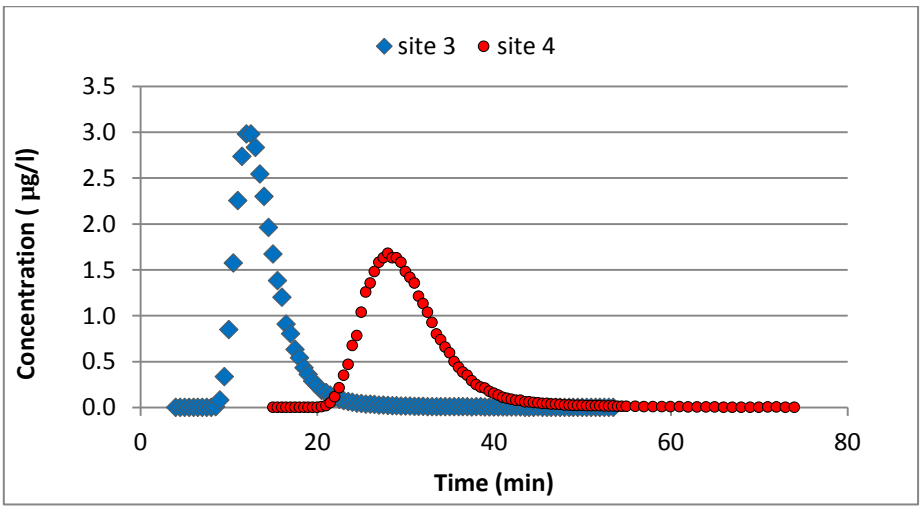

Experiment 11: Temporal concentration profiles

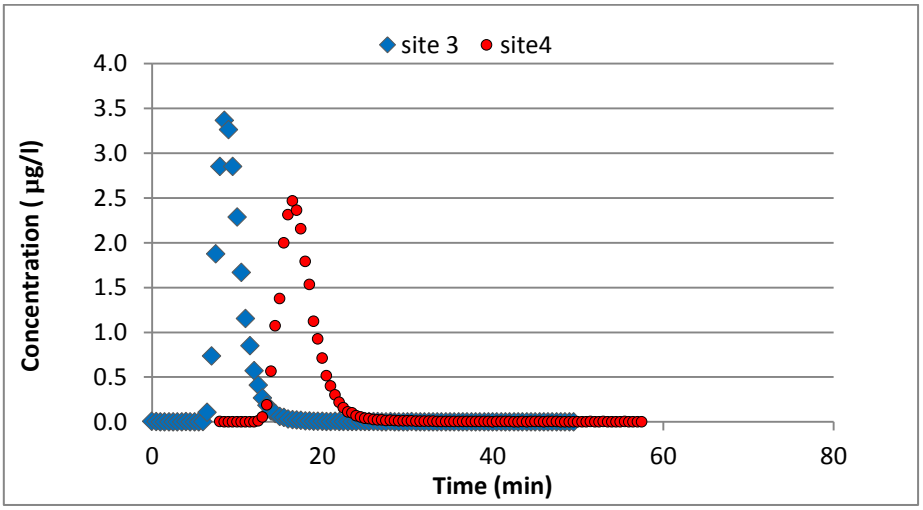

Experiment 12: Temporal concentration profiles

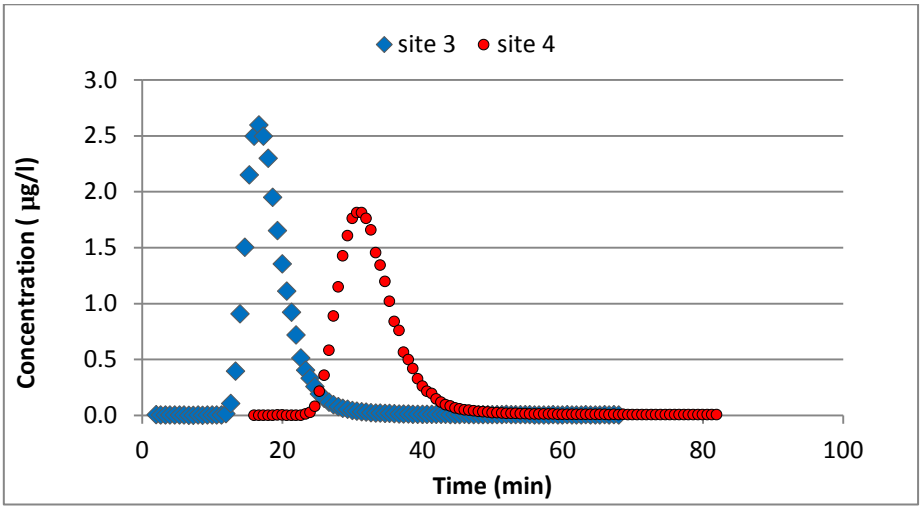

Experiment 13: Temporal concentration profiles

Appendix C. Routing procedure profiles

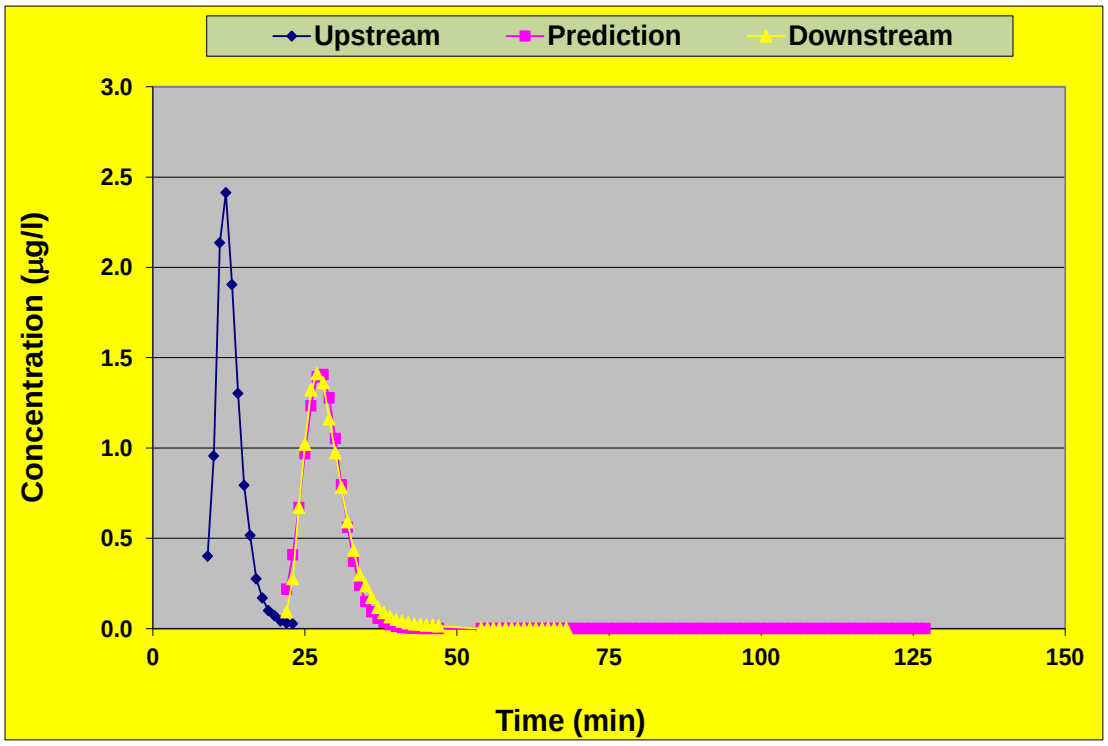

Experiment 3: Routing procedure (using scaled, truncated data)

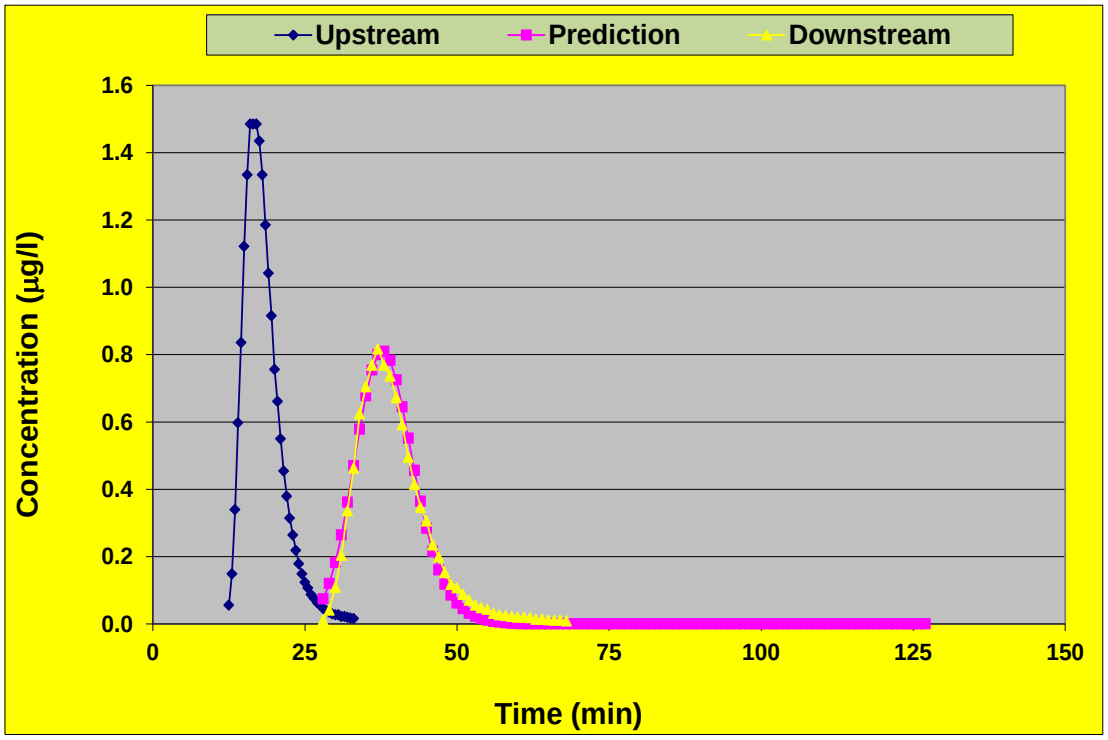

Experiment 4: Routing procedure

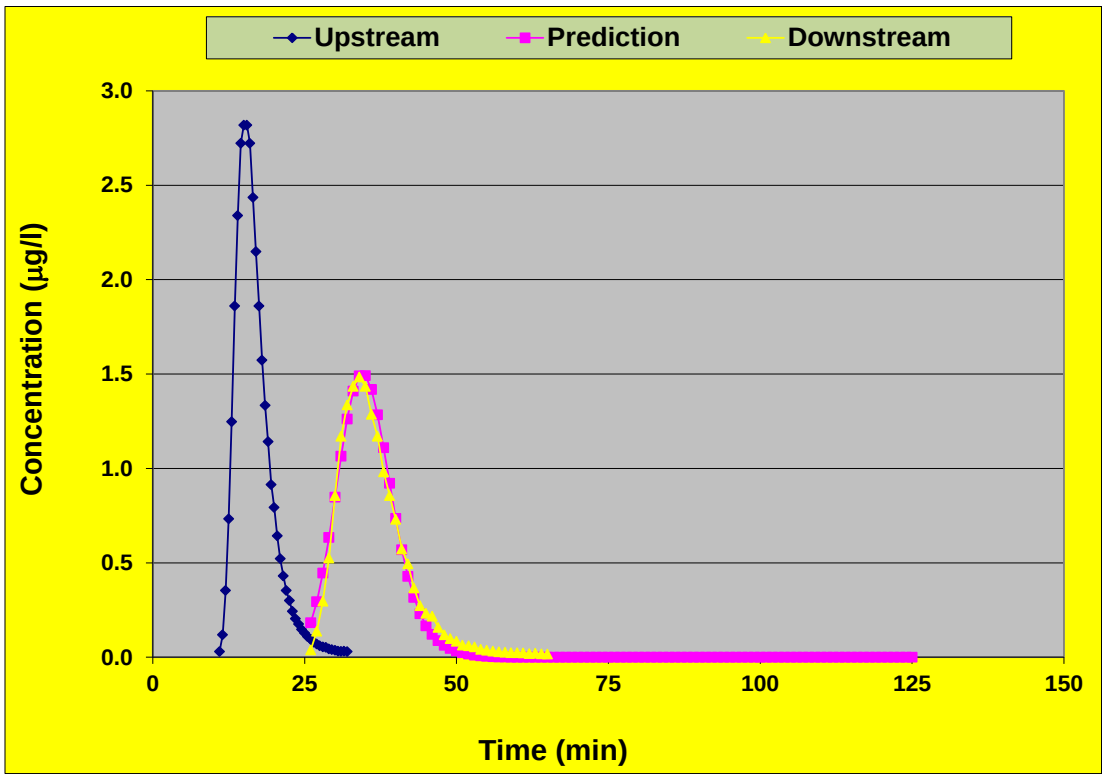

Experiment 5: Routing procedure

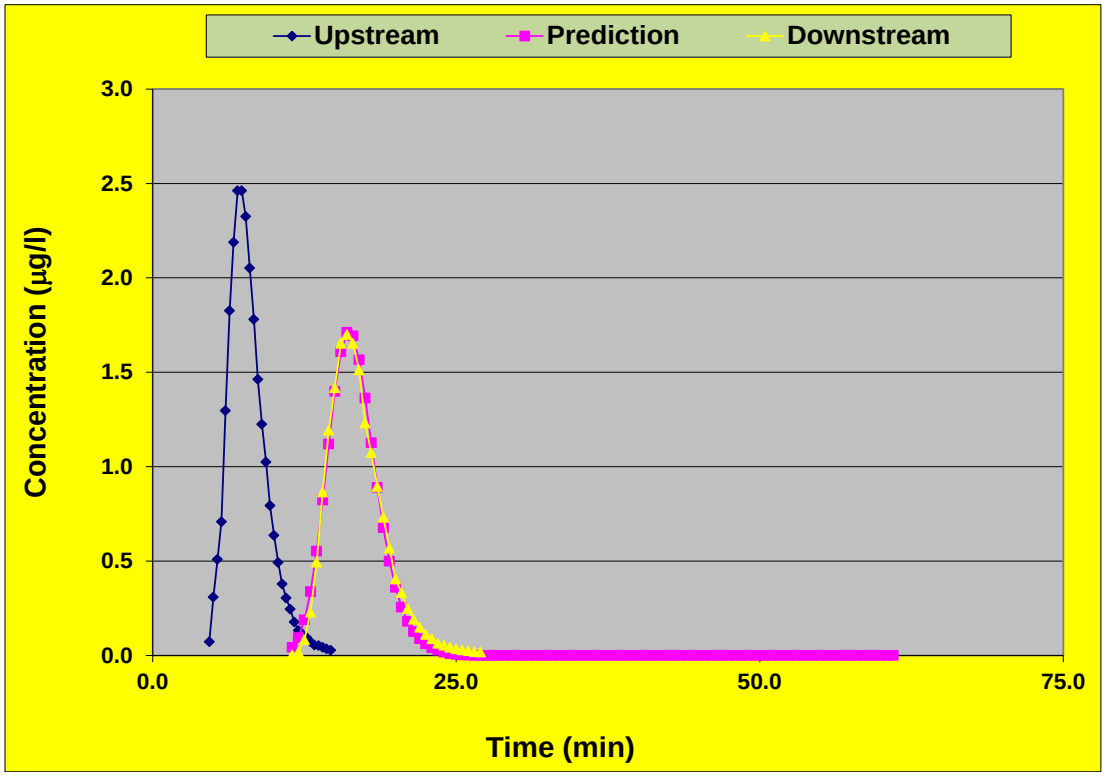

Experiment 6: Routing procedure

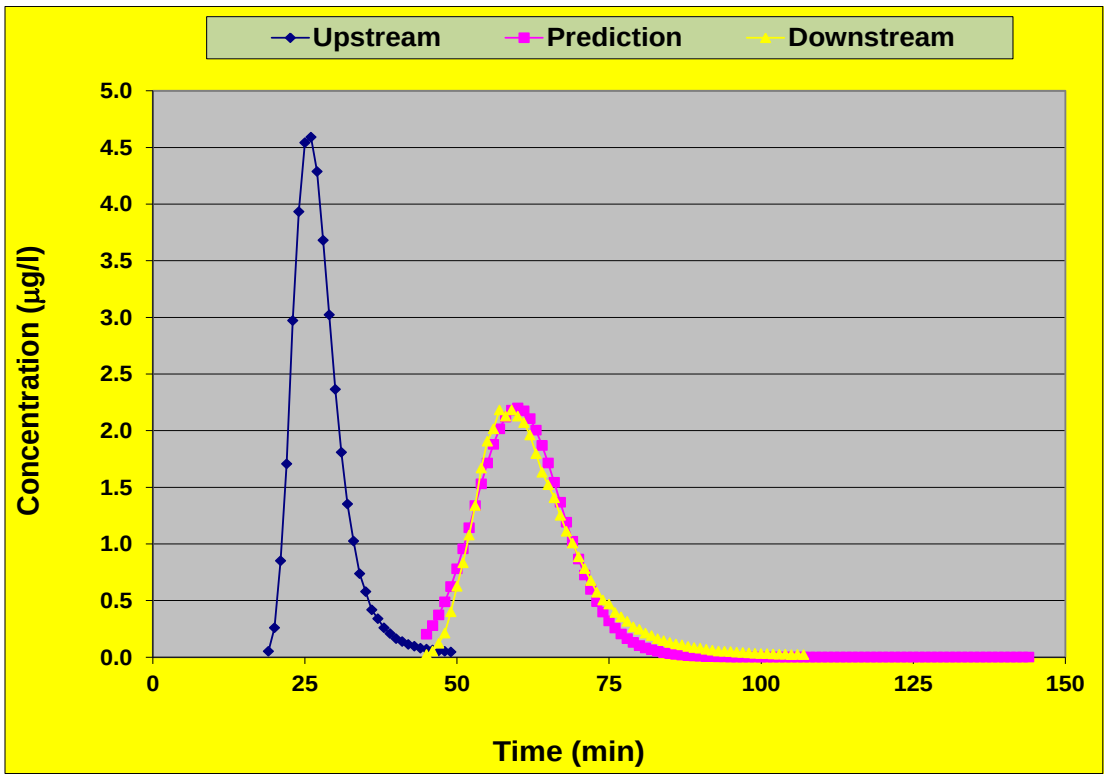

Experiment 7: Routing procedure

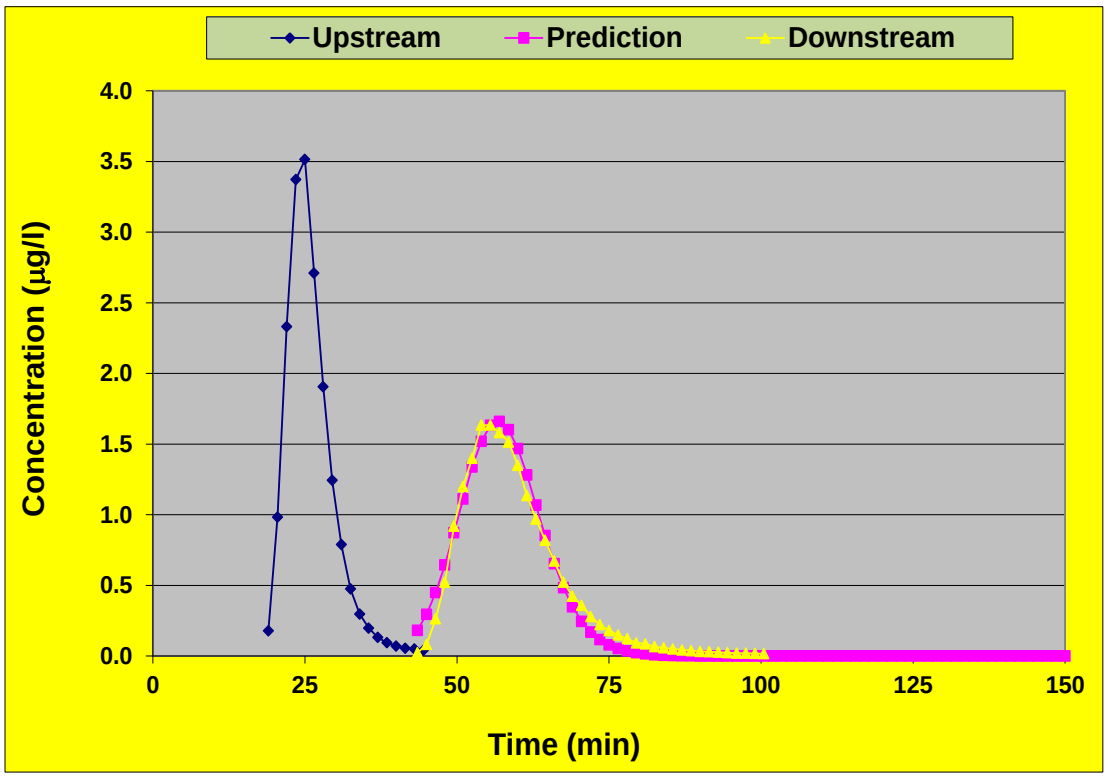

Experiment 8: Routing procedure

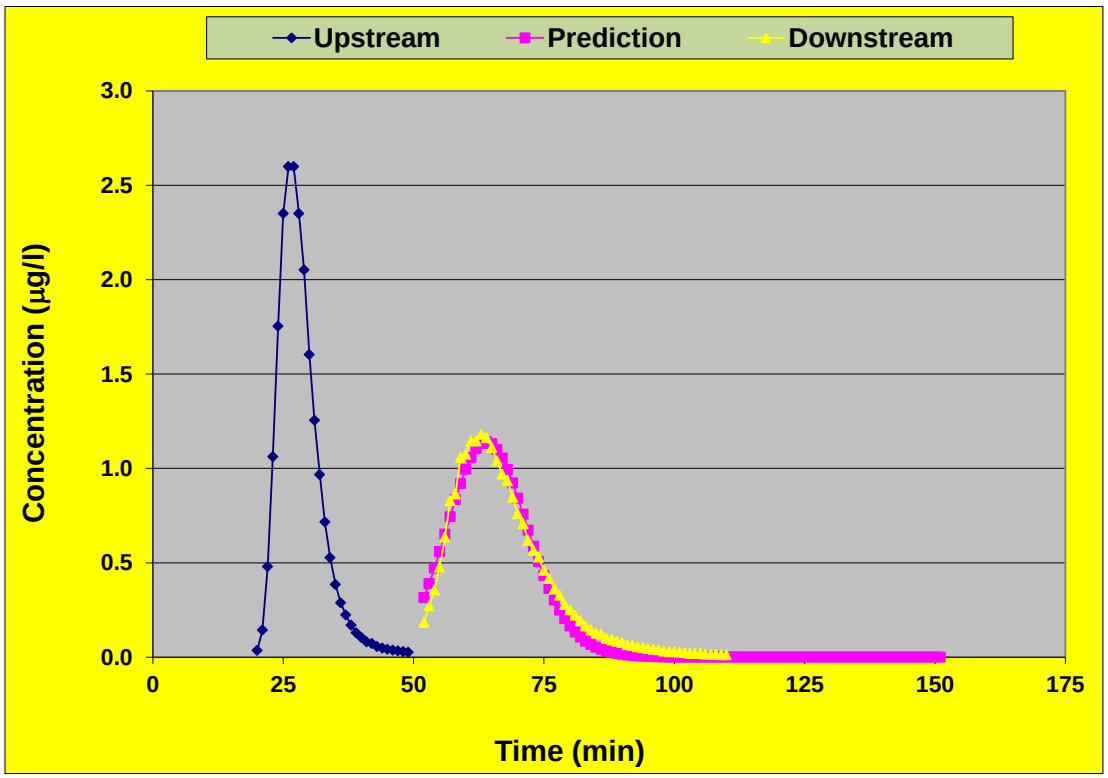

Experiment 9: Routing procedure

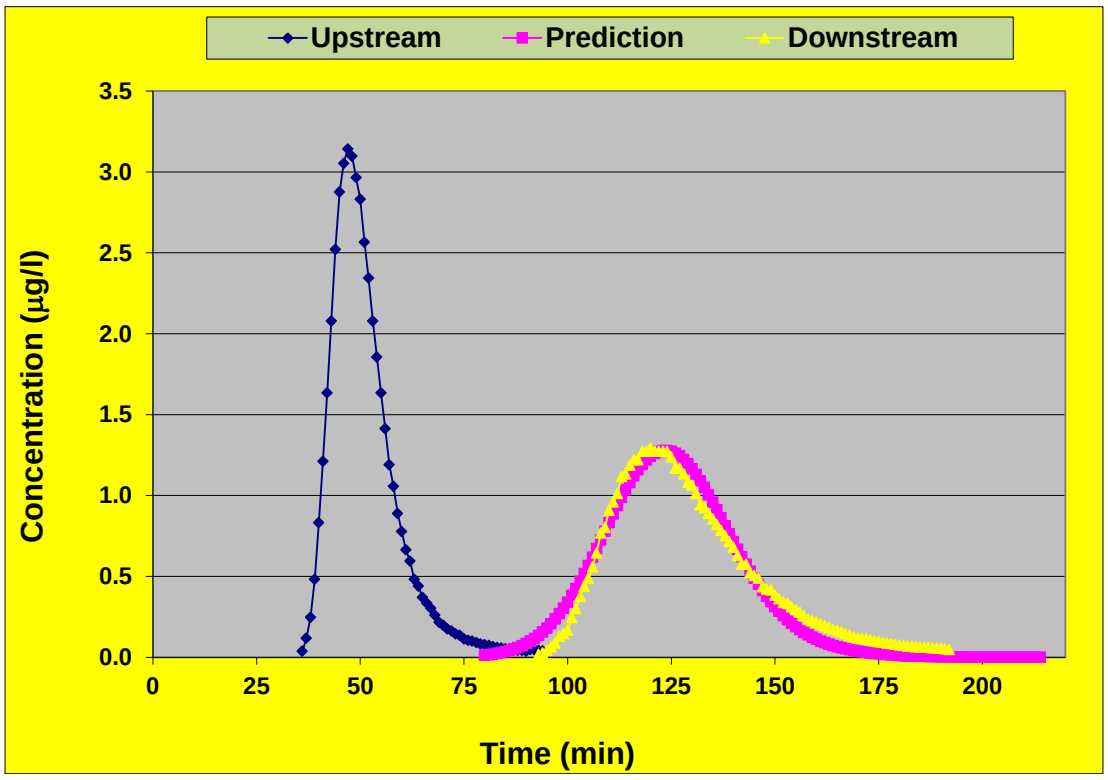

Experiment 10: Routing procedure

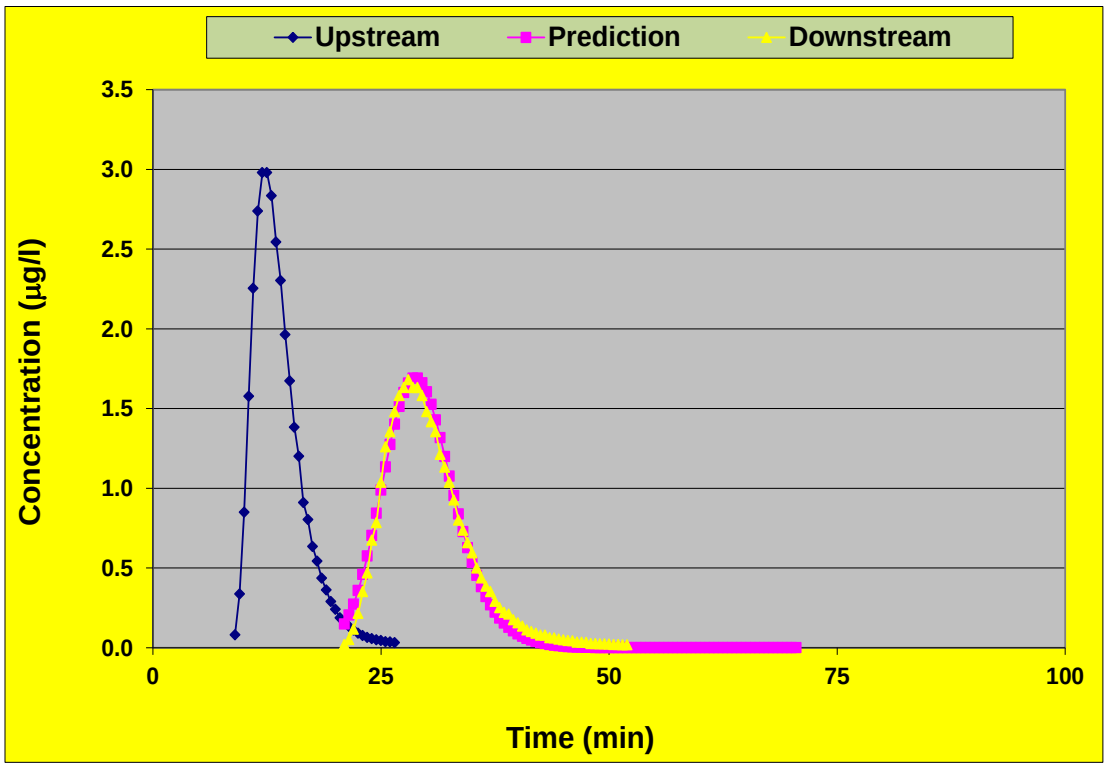

Experiment 11: Routing procedure

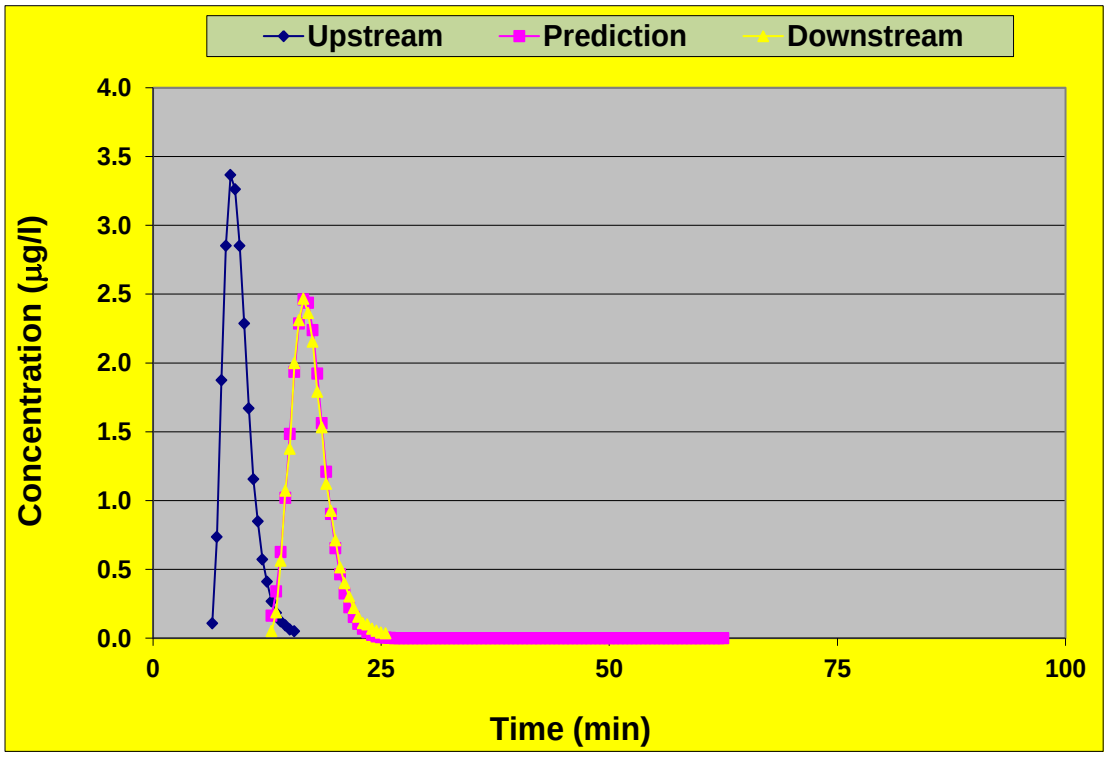

Experiment 12: Routing procedure

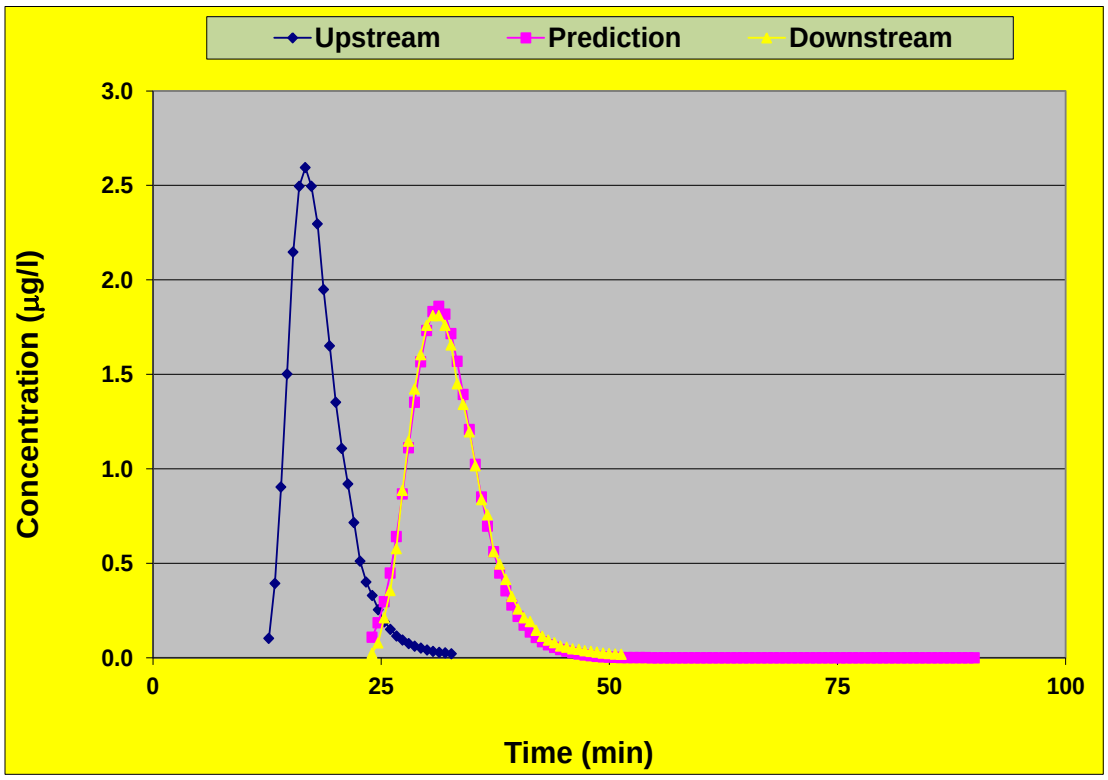

Experiment 13: Routing procedure

Appendix D. Analytical solution profiles

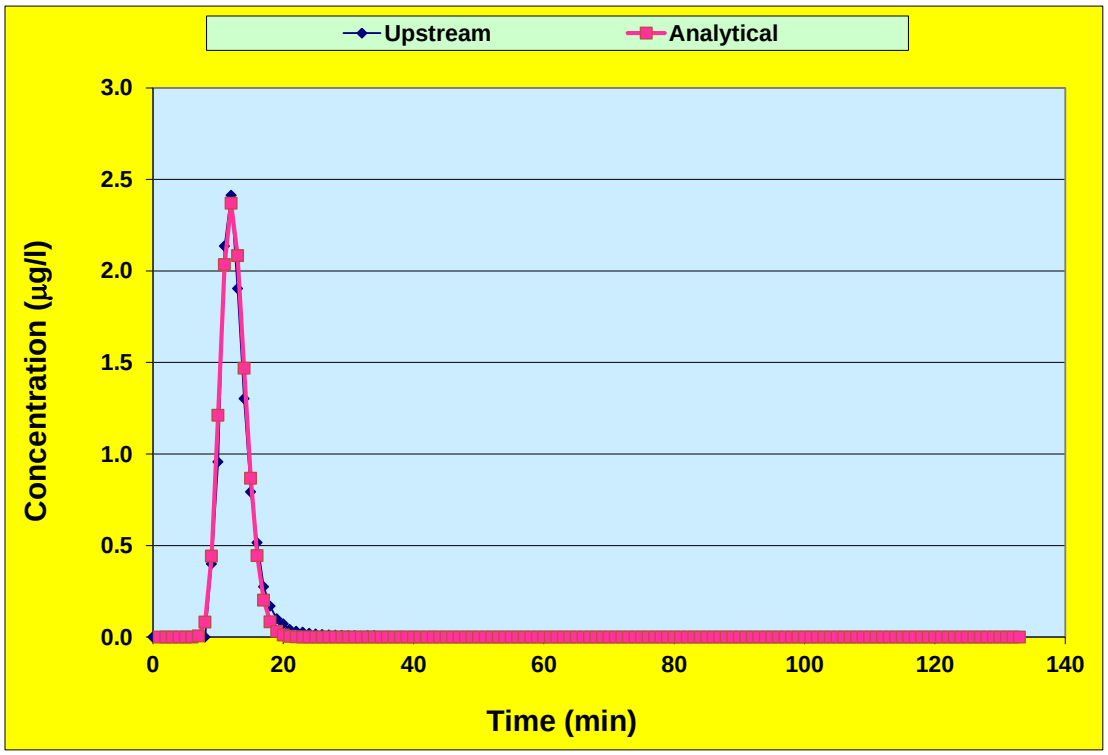

Experiment 3: Analytical solution upstream

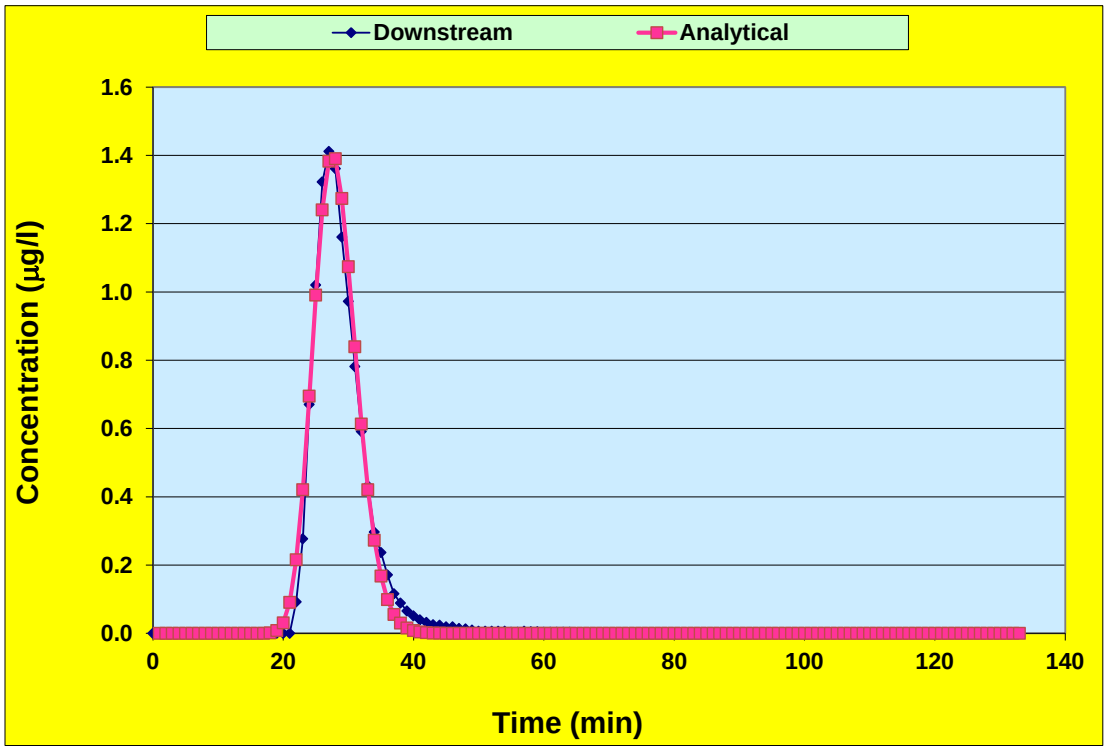

Experiment 3: Analytical solution downstream

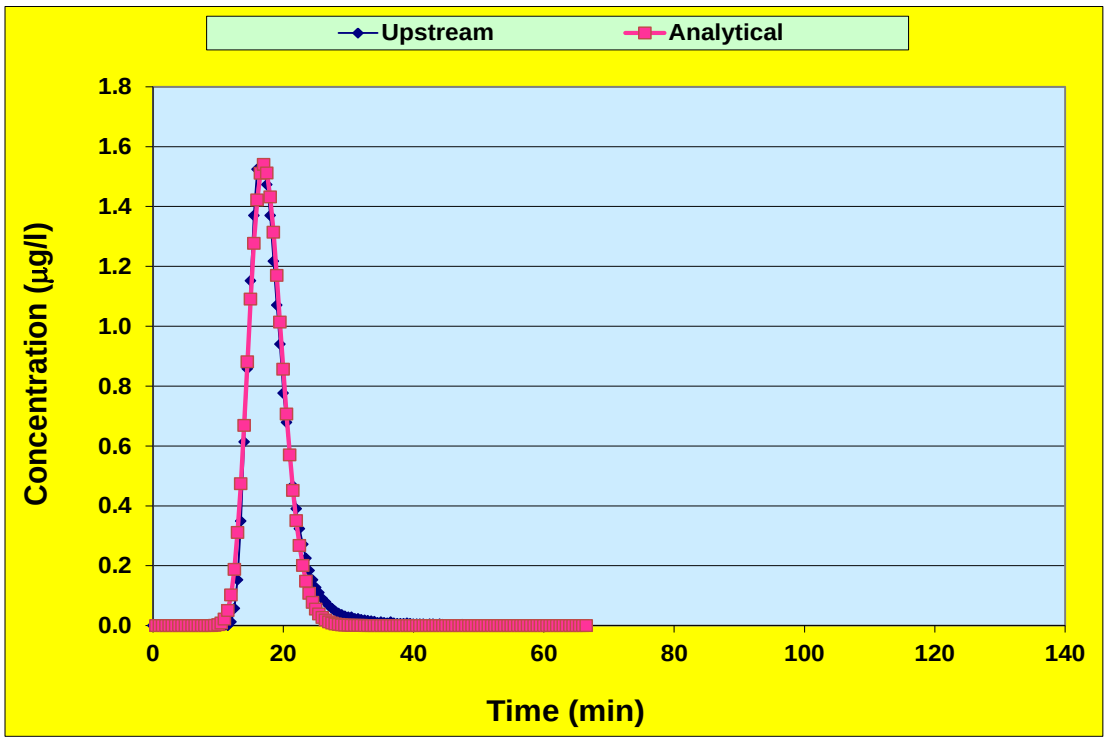

Experiment 4: Analytical solution upstream

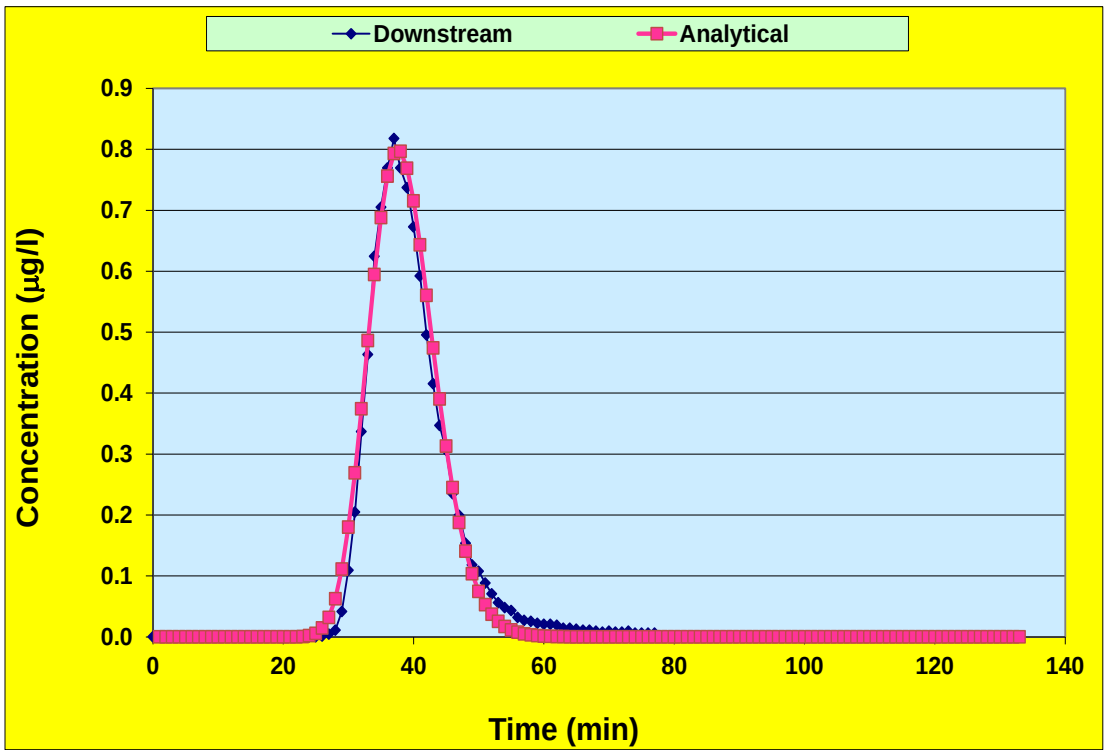

Experiment 4: Analytical solution downstream

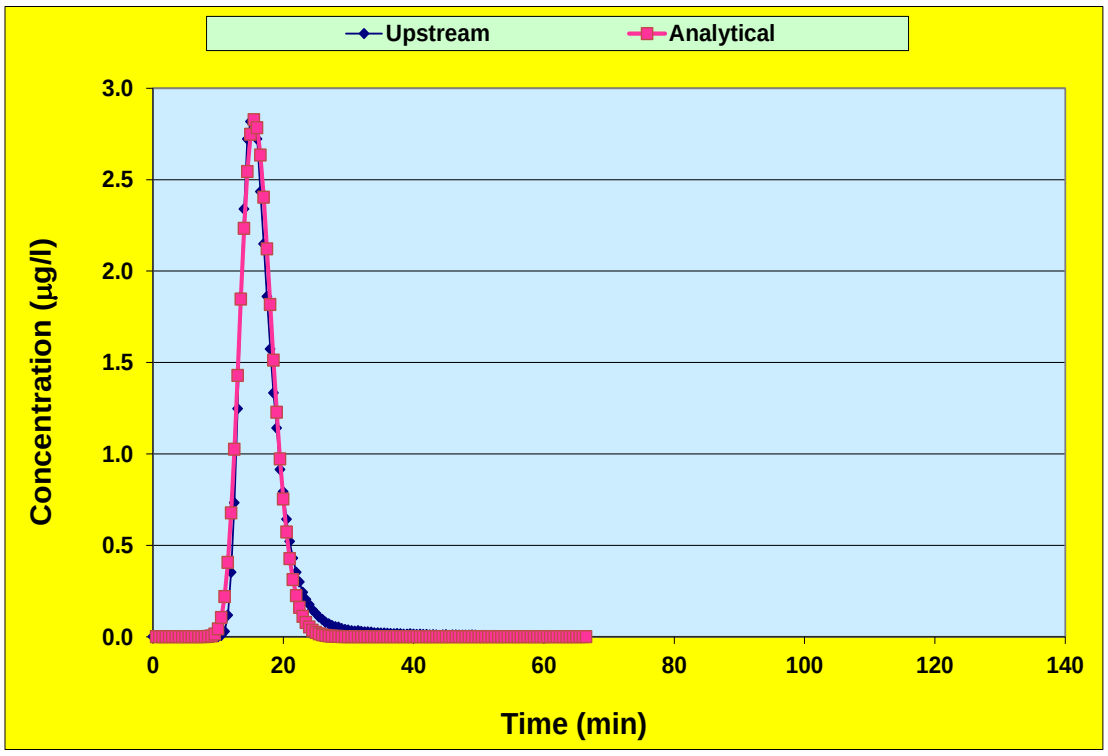

Experiment 5: Analytical solution upstream

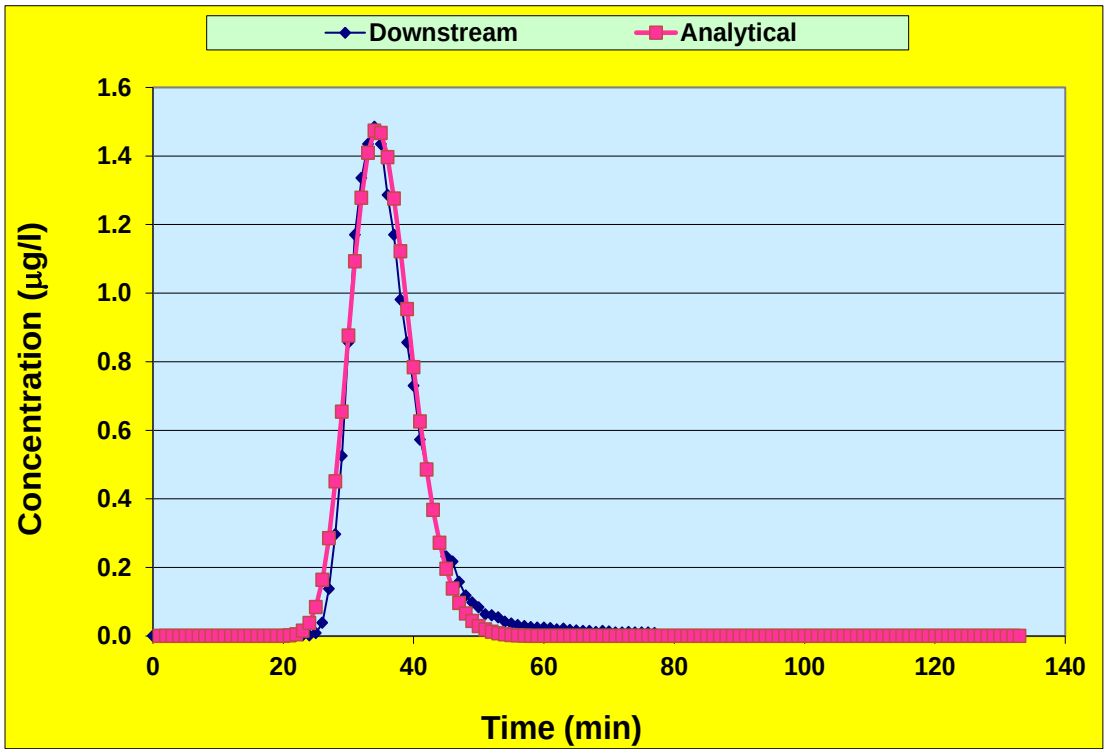

Experiment 5: Analytical solution downstream

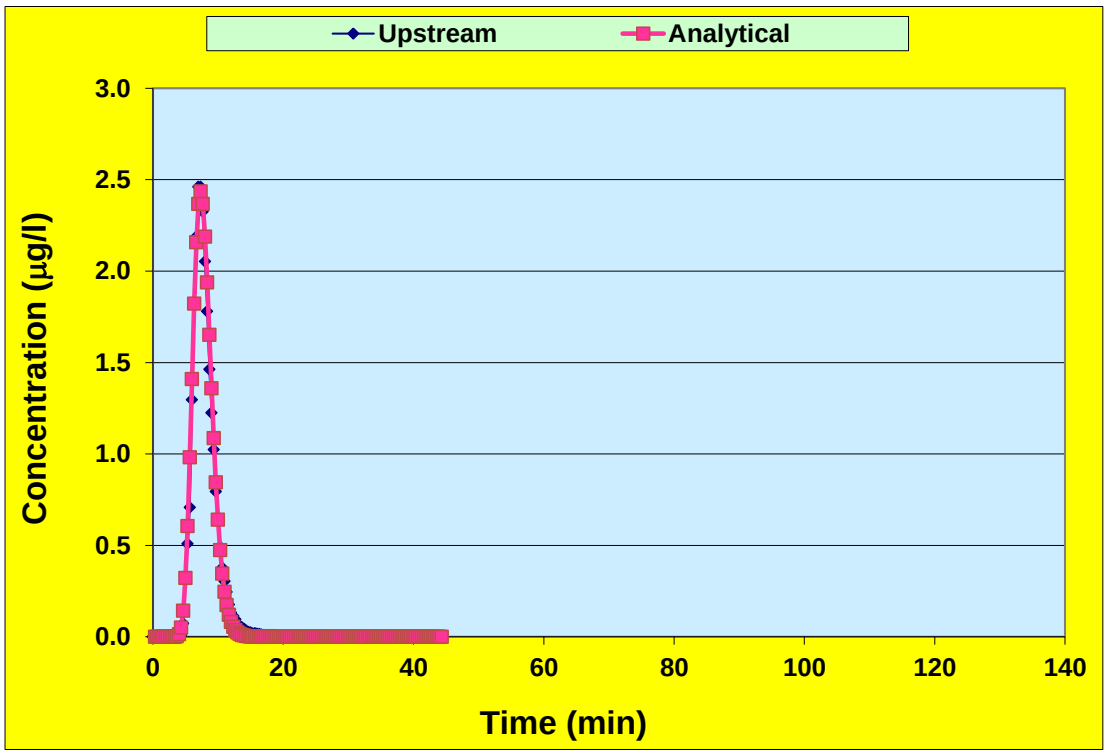

Experiment 6: Analytical solution upstream

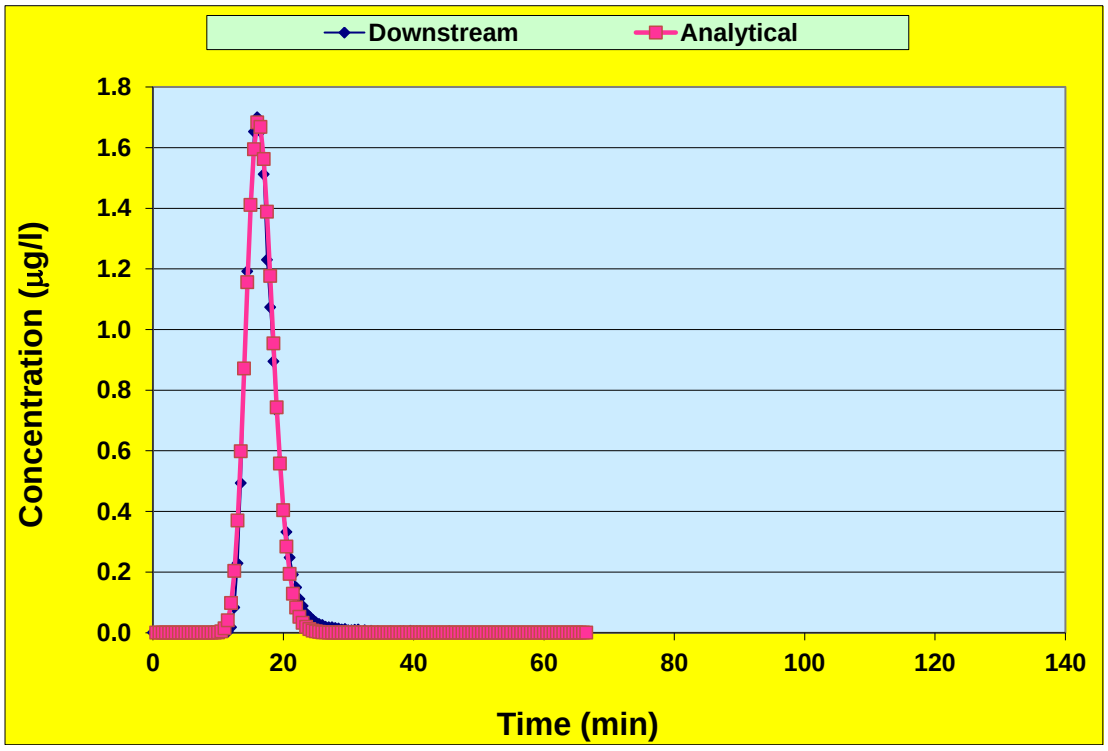

Experiment 6: Analytical solution downstream

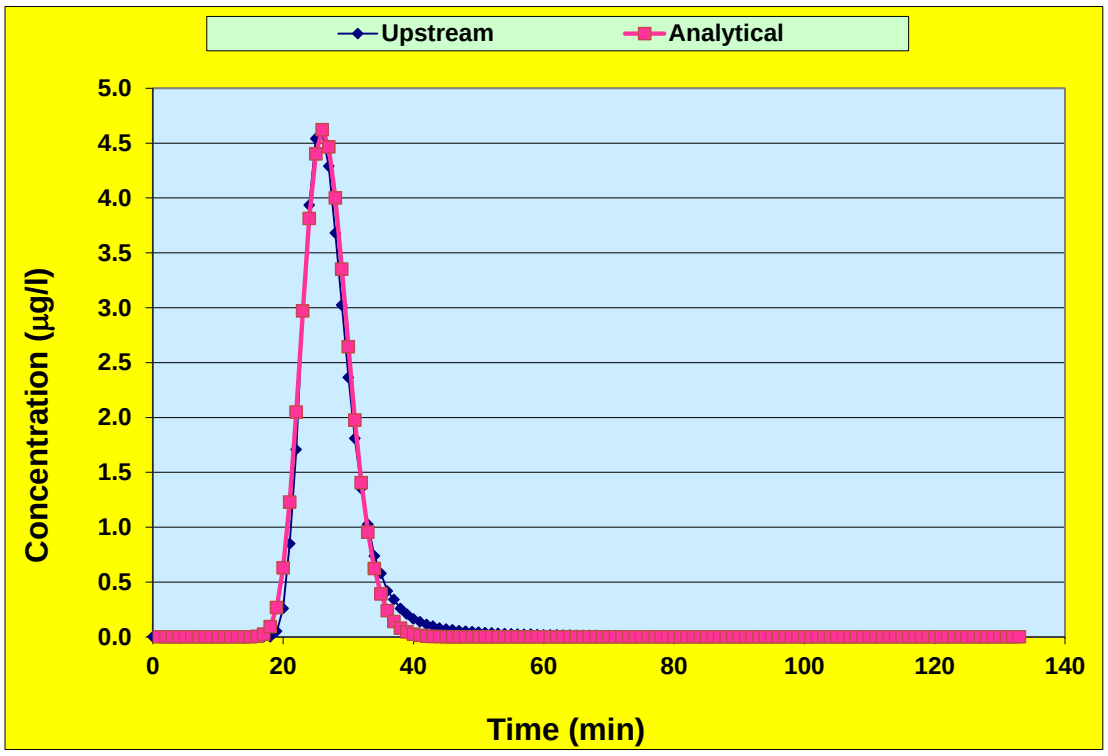

Experiment 7: Analytical solution upstream

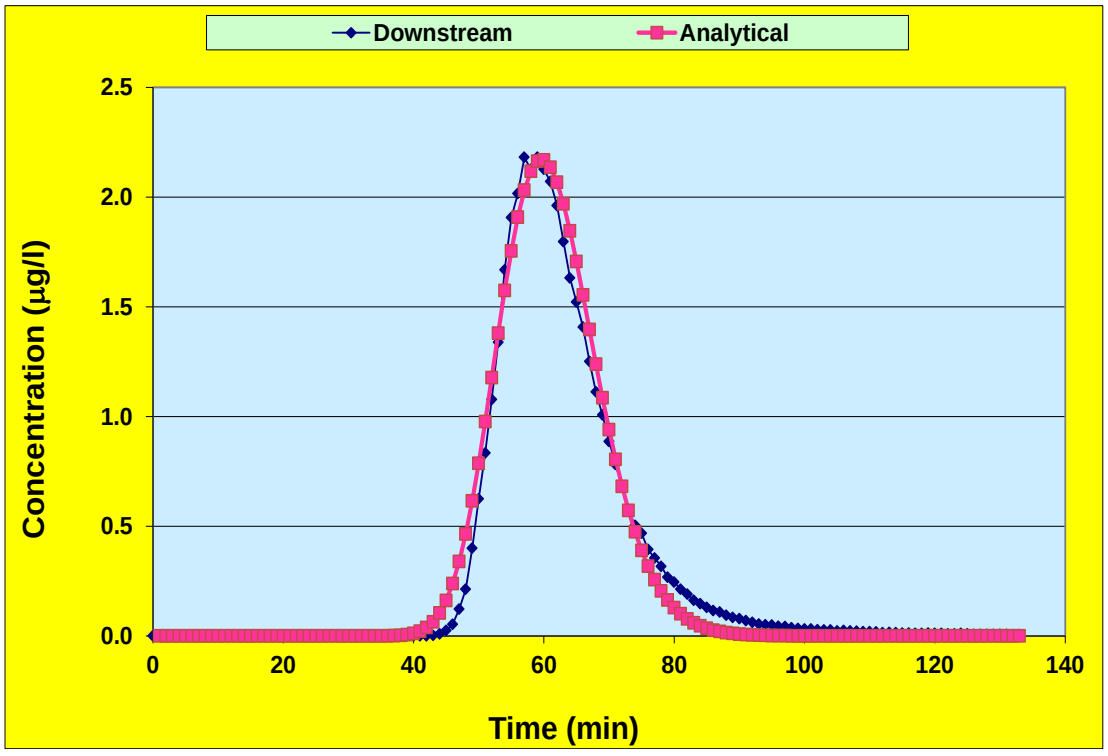

Experiment 7: Analytical solution downstream

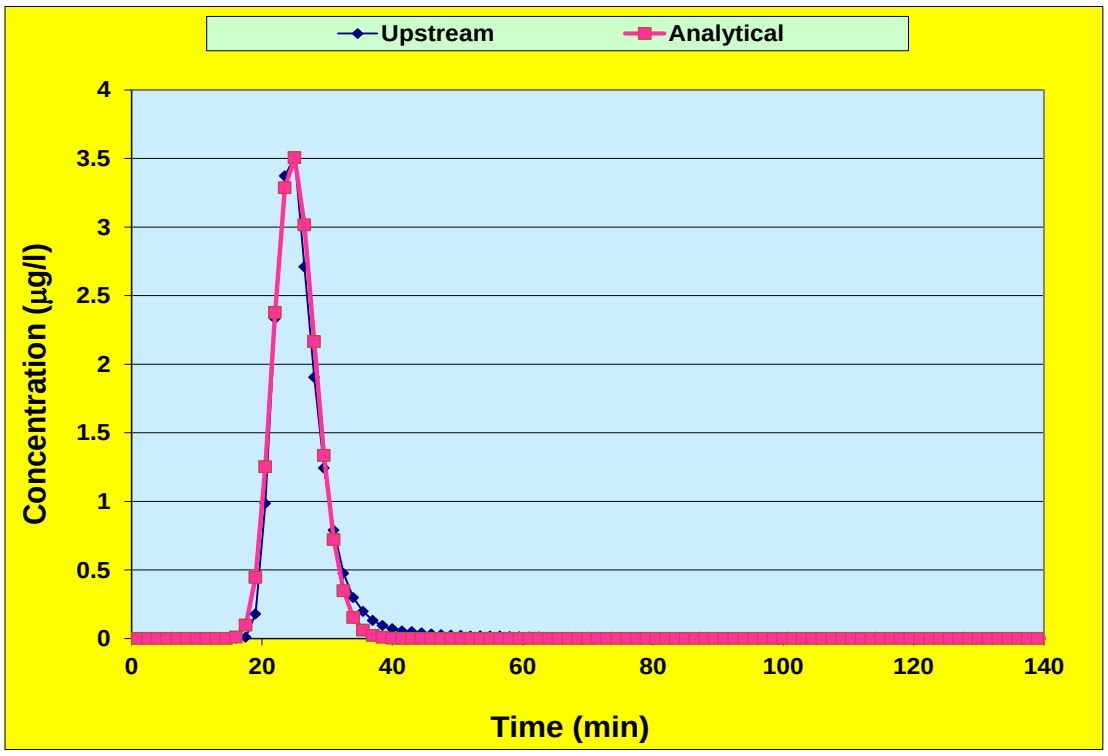

Experiment 8: Analytical solution upstream

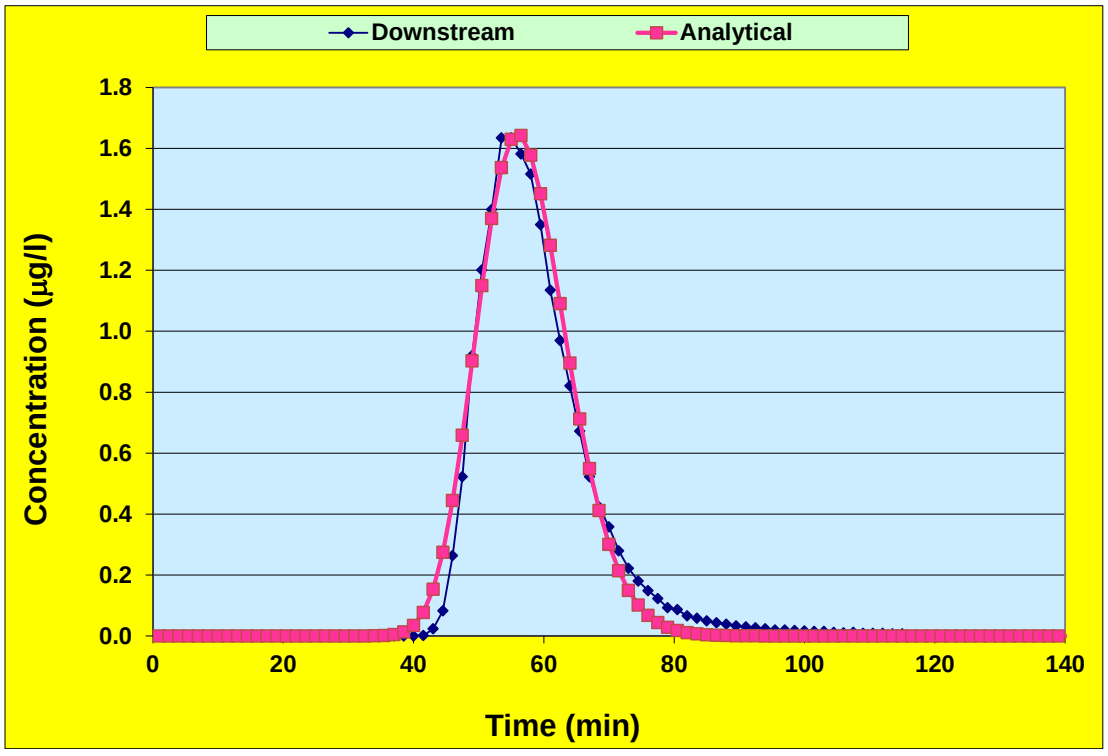

Experiment 8: Analytical solution downstream

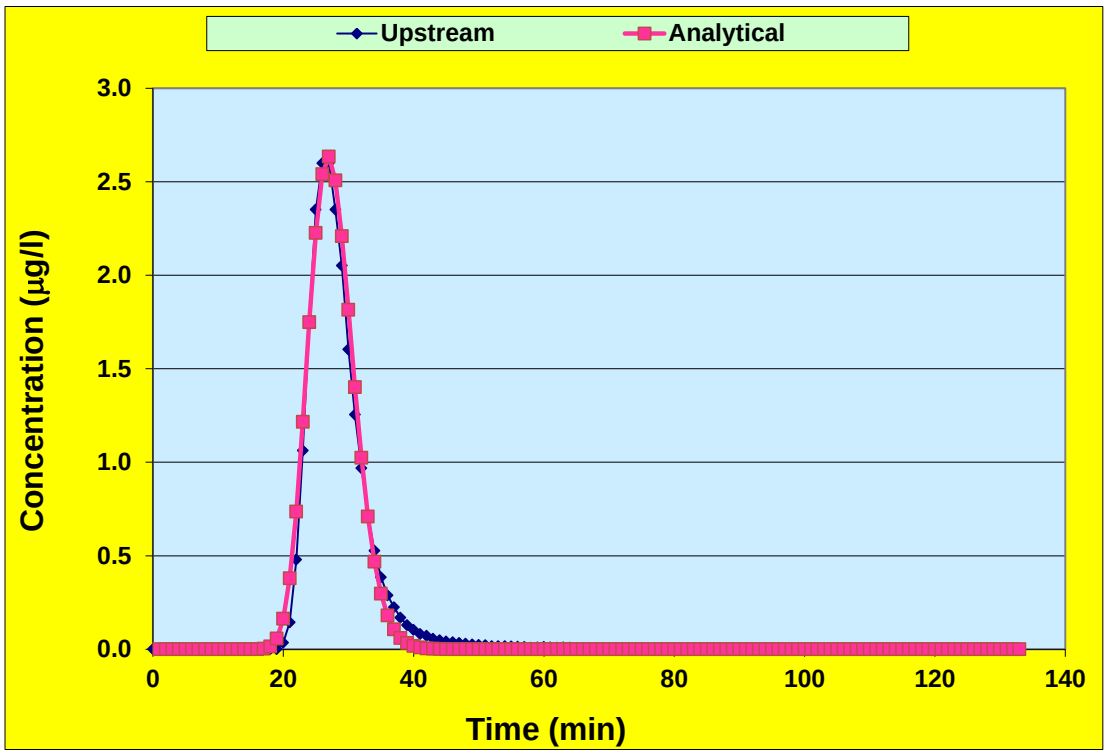

Experiment 9: Analytical solution upstream

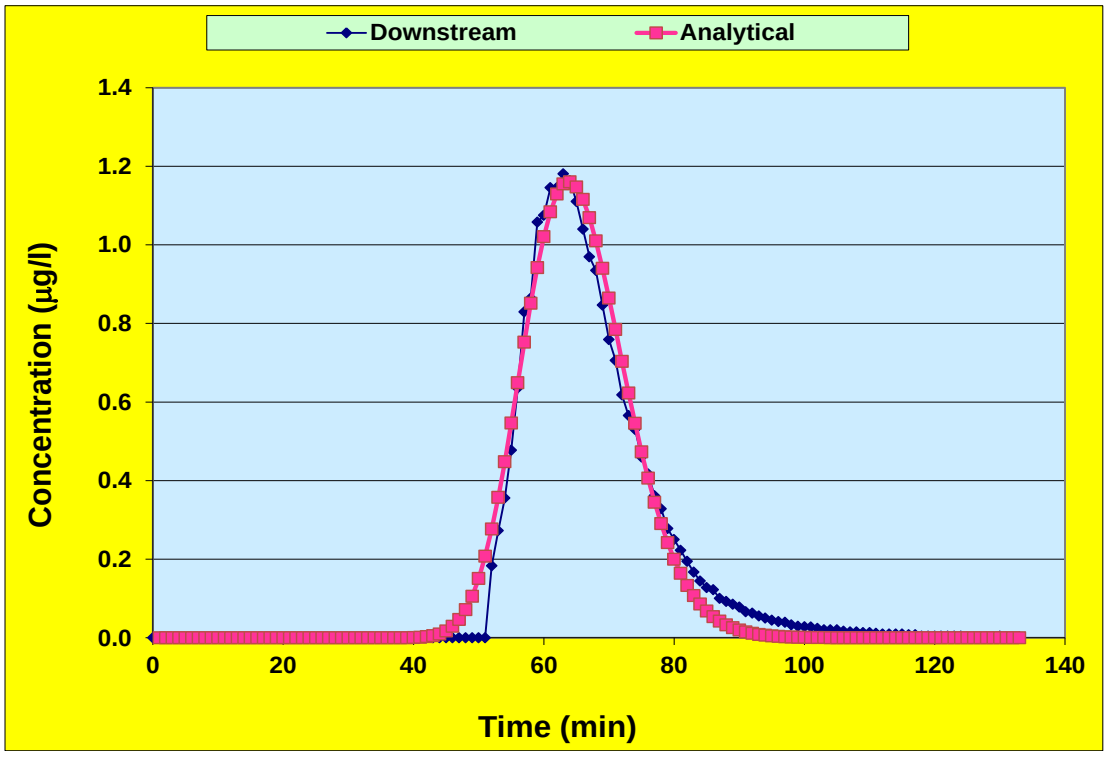

Experiment 9: Analytical solution downstream

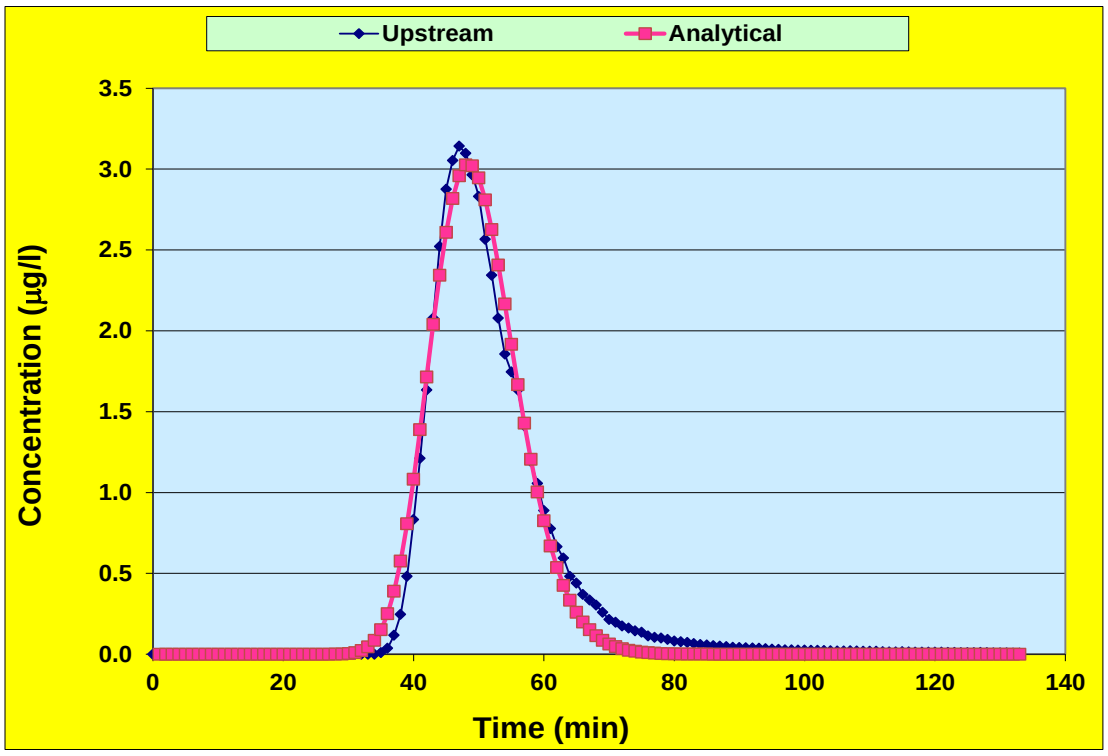

Experiment 10: Analytical solution upstream

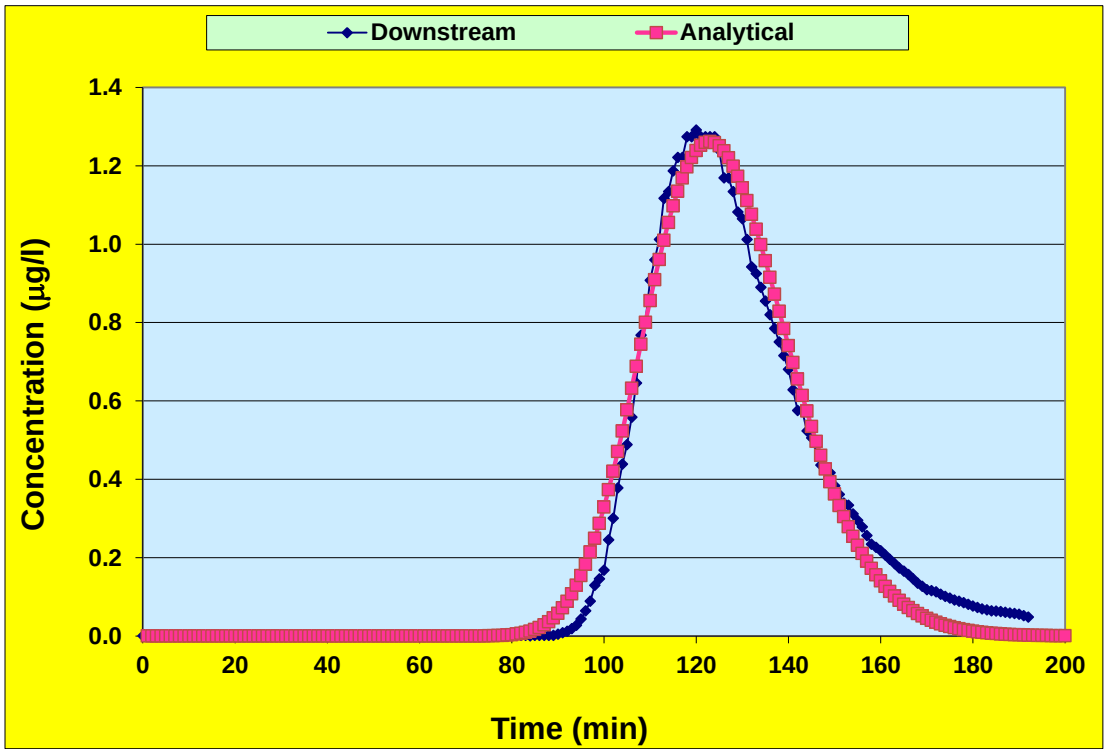

Experiment 10: Analytical solution downstream

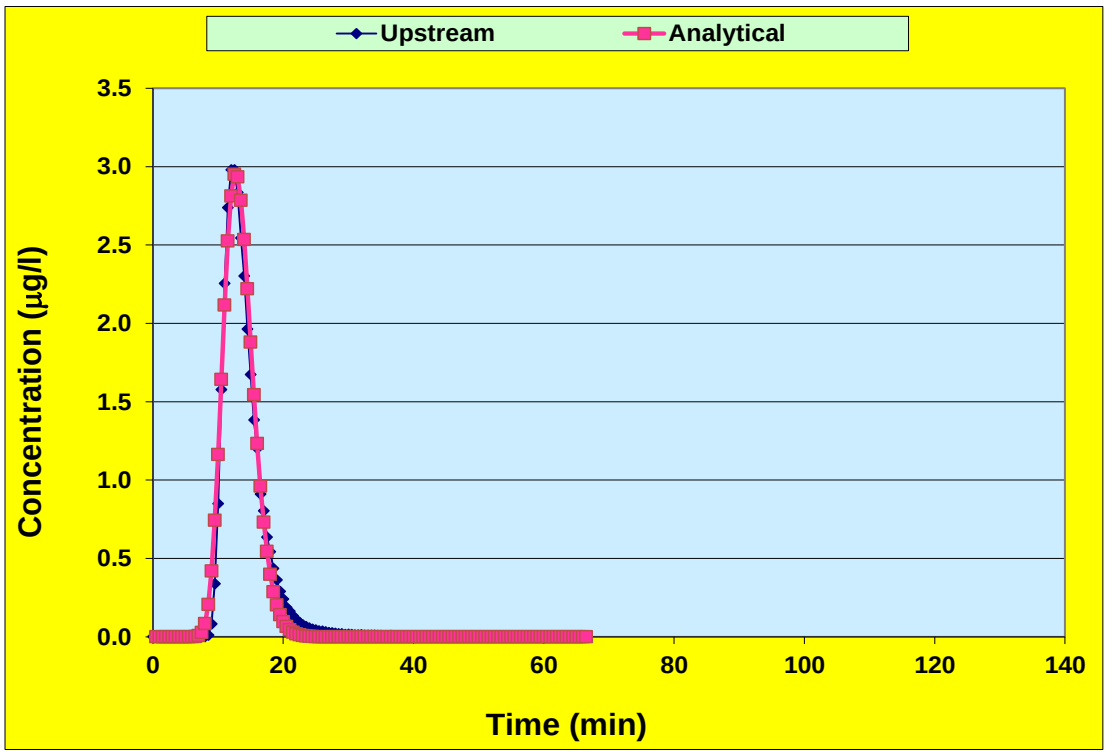

Experiment 11: Analytical solution upstream

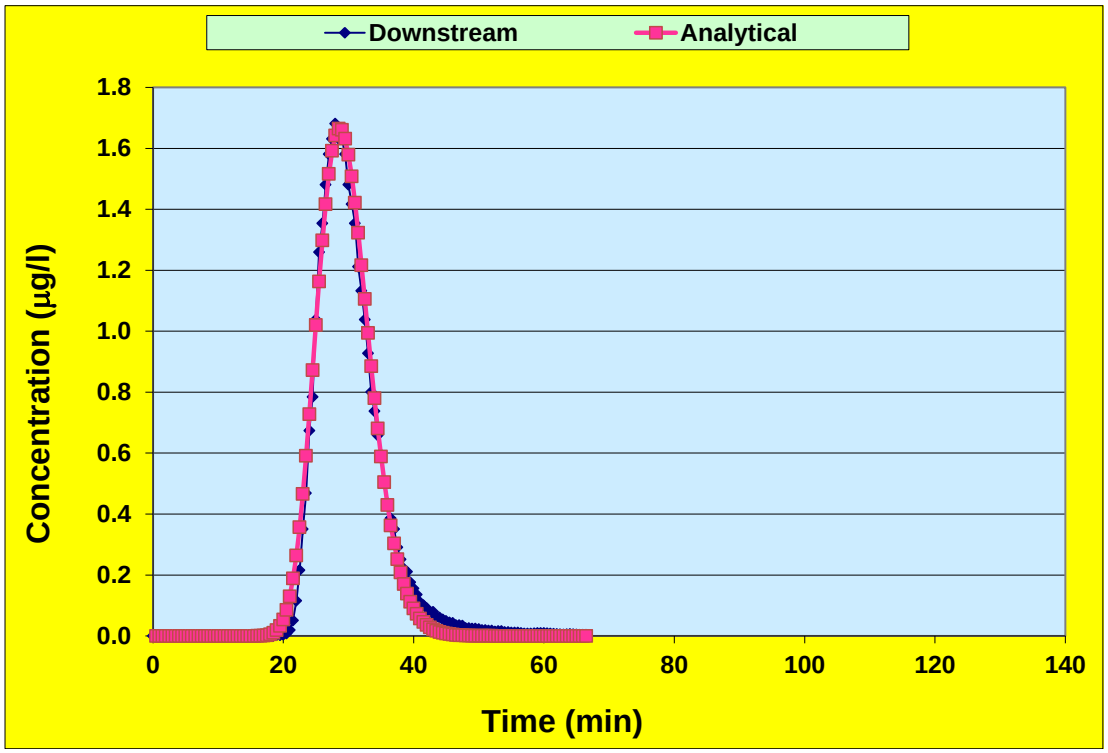

Experiment 11: Analytical solution downstream

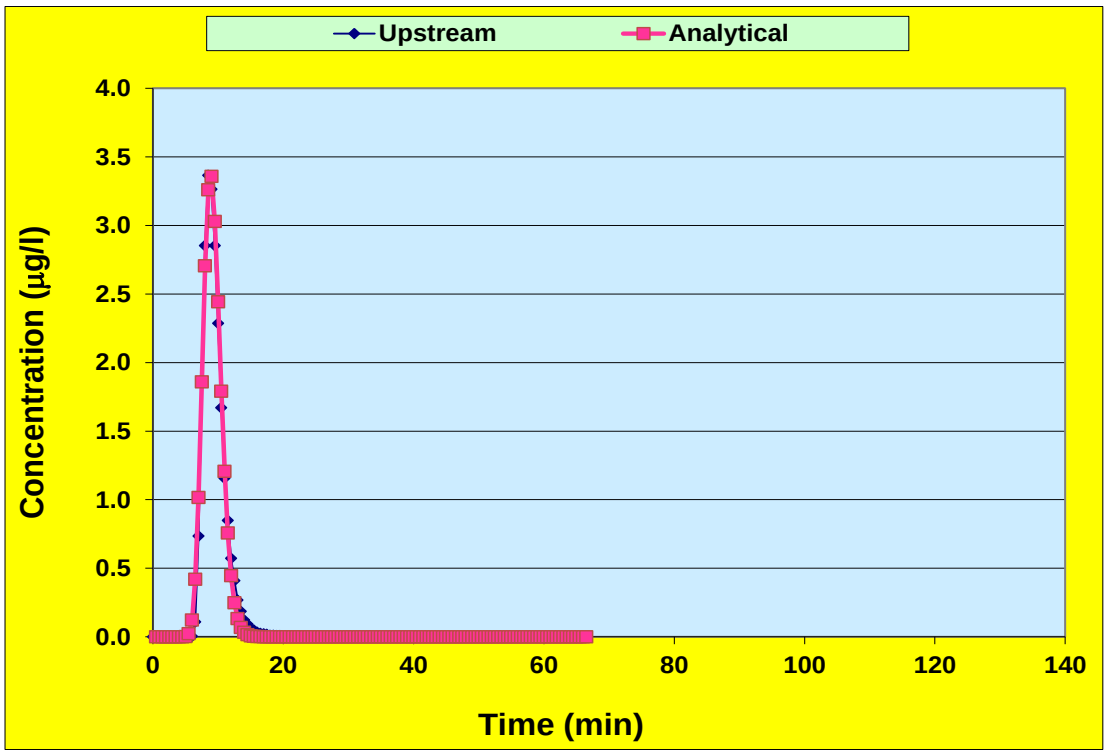

Experiment 12: Analytical solution upstream

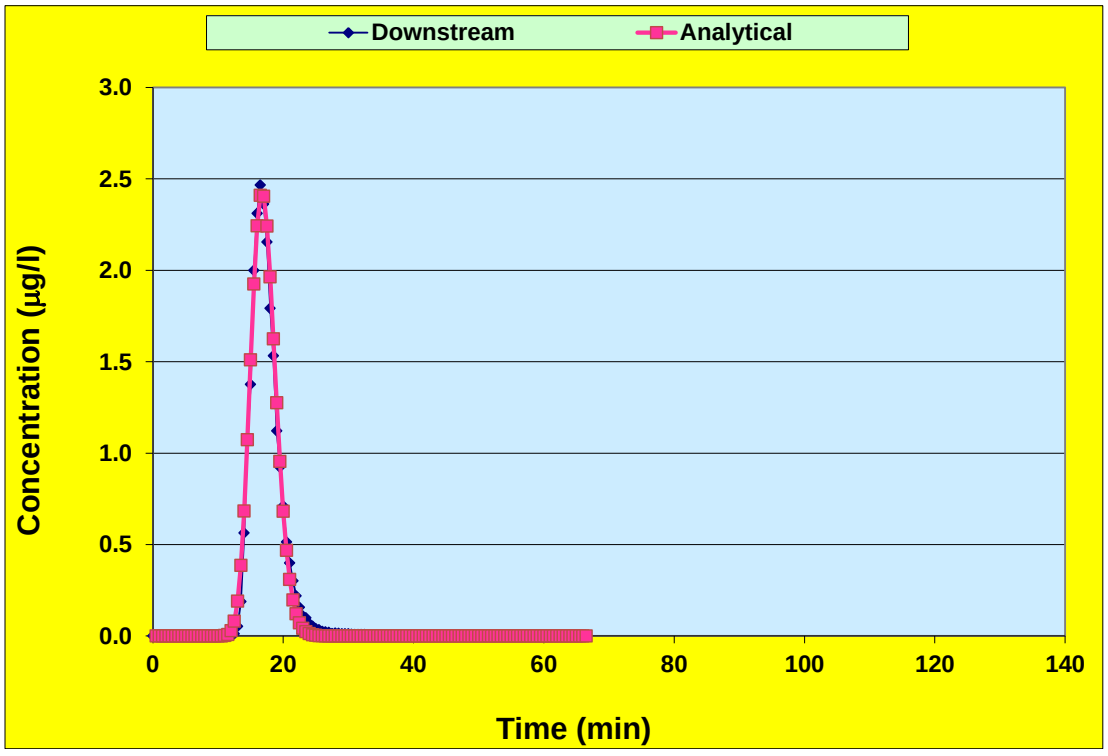

Experiment 12: Analytical solution downstream

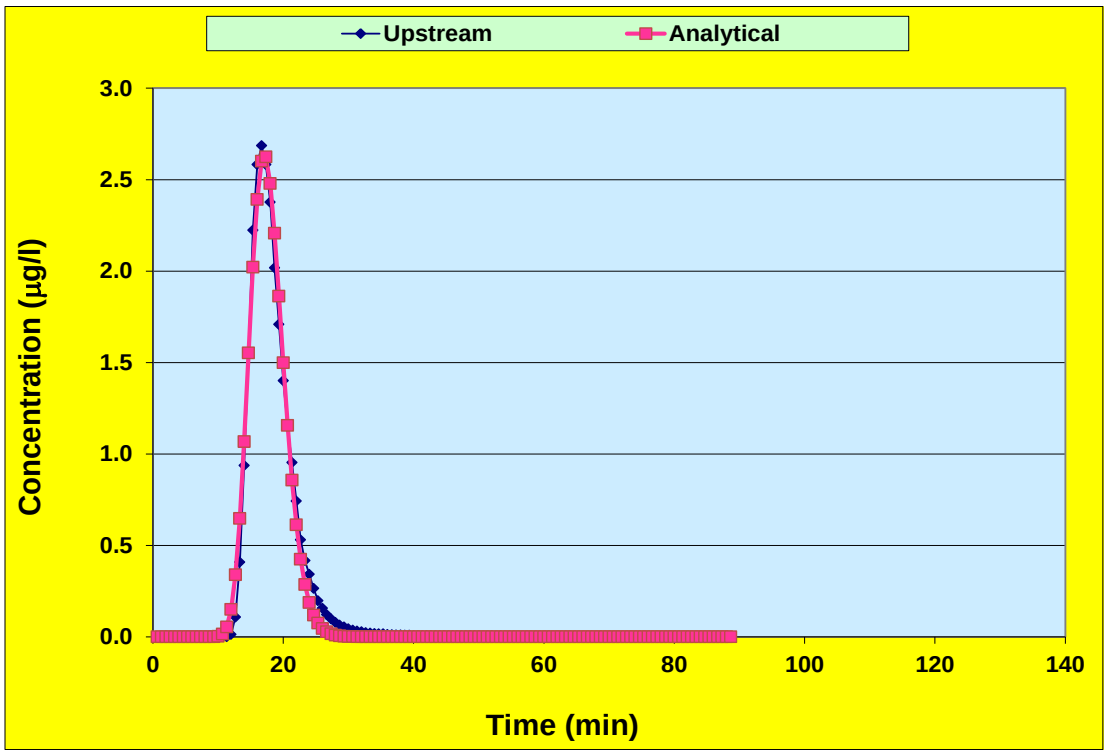

Experiment 13: Analytical solution upstream

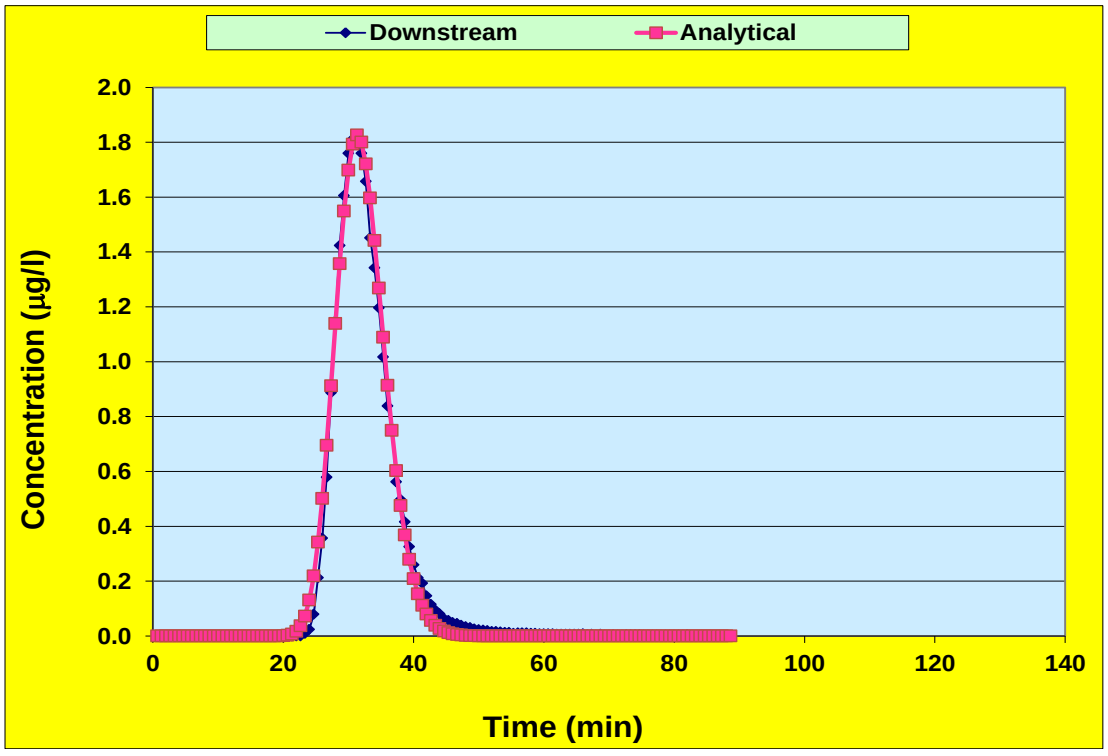

Experiment 13: Analytical solution downstream

Appendix E Velocity and dispersion coefficient tables, all methods

Experiment	Stream flow rate (l/s)	Standard data (m/s)	Truncated data (m/s)	% difference
3	147	0.204	0.204	0
4	84	0.146	0.146	0
5	97	0.161	0.161	0
6	385	0.341	0.341	0
7	41	0.085	0.085	0
8	44	0.106	0.106	0
9	37	0.083	0.083	0
10	17	0.042	0.042	0
11	150	0.192	0.192	0
12	436	0.383	0.383	0
13	148	0.219	0.219	0

Table 5.2 Velocity derived from Peak Reduction analysis

Experiment	Stream flow rate (l/s)	Standard data (m/s)	Truncated data (m/s)	% difference
3	147	0.194	0.191	+1.6
4	84	0.140	0.143	-2.2
5	97	0.151	0.156	-3.1
6	385	0.338	0.326	+3.7
7	41	0.087	0.087	+0.1
8	44	0.092	0.103	-12.1
9	37	0.080	0.079	+0.9
10	17	0.040	0.038	+4.6
11	150	0.187	0.187	-0.2
12	436	0.378	0.387	-2.3
13	148	0.212	0.213	-0.5

Table 5.3 Velocity derived from Method of Moments analysis

Experiment	Stream flow rate (l/s)	Standard data (m/s)	Truncated data (m/s)	% difference
3	147	0.215	0.201	+6.5
4	84	0.151	0.152	-0.1
5	97	0.166	0.166	-0.1
6	385	0.353	0.353	+0.1
7	41	0.093	0.093	-0.0
8	44	0.098	0.098	-0.0
9	37	0.085	0.085	+0.1
10	17	0.042	0.042	+0.7
11	150	0.196	0.197	-0.1
12	436	0.397	0.397	-0.0
13	148	0.220	0.220	-0.3

Table 5.4 Velocity derived from Routing Procedure analysis

Experiment	Stream flow rate (l/s)	Reach A (m/s)	Reach B (m/s)	Study Reach (m/s)
3	147	0.324	0.252	0.197
4	84	0.229	0.185	0.148
5	97	0.250	0.202	0.162
6	385	0.527	0.429	0.347
7	41	0.150	0.116	0.091
8	44	0.158	0.124	0.097
9	37	0.145	0.109	0.083
10	17	0.081	0.056	0.041
11	150	0.305	0.242	0.191
12	436	0.558	0.479	0.389
13	148	0.289	0.255	0.214

Table 5.5 Velocity derived from Analytical Solution analysis: standard data

Experiment	Stream flow rate (l/s)	Reach A (m/s)	Reach B (m/s)	Study Reach (m/s)	% difference
3	147	0.324	0.252	0.197	+0.0
4	84	0.229	0.184	0.148	+0.1
5	97	0.250	0.202	0.162	-0.0
6	385	0.527	0.429	0.347	+0.0
7	41	0.150	0.117	0.091	-0.4
8	44	0.158	0.123	0.096	+1.6
9	37	0.145	0.110	0.084	-1.2
10	17	0.081	0.056	0.041	+0.3
11	150	0.305	0.242	0.191	-0.3
12	436	0.558	0.479	0.389	+0.0
13	148	0.289	0.255	0.215	-0.1

Table 5.6 Velocity derived from Analytical Solution analysis: truncated data (final column shows difference between Study Reach values for standard and truncated data)

Experiment	Stream flow rate (l/s)	Standard data (m^2/s)	Truncated data (m^2/s)	% difference
3	147	0.237	0.237	0
4	84	0.161	0.161	0
5	97	0.156	0.156	0
6	385	1.168	1.168	0
7	41	0.047	0.047	0
8	44	0.049	0.049	0
9	37	0.041	0.041	0
10	17	0.018	0.018	0
11	150	0.288	0.288	0
12	436	1.071	1.071	0
13	148	0.441	0.441	0

Table 5.7 Dispersion coefficient derived from Peak Reduction analysis

Experiment	Stream flow rate (l/s)	Standard data (m^2/s)	Truncated data (m^2/s)	% difference
3	147	0	0.666	-
4	84	1.406	0.765	+45.6
5	97	2.179	0.889	+59.2
6	385	1.920	0.979	+49.0
7	41	0.474	0.426	+10.1
8	44	0.525	0.605	-15.2
9	37	0.283	0.346	-22.3
10	17	0.121	0.180	-48.7
11	150	1.114	0.909	+18.4
12	436	2.922	1.092	+62.6
13	148	1.007	0.735	+27.0

Table 5.8 Dispersion coefficient derived from Method of Moments analysis

Experiment	Stream flow rate (l/s)	Standard data (m^2/s)	Truncated data (m^2/s)	% difference
3	147	0.541	0.442	+18.3
4	84	0.528	0.508	+3.8
5	97	0.566	0.579	-2.3
6	385	0.738	0.740	-0.3
7	41	0.282	0.287	-1.8
8	44	0.280	0.286	-2.1
9	37	0.267	0.268	-0.4
10	17	0.122	0.122	0
11	150	0.655	0.666	-1.7
12	436	0.859	0.867	-0.9
13	148	0.554	0.564	-1.9

Table 5.9 Dispersion coefficient derived from Routing Procedure analysis

Experiment	Stream flow rate (l/s)	Reach A (m^2/s)	Reach B (m^2/s)	Study Reach (m^2/s)
3	147	0.949	0.718	0.538
4	84	0.610	0.667	0.714
5	97	0.703	0.759	0.805
6	385	2.272	1.424	0.709
7	41	0.312	0.376	0.426
8	44	0.309	0.385	0.445
9	37	0.273	0.335	0.380
10	17	0.169	0.189	0.202
11	150	1.104	0.973	0.868
12	436	1.930	1.457	0.920
13	148	0.955	0.846	0.714

Table 5.10 Dispersion coefficient derived from Analytical Solution analysis: standard data

Experiment	Stream flow rate (l/s)	Reach A (m^2/s)	Reach B (m^2/s)	Study Reach (m^2/s)	% difference
3	147	0.949	0.720	0.542	-0.7
4	84	0.632	0.667	0.696	+2.6
5	97	0.702	0.761	0.810	-0.6
6	385	2.271	1.424	0.710	-0.1
7	41	0.308	0.356	0.393	+7.6
8	44	0.309	0.374	0.425	+4.4
9	37	0.273	0.299	0.318	+16.4
10	17	0.163	0.189	0.206	-1.9
11	150	1.104	0.947	0.821	+5.4
12	436	1.930	1.456	0.917	+0.2
13	148	0.983	0.831	0.648	+9.4

Table 5.11 Dispersion coefficient derived from Analytical Solution analysis: truncated data (final column shows difference between Study Reach values for standard and truncated data)

Appendix F Dispersion coefficient example calculations

Example from Experiment 5

Reduction of peak

Site 3 CP 2.82 μg/l

Site 3 TP 15 mins

Site 4 CP 1.48 μg/l

Site 4 TP 34 mins

Slope 119106 figure (3.2)

Mass 100 mg

C S Area 0.60 m^2

K 0.156 m^2/s equation (3.5) $K = \frac{1}{4\pi}\left(\frac{M}{SA}\right)^2$

Method of Moments

Site 3 centroid (μ) 17.07 min

Site 3 variance (σ^2) 18.19 min^2

Site 4 centroid (μ) 37.32 min

Site 4 variance (σ^2) 82.89 min^2

K 2.18 m^2/s equation (3.14) $K = \frac{V^3}{2}\frac{(\sigma_2^2-\sigma_1^2)}{(x_2-x_1)}$

V 0.15 m/s equation (3.15) $V = \frac{x_2-x_1}{\mu_2-\mu_1}$

Routing Procedure Evolution of the process

The following three charts shows how the error criterion reduces to a minimum as the calibration coefficients change.

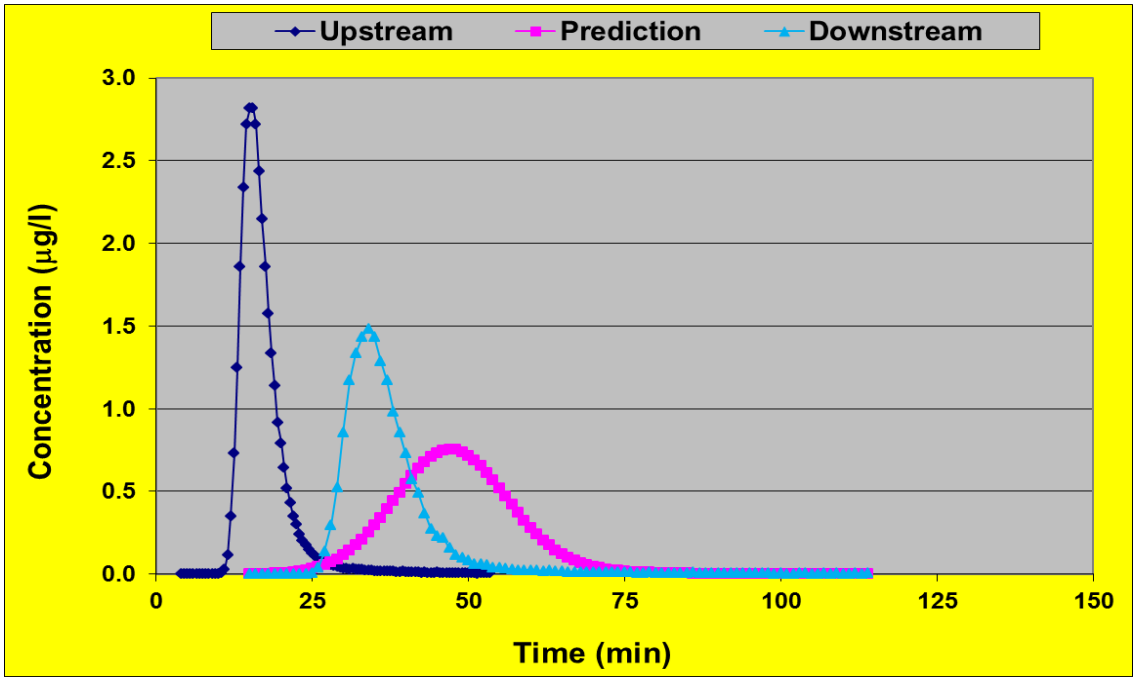

calibration coefficients			error criterion
velocity	0.1	m/s	0.1422 $(\mu g/l)^2$
dispersion	0.7	m^2/s	**Non optimum**

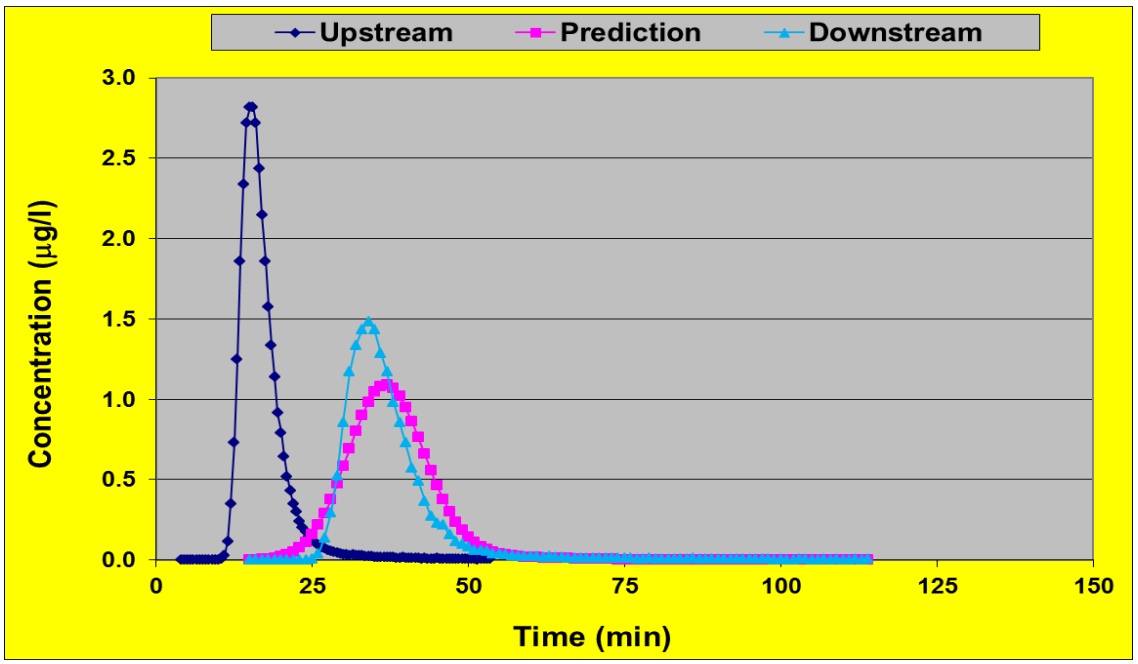

calibration coefficients			error criterion
velocity	0.15	m/s	0.0197 $(\mu g/l)^2$
dispersion	1	m^2/s	**Non optimum**

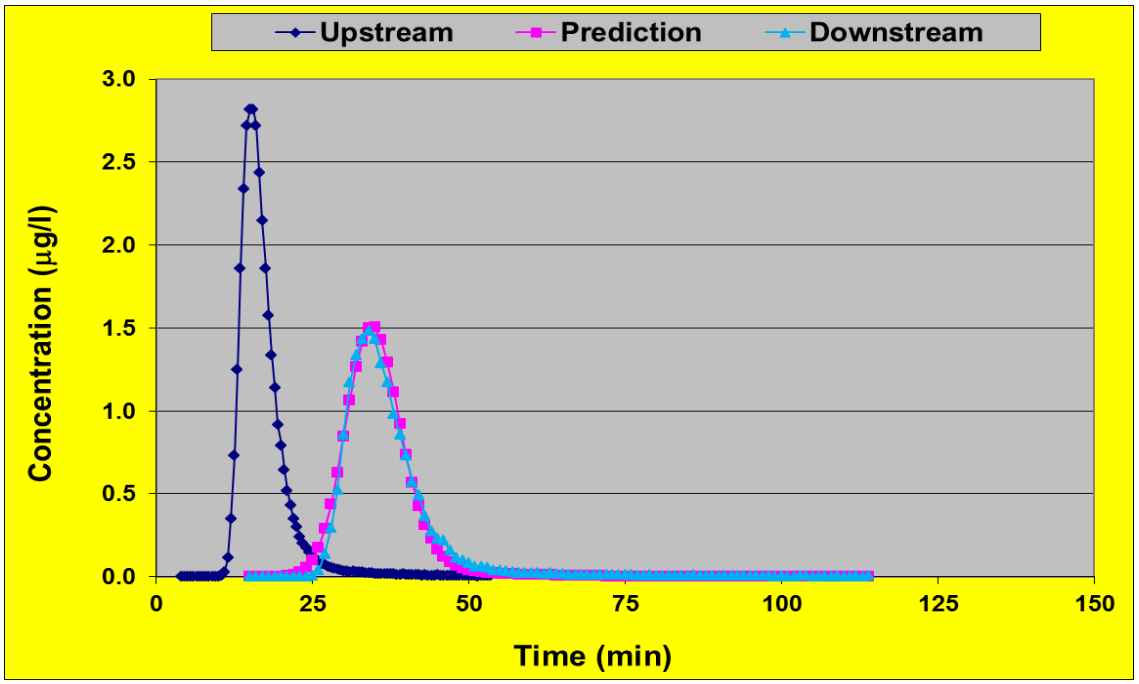

calibration coefficients			error criterion
velocity	0.166	m/s	0.002 $(\mu g/l)^2$
dispersion	0.566	m^2/s	**Optimum**

Analytical solution Evolution of the process, showing downstream data only

The following three charts shows how the error criterion reduces to a minimum as the calibration coefficients change.

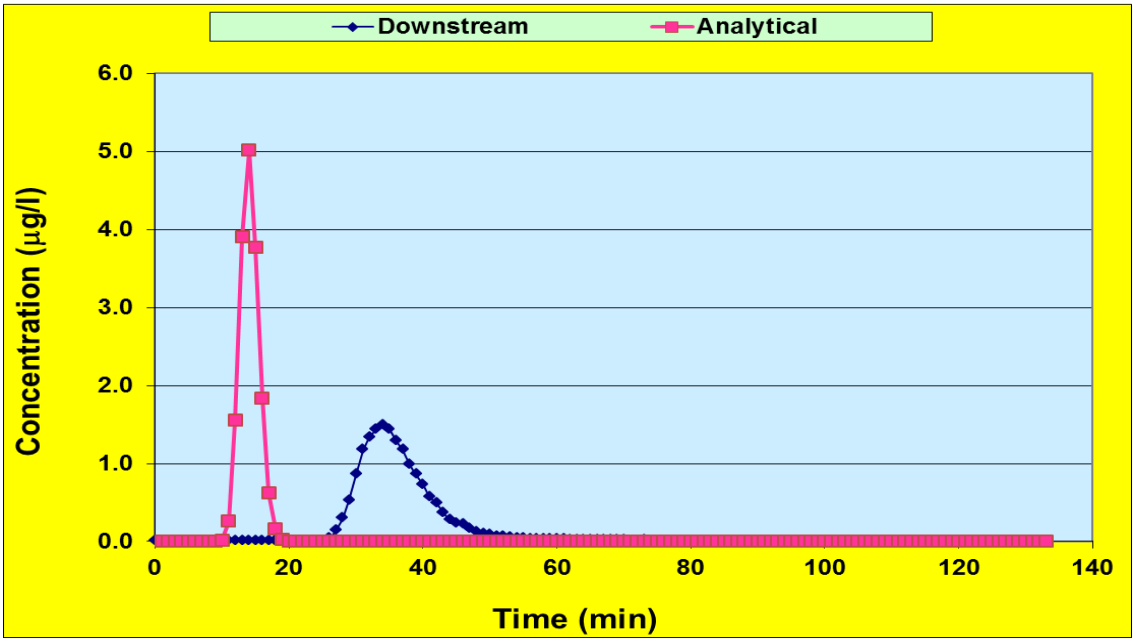

calibration coefficients			error criterion
velocity	0.5	m/s	0.5806 $(\mu g/l)^2$
dispersion	1	m^2/s	**Non optimum**

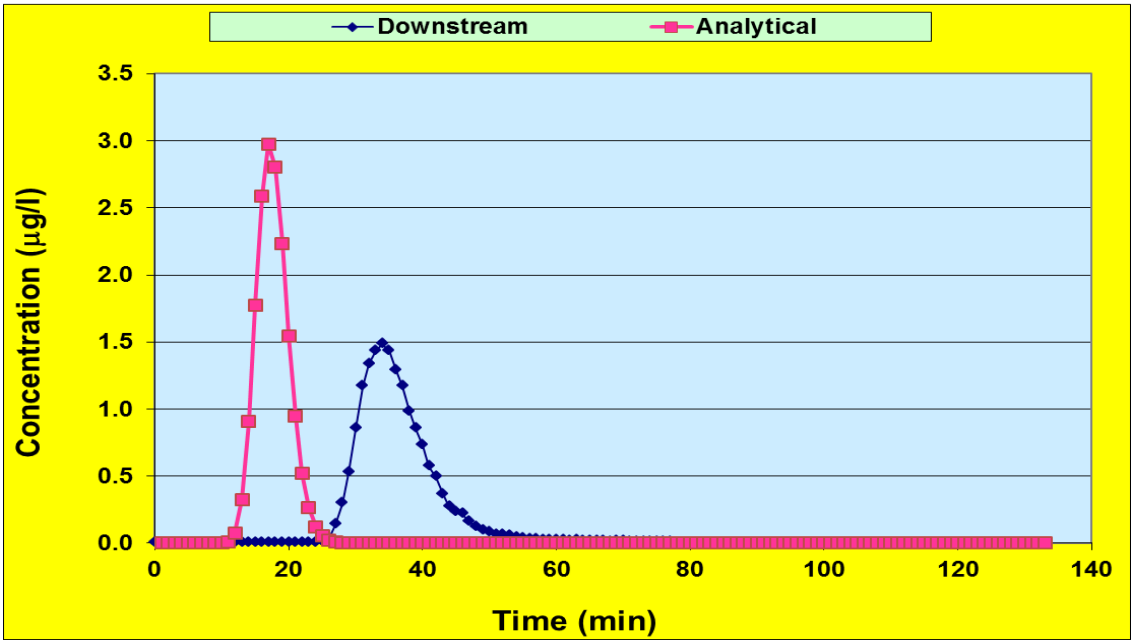

calibration coefficients			error criterion
velocity	0.404	m/s	0.3951 $(\mu g/l)^2$
dispersion	1.5	m^2/s	**Non optimum**

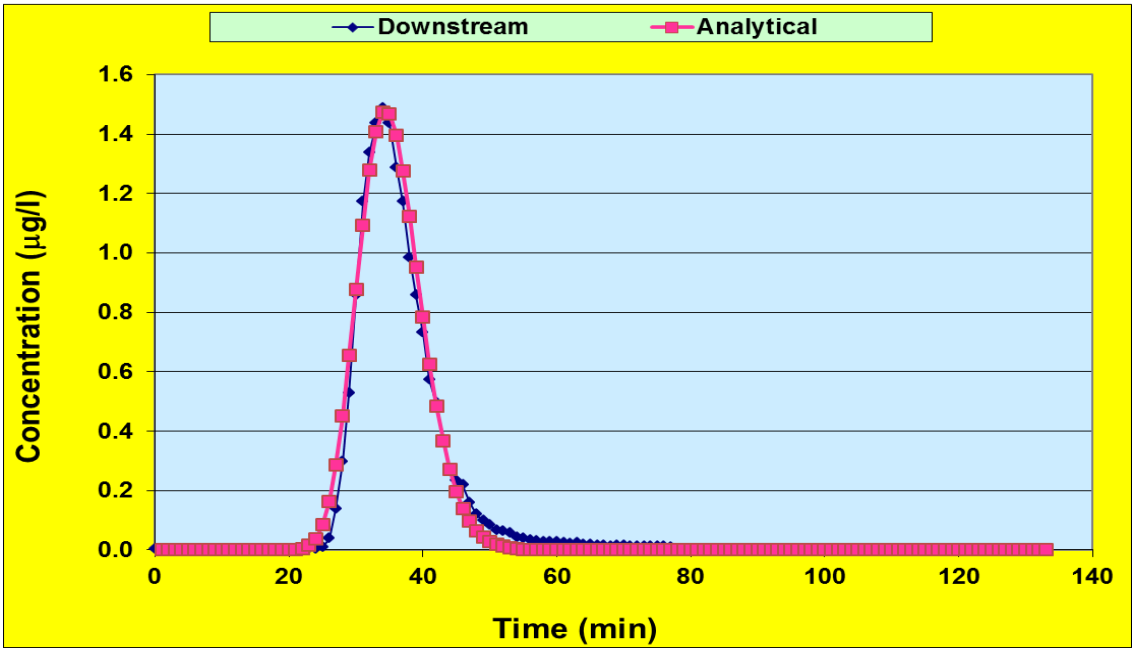

calibration coefficients			error criterion
velocity	0.202	m/s	0.0014 $(\mu g/l)^2$
dispersion	0.759	m^2/s	**Optimum**

Appendix G Process of serial dilution used to obtain the Rhodamine WT standards

Serial dilution process using Rhodamine WT 20%

1g/l = 1000mg/l = 1000000 μg/l

1 mg of 20% aqueous RWT contains 0.2 % RWT

1g of 20% aqueous RWT contains 0.2 % RWT

(1g/l RWT requires 5 g of 20% in 1 ltr)

For 1g/l take 10 g RWT and make up to 2L

For 1mg/l:

Take 2ml from stock (1g/l) and make up to 2L to create 1 mg/l

Now have 1mg/l stock standard for next dilutions

Take 2.5ml from stock (1mg/l) and make up to 500ml to create 5 μg/l

2ml from stock (1mg/l) and make up to 500ml to create 4 μg/l

1.5ml from stock (1mg/l) and make up to 500ml to create 3 μg/l

1ml from stock (1mg/l) and make up to 500ml to create 2 μg/l

1ml from stock (1mg/l) and make up to 1L to create 1 μg/l**need 3L

Now have 1μg/l stock standard for next dilutions:

Take 50ml of 1μg/l make up to 500ml = 0.1 μg/l**need 3L

100ml of 1μg/l make up to 500ml = 0.2 μg/l

150ml of 1μg/l make up to 500ml = 0.3 μg/l

200ml of 1μg/l make up to 500ml = 0.4 μg/l

250ml of 1μg/l make up to 500ml = 0.5 μg/l

300ml of 1μg/l make up to 500ml = 0.6 μg/l

350ml of 1μg/l make up to 500ml = 0.7 μg/l

400ml of 1μg/l make up to 500ml = 0.8 μg/l

Now have 0.1μg/l stock standard for next dilutions:

Take 50ml of 0.1μg/l make up to 500ml = 0.01 μg/l

100ml of 0.1μg/l make up to 500ml = 0.02 μg/l

150ml of 0.1μg/l make up to 500ml = 0.03 μg/l

200ml of 0.1μg/l make up to 500ml = 0.04 μg/l

250ml of 0.1μg/l make up to 500ml = 0.05 μg/l

300ml of 0.1μg/l make up to 500ml = 0.06 μg/l

350ml of 0.1μg/l make up to 500ml = 0.07 μg/l

400ml of 0.1μg/l make up to 500ml = 0.08 μg/l

To make up 100 milligrams of tracer for injection use 100 ml of 1 g/l solution

To make up 200 milligrams of tracer for injection use 200 ml of 1 g/l solution and so on.

References

Ani, E-C., Wallis, S.G., Kraslawski, A. & Agachi, P.S. (2009) Development, calibration and evaluation of two mathematical models for pollutant transport in a small river. Environmental Modelling and Software, 24(10), 1139-1152.

Baek, K., Seo, I., and Jeong, S. (2006). Evaluation of dispersion coefficients in meandering channels from transient tracer tests. Journal of Hydraulic Engineering, ASCE, 132(10), 1021–1032.

Baker, A. (2002) Fluorescence properties of some farm wastes: Implications for water quality monitoring. Water Research, 36, 189-195.

Barnett, A.G. (1983) Exact and approximate solutions of the advection-diffusion equation. Proceedings of the 20th IAHR Congress, Moscow, September, 1983, Vol. 3, 180-190.

Beer, T., and Young, P.C. (1983) Longitudinal dispersion in natural streams. Journal of Environmental Engineering, ASCE, 109(5), 1049-1067.

Bencala K.E. and Walters R.A. (1983) Simulation of solute transport in a mountain pool-and-riffle stream: A transient storage model. Water Resources Research, 19(3), 718-724.

Boxall, J.B., Guymer, I. and Marion, A. (2003) Transverse mixing in sinuous natural open channel flows. Journal of Hydraulic Engineering and Research, 41(2), 153-165.

Burke, N. A. (2002) Travel time and flow characteristics of a small stream system. Ph.D. thesis, Heriot-Watt University, Edinburgh.

Carr, M.L. and Rehmann, C.R. (2007) Measuring the dispersion coefficient with acoustic Doppler current profilers. Journal of Hydraulic Engineering, ASCE, 133(8), 977-982.

Chanson, H. (2004) Environmental Hydraulics of Open Channel Flows. Elsevier, Oxford, UK.

Chatwin, P.C. and Allen, C.M. (1985) Mathematical models of dispersion in rivers and estuaries. Annual Review of Fluid Mechanics, 17, 119-149.

Chin, D.A. (2013) Water-Quality Engineering in Natural Systems, 2nd Ed. Wiley, Hoboken, New Jersey, USA.

Davis, W.M. (1899) The geographical cycle. Geographical Journal, 14, 481-504.

Day, T.J. (1977) Observed mixing lengths in mountain streams. Journal of Hydrology, 35(1–2), 125–136.

Day, T.J. and Wood, I.R. (1976) Similarity of the mean motion of fluid particles dispersing in a natural channel. Water Resources Research, 12, 655-666.

Deng, Z-Q, Bengtsson, L., Singh, V.P. and Adrian, D.D. (2002) Longitudinal dispersion coefficient in single-channel streams. Journal of Hydraulic Engineering, ASCE, 128, 901-916.

Deng, Z-Q, Singh, V.P. and Bengtsson, L. (2001) Longitudinal dispersion coefficient in straight rivers. Journal of Hydraulic Engineering, ASCE, 127, 919-927.

Edmunds, W.M. and Kinniburgh, D.G. (1986) The susceptibility of UK groundwaters to acidic deposition. Journal of the Geological Society, 143(4), 707-720.

J. W. Elder (1959). The dispersion of marked fluid in turbulent shear flow. Journal of Fluid Mechanics, Vol 5, issue 4, pp 544-560.

Fischer, H. B., List, E. J., Koh, R. C. Y., Imberger, J., and Brooks, N. H. (1979) Mixing in Inland and Coastal Waters. Academic Press, New York.

Fischer, H.B. (1966) Longitudinal dispersion in laboratory and natural streams. Technical Report KH-R-12, California Institute of Technology, Pasadena, USA.

Fischer, H.B. (1967) The mechanics of dispersion in natural streams. Journal of the Hydraulics Division, ASCE, 93(HY6), 187-215.

Fischer, H.B. (1968) Dispersion predictions in natural streams. Journal of the Sanitary Engineering Division, ASCE, 94, 927-944.

Fischer, H.B. (1969) The effects of bends on dispersion in streams. Water Resources Research, 5, 496-506.

Fischer, H.B. (1975) Discussion of "Simple method for predicting dispersion in streams", R.S. McQuivey and T.N. Keefer. Journal of the Environmental Engineering Division, ASCE, 101, 453-455.

Godfrey, R. G. and Frederick, B. J. 1963. Dispersion in natural streams. Open-File report, US Geological Survey.

Harriman, R. and Morrison, B.R.S. (1982) Ecology of streams draining forested and non-forested catchments in an area of central Scotland subject to acid precipitation. Hydrobiologia, 88, 251-263.

Herschy, R.W (1995) Streamflow Measurement.Second Edition. E and F.N.Spon. London UK. ISBN 0 419 19490 8

IBIS (2012) Report of Workshop on Small Streams: Contribution to populations of trout and sea trout. Carlingford, Ireland, September, 2012.

Kashefipour S.M. and Falconer, R.A. (2002) Longitudinal dispersion coefficients in natural channels. Water Research, 36(6), 1596-1608.

Kashefipour, S.M., Falconer, R.A. and Lin, B. (2002) Modelling longitudinal dispersion in natural flows using ANNs. Proceedings of River Flow 2002, Louvain-le-Neuve, Belgium, 111-116.

Liu, H. (1977) Predicting dispersion coefficient of streams. Journal of the Environmental Engineering Division, ASCE, 103, 59-69.

Nordin, C.F. and Troutman, B.M. (1980) Longitudinal dispersion in rivers: The persistence of skewness in observed data. Water Resources Research, 16, 123-128.

Piotrowski, A.A., Napiorkowski, J.J., Rowinski, P.M. and Wallis, S.G. (2011) Evaluation of temporal concentration profiles for ungauged rivers following pollution incidents. Hydrological Sciences Journal, 56(5), 883-894.

Rosgen, D.L. A Classificationof Natural Rivers (1994) Catena, vol 22:169-199 Elsevier Science, B.V. Amsterdam. .

Rowinski, P.M., Piotrowski, A. and Napiorkowski, J.J. (2005) Are artificial neural network techniques relevant for the estimation of longitudinal dispersion coefficient in rivers? Journal of Hydrological Sciences, 50 (1), 175-187.

Rowinski, P.M., Guymer, I., Bielonko, A., Napiorkowski, J.J., Pearson, J. and Piotrowski, A. (2007) Large scale tracer study of mixing in a natural lowland river. Proceedings of the 32nd IAHR Congress, Venice, Italy, 1-6 July, paper SS08-05-O.

Runkel, R.L. (1998) One-dimensional transport with inflow and storage (OTIS): A solute transport model for streams and rivers. Water Resources Investigations Report 98-4018, US Geological Survey.

Rutherford, J.C. (1994) River Mixing. Wiley, Chichester, UK.

Sayre, W. W. (1968) Dispersion of Mass in Open Channel Flow. Hydraulics Papers, NO: 3, Colorado State University, Fort Collins, Colorado.

Schmid, B.H. (2002) Persistence of skewness in longitudinal dispersion data: Can the dead zone model explain it after all? Journal of Hydraulic Engineering, ASCE, 128(9), 848-854.

Seo, I.W. and Baek, K.O. (2002) Estimation of longitudinal dispersion coefficient for streams. Proceedings of River Flow 2002, Louvain-le-Neuve, Belgium, 143-150.

Seo, I.W. and Cheong, T.S. (1998) Predicting longitudinal dispersion coefficient in natural streams. Journal of Hydraulic Engineering, ASCE, 124, 25-32.

Shen, C., Niu, J., Anderson, E.J. and Phanikumar, M.S. (2010) Estimating longitudinal dispersion in rivers using acoustic Doppler current profilers. Advances in Water Resources, 33, 616-623.

Shucksmith, J., Boxall, J. and Guymer, I. (2007) Importance of advective zone in longitudinal mixing experiments. Acta Geophysica, 55(1), 95-103.

Silavwe, D.D., (2009) Application of routing procedures to solute transport in a small stream. M.S.c. thesis, Heriot-Watt University, Edinburgh.

Singh, S.K. and Beck, M.B. (2003) Dispersion coefficient of streams from tracer experiment data. Journal of Environmental Engineering, ASCE, 129(6), 539-546.

Smart, P.L. and Laidlaw, I.M.S. (1977) An evaluation of some fluorescent dyes for water tracing. Water Resources Research, 13(1), 15-33.

Strahler, A.N. (1952) Hypsometric (area-altitude) analysis of erosional topography. Geological Society Bulletin, 63, 1117-1142.

Sukhodolov, A.N., Nikora, V.I., Rowinski, P.M. and Czernuszenko W. (1997) A case study of longitudinal dispersion in small lowland rivers. Water Environment Research, 69 (7), 1246-1253.

Taylor, G.I. (1921) Diffusion by continuous movements. Proceedings of the London Mathematical Society, Series 2, 20, 196-212.

Taylor, G.I. (1953) Dispersion of soluble matter in solvent flowing slowly through a tube. Proceedings of the Royal Society of London, Series A, 219, 186-203.

Taylor, G.I. (1954) The dispersion of matter in turbulent flow through a pipe. Proceedings of the Royal Society of London, Series A, 223, 446-468.

Valentine, E.M. and Wood, I.R. (1979) Experiments in longitudinal dispersion with dead zones. Journal of the Hydraulics Division, ASCE, 105(HY8), 999-1016.

Wallis, S.G and Manson, J. R. (2004) Methods for predicting dispersion coefficients in rivers. Water Management, Proceedings of the Institution of Civil Engineers, 157(3), 131-141.

Wallis, S.G and Manson, J. R. (2005) Modelling solute transport in a small stream using DISCUS. Acta Geophysica Polonica 53(4), pp 501-515

Wallis, S.G., Piotrowski, A., Rowinski, P.M. and Napiorkowski, J.J. (2007) Prediction of dispersion coefficients in a small stream using artificial neural networks. Proceedings of the 32nd IAHR Congress, Venice, Italy, 1-6 July, Paper B2b-083-O.

Wallis, S.G. (2011) Pollutant Transport in Rivers. MSc Course Notes, Heriot-Watt University, Edinburgh, UK.

Wallis, S.G., Young, P.C. and Beven, K.J. (1989) Experimental investigation of the aggregated dead zone model for longitudinal solute transport in stream channels. Proceedings of the Institution of Civil Engineers, Part 2, 1989, 87 (Mar), 1-22.

Yotsukura N., Fischer H.B. Sayre W.W (1970) Measurement of the mixing characteristics of the Missouri River between Sioux City, Iowa and Plattsmouth, Nebraska. Water Supply Paper 1899-G, US Geological Survey.

Zeng, H.Y and Huai X.W. (2014) Estimation of longitudinal dispersion coefficient in rivers. Journal of Hydro-environment Research, 8, 2-8.

Zhang, W and Boufadel, M.C. (2010) Pool Effects on Longitudinal Dispersion in Streams and Rivers. Journal of Water Resource and Protection, 2010, 2, 960-971